



Geologic Framework for the National Assessment of Carbon Dioxide Storage Resources—Southern Rocky Mountain Basins

By Matthew D. Merrill, Ronald M. Drake II, Marc L. Buursink, William H. Craddock, Joseph A. East, Ernie R. Slucher, Peter D. Warwick, Sean T. Brennan, Madalyn S. Blondes, Philip A. Freeman, Steven M. Cahan, Christina A. DeVera, and Celeste D. Lohr

Chapter M of

Geologic Framework for the National Assessment of Carbon Dioxide Storage Resources

Edited by Peter D. Warwick and Margo D. Corum

Open-File Report 2012–1024–M

U.S. Department of the Interior
SALLY JEWELL, Secretary

U.S. Geological Survey
Suzette M. Kimball, Director

U.S. Geological Survey, Reston, Virginia: 2016

For more information on the USGS—the Federal source for science about the Earth, its natural and living resources, natural hazards, and the environment—visit <http://www.usgs.gov> or call 1-888-ASK-USGS (1-888-275-8747).

For an overview of USGS information products, including maps, imagery, and publications, visit <http://store.usgs.gov/>.

Any use of trade, firm, or product names is for descriptive purposes only and does not imply endorsement by the U.S. Government.

Although this information product, for the most part, is in the public domain, it also may contain copyrighted materials as noted in the text. Permission to reproduce copyrighted items must be secured from the copyright owner.

Suggested citation:

Merrill, M.D., Drake, R.M., II, Buursink, M.L., Craddock, W.H., East, J.A., Slucher, E.R., Warwick, P.D., Brennan, S.T., Blondes, M.S., Freeman, P.A., Cahan, S.M., DeVera, C.A., and Lohr, C.D., 2016, Geologic framework for the national assessment of carbon dioxide storage resources—Southern Rocky Mountain Basins, chap. M of Warwick, P.D., and Corum, M.D., eds., Geologic framework for the national assessment of carbon dioxide storage resources: U.S. Geological Survey Open-File Report 2012–1024–M, 59 p., at <http://dx.doi.org/10.3133/ofr20121024M>.

Editors' Preface

By Peter D. Warwick and Margo D. Corum

The 2007 Energy Independence and Security Act (Public Law 110–140; U.S. Congress, 2007) directs the U.S. Geological Survey (USGS) to conduct a national assessment of potential geologic storage resources for carbon dioxide (CO₂) and to consult with other Federal and State agencies to locate the pertinent geological data needed for the assessment. The geologic storage of CO₂ is one possible way to mitigate its effects on climate change.

The methodology used by the USGS for the assessment was described by Brennan and others (2010), who revised the methodology by Burruss and others (2009) according to comments from peer reviewers, an external panel of experts, and members of the public. During the implementation phase of the assessment (from 2010 to 2012), several practical steps were added to the assessment methodology of Brennan and others (2010). The details of the methodology used in the assessment are described in Blondes and others (2013). The assessment methodology is non-economic and is intended to be used at regional to subbasinal scales.

The operational unit of the assessment is a storage assessment unit (SAU), which is composed of a porous storage formation with fluid flow and an overlying fine-grained sealing unit. Assessments are conducted at the SAU level and are aggregated to basinal and regional results. SAUs have a minimum depth of 3,000 feet (ft), which ensures that the CO₂ is in a supercritical state, and thus occupies less pore space than a gas. Standard SAUs have a maximum depth of 13,000 ft below the surface, a depth accessible with average injection pipeline pressures (Burruss and others, 2009; Brennan and others, 2010; Blondes and others, 2013). Where geologic conditions favor CO₂ storage below 13,000 ft, an additional deep SAU is assessed.

The assessments are also constrained by the occurrence of relatively fresh formation water. Any formation water having a salinity less than 10,000 parts per million (ppm) total dissolved solids (TDS), regardless of depth, has the potential to be used as a potable water supply (U.S. Environmental Protection Agency, 2009). The U.S. Environmental Protection Agency (EPA) (2010) defines the lower limit of 10,000 ppm (equivalent to 10,000 mg/L) TDS for injection of CO₂. Therefore, the potential storage resources for CO₂ in formations where formation waters have salinities less than 10,000 ppm TDS are not assessed (Brennan and others, 2010; Blondes and others, 2013).

This report series contains a geologic description of each SAU identified within each report's assessed basins and focuses on particular characteristics specified in the methodology that influence the potential CO₂ storage resource. The geologic framework information contained in these reports was used to calculate a statistical Monte Carlo-based distribution of potential storage space in the various SAUs following Brennan and others (2010) and Blondes and others (2013). Assessment data, results, and a summary can be found in the U.S. Geological Survey Geologic Carbon Dioxide Storage Resources Assessment Team's (2013a,b,c) reports. The map figures in this report series show the SAU boundaries and cells representing well-penetration density. The well-penetration density is the number of wells within one square mile that penetrate through the sealing unit into the top of the storage formation. Wells sharing the same well borehole are treated as a single penetration. The well-penetration-density cell maps are derived from interpretations of incompletely attributed well data from IHS Energy Group (2011) (and other data as available), which is a digital compilation that is known not to include all drilling. The USGS does not expect to know the location of all wells and cannot guarantee the amount of drilling through specific formations in any given cell shown on the cell maps.

References Cited

- Blondes, M.S., Brennan, S.T., Merrill, M.D., Buursink, M.L., Warwick, P.D., Cahan, S.M., Cook, T.A., Corum, M.D., Craddock, W.H., DeVera, C.A., Drake, R.M., II, Drew, L.J., Freeman, P.A., Lohr, C.D., Olea, R.A., Roberts-Ashby, T.L., Slucher, E.R., and Varela, B.A., 2013, National assessment of geologic carbon dioxide storage resources—Methodology implementation: U.S. Geological Survey Open-File Report 2013–1055, 26 p., at <http://pubs.usgs.gov/of/2013/1055/>.
- Brennan, S.T., Burruss, R.C., Merrill, M.D., Freeman, P.A., and Ruppert, L.F., 2010, A probabilistic assessment methodology for the evaluation of geologic carbon dioxide storage: U.S. Geological Survey Open-File Report 2010–1127, 31 p., accessed March 22, 2011, at <http://pubs.usgs.gov/of/2010/1127/>.
- Burruss, R.C., Brennan, S.T., Freeman, P.A., Merrill, M.D., Ruppert, L.F., Becker, M.F., Herkelrath, W.N., Kharaka, Y.K., Neuzil, C.E., Swanson, S.M., Cook, T.A., Klett, T.R., Nelson, P.H., and Schenk, C.J., 2009, Development of a probabilistic assessment methodology for evaluation of carbon dioxide storage: U.S. Geological Survey Open-File Report 2009–1035, 81 p., accessed March 22, 2011, at <http://pubs.usgs.gov/of/2009/1035/>.
- IHS Energy Group, 2011, ENERDEQ U.S. well data: IHS Energy Group, online database available from IHS Energy Group, 15 Inverness Way East, D205, Englewood, CO 80112, U.S.A., accessed January 20, 2011.
- U.S. Congress, 2007, Energy Independence and Security Act of 2007—Public Law 110–140: U.S. Government Printing Office, 311 p., accessed October 30, 2012, at http://frwebgate.access.gpo.gov/cgi-bin/getdoc.cgi?dbname=110_cong_public_laws&docid=f:publ140.110.pdf.
- U.S. Environmental Protection Agency, 2009, Safe Drinking Water Act (SDWA): Washington, D.C., U.S. Environmental Protection Agency Web site, accessed January 14, 2009, at <http://www.epa.gov/ogwdw/sdwa/index.html>.
- U.S. Environmental Protection Agency, 2010, Final rule for Federal requirements under the underground injection control (UIC) program for carbon dioxide (CO₂) geologic sequestration (GS) wells final rule: Washington, D.C., U.S. Environmental Protection Agency Web site, accessed October 15, 2012, at <http://water.epa.gov/type/groundwater/uic/class6/gsregulations.cfm>.
- U.S. Geological Survey Geologic Carbon Dioxide Storage Resources Assessment Team, 2013a, National assessment of geologic carbon dioxide storage resources—Summary (ver. 1.1, September 2013): U.S. Geological Survey Fact Sheet 2013–3020, 6 p., at <http://pubs.usgs.gov/fs/2013/3020/>. (Supersedes ver. 1.0 released June 26, 2013.)
- U.S. Geological Survey Geologic Carbon Dioxide Storage Resources Assessment Team, 2013b, National assessment of geologic carbon dioxide storage resources—Data (ver. 1.1, September 2013): U.S. Geological Survey Data Series 774, 13 p., plus 2 appendixes and 2 large tables in separate files, at <http://pubs.usgs.gov/ds/774/>. (Supersedes ver. 1.0 released June 26, 2013.)
- U.S. Geological Survey Geologic Carbon Dioxide Storage Resources Assessment Team, 2013c, National assessment of geologic carbon dioxide storage resources—Results (ver. 1.1, September 2013): U.S. Geological Survey Circular 1386, 41 p., at <http://pubs.usgs.gov/circ/1386/>. (Supersedes ver. 1.0 released June 26, 2013.)

Contents

Editors' Preface	iii
References Cited	iv
Conversion Factors	vii
Abbreviations	viii
Abstract	1
Report Overview	1
Uinta and Piceance Basins	3
Introduction	3
Geologic History	3
Hydrocarbon Exploration and Production	5
Carbon Dioxide Storage Assessment	5
Paleozoic Composite SAU C50200101 and Paleozoic Composite Deep SAU C50200102	7
Lower Cretaceous Composite SAU C50200103 and Lower Cretaceous Composite Deep SAU C50200104	10
Green River Formation SAU C50200105	12
Paradox Basin	14
Introduction	14
Geologic History	14
Hydrocarbon and Carbon Dioxide Production and Exploration	16
Carbon Dioxide Storage Assessment	16
Paleozoic Composite SAU C50210101	18
San Juan Basin	21
Introduction	21
Geologic History	21
Hydrocarbon Exploration and Production	22
Carbon Dioxide Storage Assessment	22
Entrada Sandstone SAU C50220101	25
Dakota Sandstone SAU C50220102	27
Gallup Sandstone SAU C50220103	29
Lewis Shale and Mesaverde Group SAU C50220104	31
Eastern Great Basin	33
Introduction	33
Geologic History	33
Hydrocarbon Exploration and Production	34
Carbon Dioxide Storage Assessment	34
Joana Limestone SAU C50190101	37
Navajo Sandstone SAU C50190102	40
Raton Basin	42
Introduction and Geologic History	42
Hydrocarbon and Carbon Dioxide Exploration and Production	42
Carbon Dioxide Storage Assessment	42
Dakota Sandstone SAU C50410101	45
Black Mesa Basin	47
Acknowledgments	47
References Cited	47

Figures

1. Map of the southern Rocky Mountain basins of Arizona, Colorado, Idaho, Nevada, New Mexico, and Utah showing the basins that were evaluated for their geologic carbon dioxide storage potential.....	2
2. Map showing the Uinta and Piceance Basins study area, including major structural features.....	4
3. Generalized stratigraphic column of geologic units in the Uinta and Piceance Basins study area of Utah and Colorado	6
4. Map of the Paleozoic Composite C50200101 and Paleozoic Composite Deep C50200102 Storage Assessment Units (SAUs) in the Uinta and Piceance Basins	9
5. Map of the Lower Cretaceous Composite C50200103 and Lower Cretaceous Composite Deep C50200104 Storage Assessment Units (SAUs) in the Uinta and Piceance Basins.....	11
6. Map of the Green River Formation C50200105 Storage Assessment Unit (SAU) in the Uinta and Piceance Basins	13
7. Map showing the Paradox Basin study area, including major structural features	15
8. Generalized stratigraphic column of geologic units in the Paradox Basin study area, Utah, Colorado, Arizona, and New Mexico.....	17
9. Map of the Paleozoic Composite C50210101 Storage Assessment Unit (SAU) in the Paradox Basin	20
10. Map showing the San Juan Basin study area, including major structural features	23
11. Generalized stratigraphic column of geologic units in the San Juan Basin study area of New Mexico and Colorado	24
12. Map of the Entrada Sandstone C50220101 Storage Assessment Unit (SAU) in the San Juan Basin.....	26
13. Map of the Dakota Sandstone C50220102 Storage Assessment Unit (SAU) in the San Juan Basin	28
14. Map of the Gallup Sandstone C50220103 Storage Assessment Unit (SAU) in the San Juan Basin	30
15. Map of the Lewis Shale and Mesaverde Group C50220104 Storage Assessment Unit (SAU) in the San Juan Basin	32
16. Map showing the Eastern Great Basin study area, including major structural features.....	35
17. Generalized stratigraphic column of geologic units in the Eastern Great Basin study area of Nevada, Utah, Arizona, and Idaho.....	36
18. Map of the Joana Limestone nonquantitative C50190101 Storage Assessment Unit (SAU) in the Eastern Great Basin	39
19. Map of the Navajo Sandstone C50190102 Storage Assessment Unit (SAU) in the Eastern Great Basin	41
20. Map showing the Raton Basin study area, including major structural features.....	43
21. Generalized stratigraphic column of geologic units in the Raton Basin study area of Colorado and New Mexico	44
22. Map of the Dakota Sandstone C50410101 Storage Assessment Unit (SAU) in the Raton Basin	46

Conversion Factors

Multiply	By	To obtain
Length		
inch (in.)	2.54	centimeter (cm)
foot (ft)	0.3048	meter (m)
mile (mi)	1.609	kilometer (km)
Area		
acre	0.4047	hectare (ha)
acre	0.004047	square kilometer (km ²)
square mile (mi ²)	2.5899	square kilometer (km ²)
Volume		
barrel (bbl), (petroleum, 1 barrel=42 gal)	0.1590	cubic meter (m ³)
cubic foot (ft ³)	0.02832	cubic meter (m ³)
1,000 cubic feet (MCF)	28.32	cubic meter (m ³)
liter (L)	0.2642	gallon (gal)
Mass		
megaton (Mt) = 1 million metric tons	1.102	million short tons

Abbreviations

BCFG	billion cubic feet of gas
Btu	British thermal unit
CH ₄	methane
CO ₂	carbon dioxide
EOR	enhanced oil recovery
EPA	U.S. Environmental Protection Agency
ft	feet
GIS	Geographic Information System
Ls	limestone
Ma	Mega-annum, or millions of years before present
Mbr	member
mD	millidarcy
mg/L	milligrams per liter
mi	mile
MMBO	million barrels of oil
Mt/y	megatons per year
N ₂	nitrogen
NOGA	national oil and gas assessment
OFR	open-file report
ppm	parts per million
SAU	storage assessment unit
Ss	sandstone
TCFG	trillion cubic feet of gas
TDS	total dissolved solids
TPS	total petroleum system
USDW	underground source of drinking water
USGS	U.S. Geological Survey

Geologic Framework for the National Assessment of Carbon Dioxide Storage Resources—Southern Rocky Mountain Basins

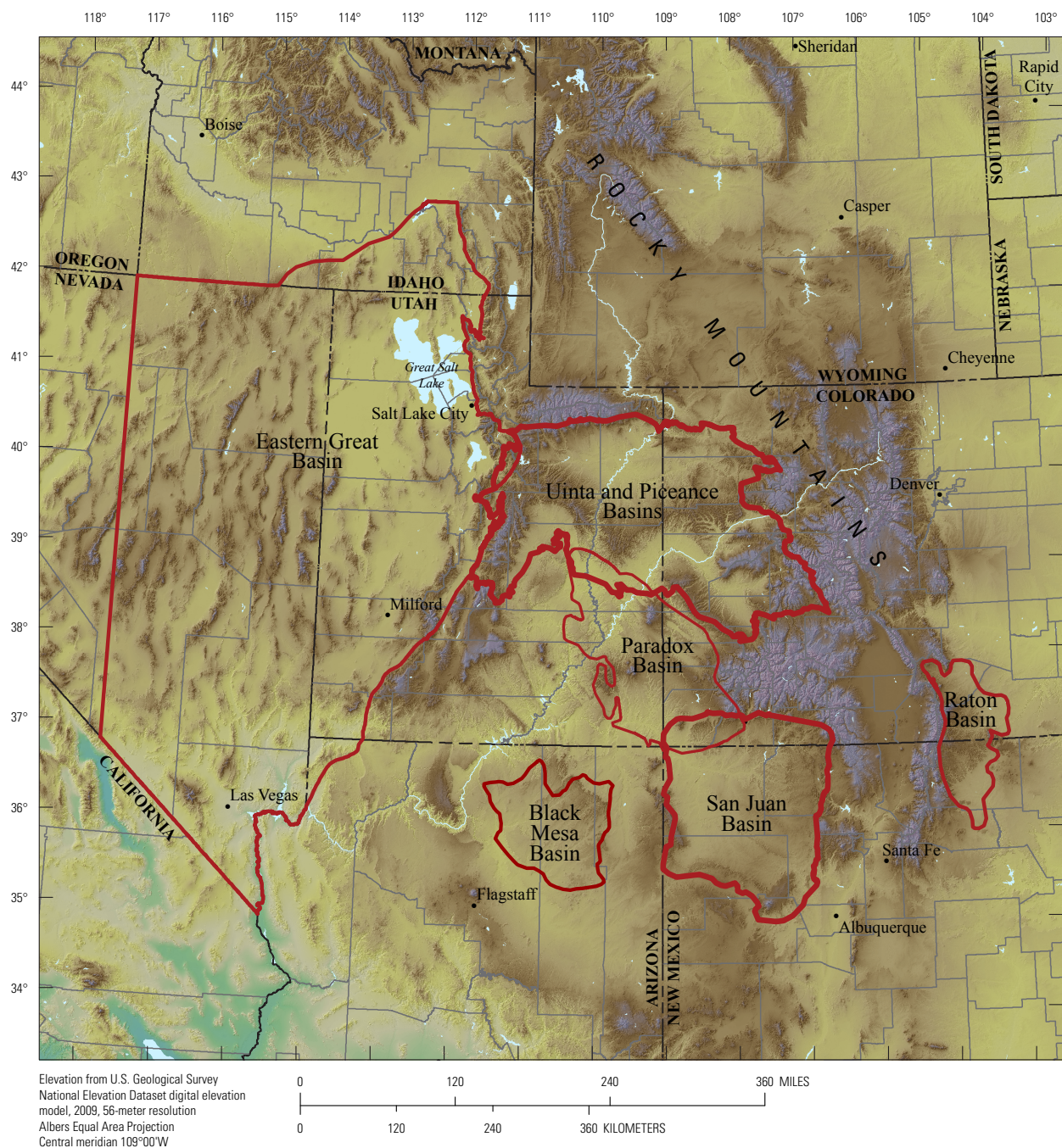
By Matthew D. Merrill, Ronald M. Drake II, Marc L. Buursink, William H. Craddock, Joseph A. East, Ernie R. Slucher, Peter D. Warwick, Sean T. Brennan, Madalyn S. Blondes, Philip A. Freeman, Steven M. Cahan, Christina A. DeVera, and Celeste D. Lohr

Abstract

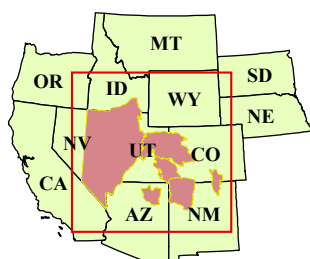
The U.S. Geological Survey has completed an assessment of the potential geologic carbon dioxide storage resources in the onshore areas of the United States. To provide geological context and input data sources for the resources numbers, framework documents are being prepared for all areas that were investigated as part of the national assessment. This report is the geologic framework document for the Uinta and Piceance, San Juan, Paradox, Raton, Eastern Great, and Black Mesa Basins, and subbasins therein of Arizona, Colorado, Idaho, Nevada, New Mexico, and Utah. In addition to a summary of the geology and petroleum resources of studied basins, the individual storage assessment units (SAUs) within the basins are described and explanations for their selection are presented. Although appendixes in the national assessment publications include the input values used to calculate the available storage resource, this framework document provides only the context and source of the input values selected by the assessment geologists. Spatial-data files of the boundaries for the SAUs, and the well-penetration density of known well bores that penetrate the SAU seal, are available for download with the release of this report.

Report Overview

This six-part U.S. Geological Survey (USGS) Open-File Report (OFR) chapter contains the geologic framework for six regionally adjacent study areas in Arizona, Colorado, Idaho, Nevada, New Mexico, and Utah: the Uinta and Piceance, Paradox, San Juan, Eastern Great, Raton, and Black Mesa Basins (fig. 1). Subbasins associated with these areas are included in this report and addressed in the basin-specific sections. The Geologic Framework for the National Assessment of Carbon Dioxide Storage Resources—Southern Rocky Mountain Basins report is chapter M of USGS OFR 2012–1024, a multiple chapter report that summarizes the geologic framework employed in the investigation of sedimentary basins for the USGS National Assessment of Geologic Carbon Dioxide Storage Resources. Complete national assessment results, other basin-framework reports, and related carbon dioxide (CO₂) sequestration investigations by the USGS are available at <http://energy.usgs.gov/EnvironmentalAspects/EnvironmentalAspectsofEnergyProductionandUse/GeologicCO2Sequestration.aspx> (U.S. Geological Survey, 2015).



EXPLANATION




 Study areas—Different line weights are used only to distinguish basins that overlap

Figure 1. Map of the southern Rocky Mountain basins of Arizona, Colorado, Idaho, Nevada, New Mexico, and Utah showing the basins that were evaluated for their geologic carbon dioxide storage potential. Major structural features are presented in the basin-specific maps. Study areas are modified from U.S. Geological Survey National Oil and Gas Assessment and other reports; citations are provided in basin-specific sections.

Uinta and Piceance Basins

By Matthew D. Merrill

Introduction

The Uinta Basin in eastern Utah and westernmost Colorado and the Piceance Basin in western Colorado formed from Late Cretaceous through Eocene time, contain sedimentary rocks ranging in age from Precambrian to Tertiary, and are bounded by basement-cored uplift features. In past U.S. Geological Survey (USGS) National Oil and Gas Assessments (NOGA), these basins have been combined and assessed together; however, for the purposes of the USGS National Assessment of Geologic Carbon Dioxide Storage Resources, the basins are also assessed as a composite. The two basins are separated by the north-south-trending Douglas Creek arch (fig. 2). Mountain ranges and structural features that bound the basins are the Uinta Mountains to the north, the Elk Mountains and White River uplift to the east, the Uncompahgre Plateau and San Rafael Swell to the south, and the Wasatch Mountains and Wasatch Plateau to the west (Dubiel, 2003).

Geologic History

Johnson (1992) provided an excellent account of the tectonic and depositional history of the Uinta and Piceance Basins region and provided a thorough explanation (with complete citations) of the evolutionary stages summarized herein; that report also supports any of the discussions on general basin evolution included throughout this assessment. Additionally, Johnson (1992) subdivided the geologic history of the region into six phases (covering Precambrian to Eocene time), each one including a period of rapid subsidence related to tectonic activity followed by a relatively stable period. This review will also refer to those stages as the basin's evolution.

Basement rocks in the study area are exposed in the surrounding mountains and underlie the Phanerozoic sedimentary rocks found in the basins (Johnson, 1992). Crystalline basement rocks in the region fall into two broad categories: (1) the northern boundary of the Uinta and Piceance Basins near the southern edge of the Wyoming province, which is an Archean craton that consists of some of the oldest continental crust in the western United States (Johnson, 1992; Lawton, 2008); and (2) the central and southern portions of the basins that represent a continental margin setting located south of the Archean craton (fig. 2). The oldest sedimentary rocks in the basins are late Proterozoic in age (1,100 to 925 million years old) (Tweto, 1987). These sediments were deposited in an east-west-trending, fault-bounded trough with a northern margin near the Archean craton suture zone. Latest late Proterozoic and early Paleozoic strata record a transition from intracontinental rifting to a passive continental margin (Johnson, 1992).

Johnson's (1992) phase 1 of basin evolution covered Cambrian to Devonian time, when the region occupied a passive margin cratonic shelf. The associated depositional environments and their resulting sediment accumulations were produced by rifting to the west. Cambrian sedimentary environments ranged from nearshore siliciclastic to offshore carbonate rocks; thicknesses increased toward the Cordilleran hingeline in the west (fig. 2). During the Ordovician, the deposition of near-shore, shallow-marine, and marine sediments continued. Silurian and Early to Middle Devonian rocks are present only west of the hingeline.

Phase 2 began with the onset of the Late Devonian Antler orogeny, which began in Nevada and possibly Idaho. The event led to an increase in subsidence as the crust thickened due to thrusting, and the former Paleozoic shelf was depressed into a retro-arc foreland basin (Speed and Sleep, 1982; Goebel, 1991). The Uinta and Piceance Basins area was largely emergent during the early stages of the orogeny, and Late Devonian rocks are only locally preserved in the area. Orogenic activity accelerated in the early Late Mississippian and subsidence rates increased in the Uinta and Piceance Basins area, resulting in the deposition of platform carbonate rocks.

Phase 3 differed from the other phases with the addition of a tectonic component from the south. The convergence of the Laurentian (North America) and Gondwanan (the African and South American continents) plates during the Early Pennsylvanian Ouachita orogeny (Kluth, 1986), the Permian assembly of the supercontinent Pangaea, and the potential effects from extensional deformation to the west (Smith and Miller, 1990) resulted in North American intraplate deformation that produced a number of "ancestral Rocky Mountain" uplifts and basins (Johnson and others, 1992).

The onset of the Sonoran orogeny in the late Permian to Triassic marked the beginning of phase 4, which was a reestablishment of a westward-thickening sediment wedge and asymmetrical foreland basin that was present during the Mississippian (Johnson, 1992). Shallow to marginal-marine redbed and evaporite deposition followed an increase in aridity and reduction in sediment input during the late Permian and Early Triassic. Phase 5 was similar to phase 4 in that the period from the Middle

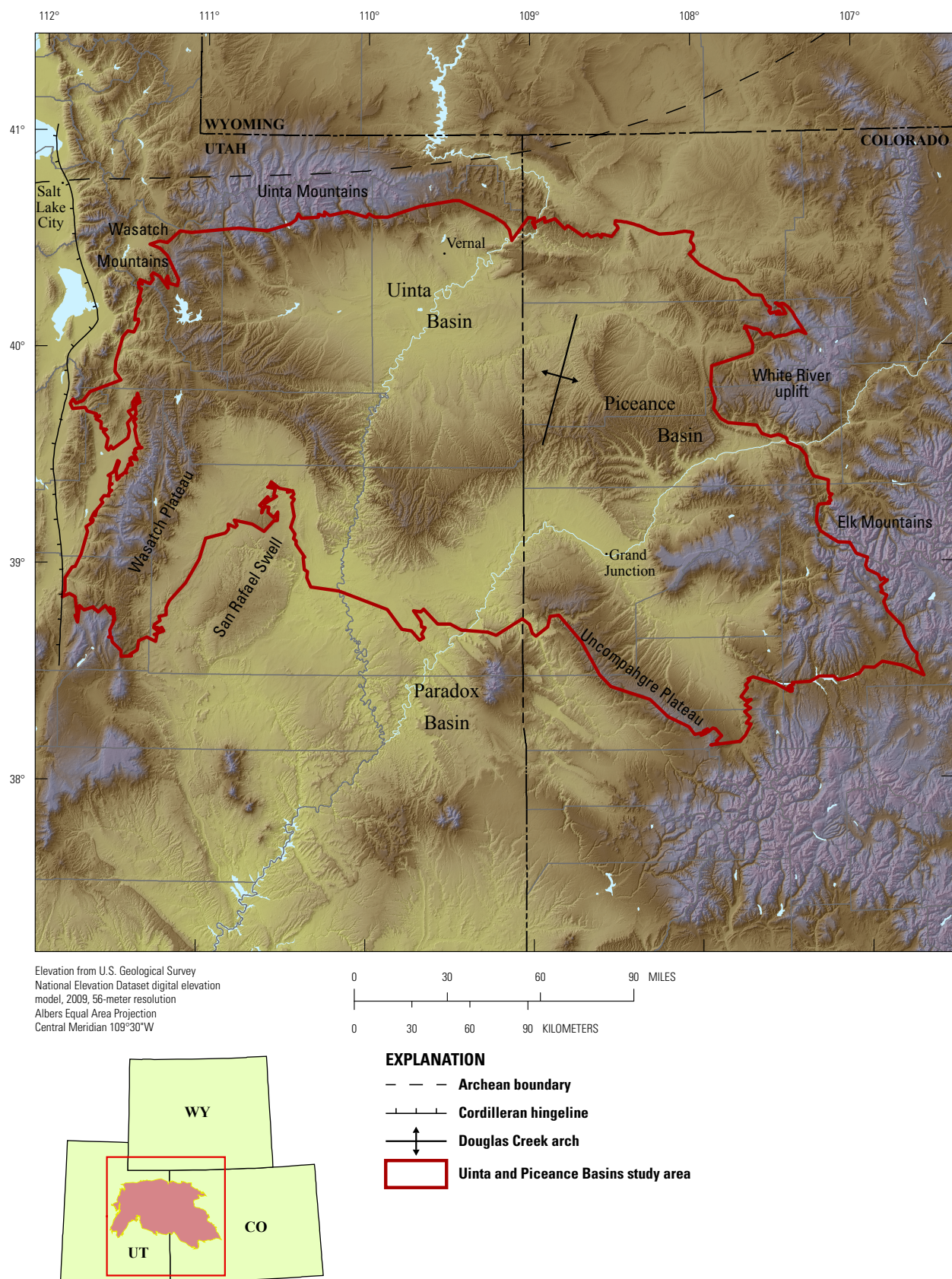


Figure 2. Map showing the Uinta and Piceance Basins study area, including major structural features (modified from U.S. Geological Survey Uinta-Piceance Assessment Team, 2003). Study area boundaries were modified from the U.S. Geological Survey National Oil and Gas Assessment (U.S. Geological Survey Uinta-Piceance Assessment Team, 2002).

Jurassic to the Early Cretaceous began with a pulse of rapid asymmetrical subsidence from thrusting during the Elko orogeny in Nevada (Thorman and others, 1991; Johnson, 1992).

The area of the Uinta and Piceance Basins entered the sixth and final phase of Johnson's geologic evolution with another period of uplift and basin filling caused by the Sevier and Laramide orogenies, which began in the Middle Cretaceous and continued into the Eocene. Lawton (2008) hypothesized that the Laramide uplifts (within the study area and beyond) occurred along basement-rooted faults commonly associated with Precambrian and late Paleozoic structural zones. Deposition in a foreland basin setting through the Cretaceous shifted by the beginning of the Paleogene to intermontane basin deposition as the Western Interior Seaway drained and the Laramide uplifts rose. Freshwater lacustrine, paludal, and alluvial environments dominated the two basins until about 52 Ma (mega-annum), when a large saline lake, Lake Uinta, expanded to cover much of the Uinta and Piceance Basins and the Douglas Creek arch (Johnson, 1985). By the latest Eocene to early Oligocene, the Laramide orogeny had ended and Lake Uinta was filled with sediment. Miocene and Holocene volcanism in the region is thought to be related to Basin and Range as well as Rio Grande rift extension. Uplift surrounding the basins began in the middle Miocene and established the modern drainage systems present today.

Hydrocarbon Exploration and Production

The Uinta and Piceance Basins are mature oil- and gas-producing provinces that have been under active exploration since the early 1900s and began major production in the 1920s and 1930s (Bowker and Jackson, 1989). As of 2008, the total production in the composite basin was 1,575 million barrels of oil (MMBO) with reserves of 253 MMBO and 9,507 trillion cubic feet of gas (TCFG) with reserves of 15,991 TCFG (Nehring Associates Inc., 2010). The Permian Weber Formation, Cretaceous Mesaverde Formation, and Eocene Wasatch and Green River Formations are major historical producers with future potential greatest in unconventional reservoirs such as tight gas and coal-bed gas in Cretaceous and Paleogene strata (U.S. Geological Survey Uinta-Piceance Assessment Team, 2002).

The USGS assessed potential undiscovered hydrocarbons in the Uinta and Piceance Basins in 2002 (U.S. Geological Survey Uinta-Piceance Assessment Team, 2002). Potential undiscovered resources totaled 20.39 MMBO and 213.12 TCFG and were calculated through the investigation of individual total petroleum systems (TPS). A TPS includes the source of hydrocarbons, as well as their maturity, migration pathways, reservoir rocks, and sealing formations (Magoon and Dow, 1994). NOGA geologists defined five TPSs in the Uinta and Piceance Basins, which include the Phosphoria, Mancos/Mowry, Ferron/Wasatch, Mesaverde, and Green River. The data collection and research required to conduct the NOGA work was also essential to the CO₂ storage assessment process; therefore, USGS NOGA data and publications are heavily cited in this report.

Carbon Dioxide Storage Assessment

The USGS Geologic Carbon Dioxide Storage Resources Assessment Team investigated and ultimately assessed five storage assessment units (SAUs) (fig. 3). A mix of Devonian through Permian sandstone and carbonate lithologies are sealed by the Park City and Phosphoria Formations and constitute the units of the Paleozoic Composite (C50200101) and Paleozoic Composite Deep (C50200102) SAUs. Sandstones in the Cedar Mountain Formation, Dakota Sandstone, Ferron Sandstone Member of the Mancos Shale, and Frontier Formation, all of which are sealed by the Mancos Shale, are included in the Lower Cretaceous Composite (C50200103) and Lower Cretaceous Composite Deep (C50200104) SAUs. The fifth SAU is the Green River Formation (C50200105), which has storage formations in the North Horn Formation, Flagstaff Limestone, and Colton Formation and is sealed by the basal Garden Gulch Member of the Green River Formation.

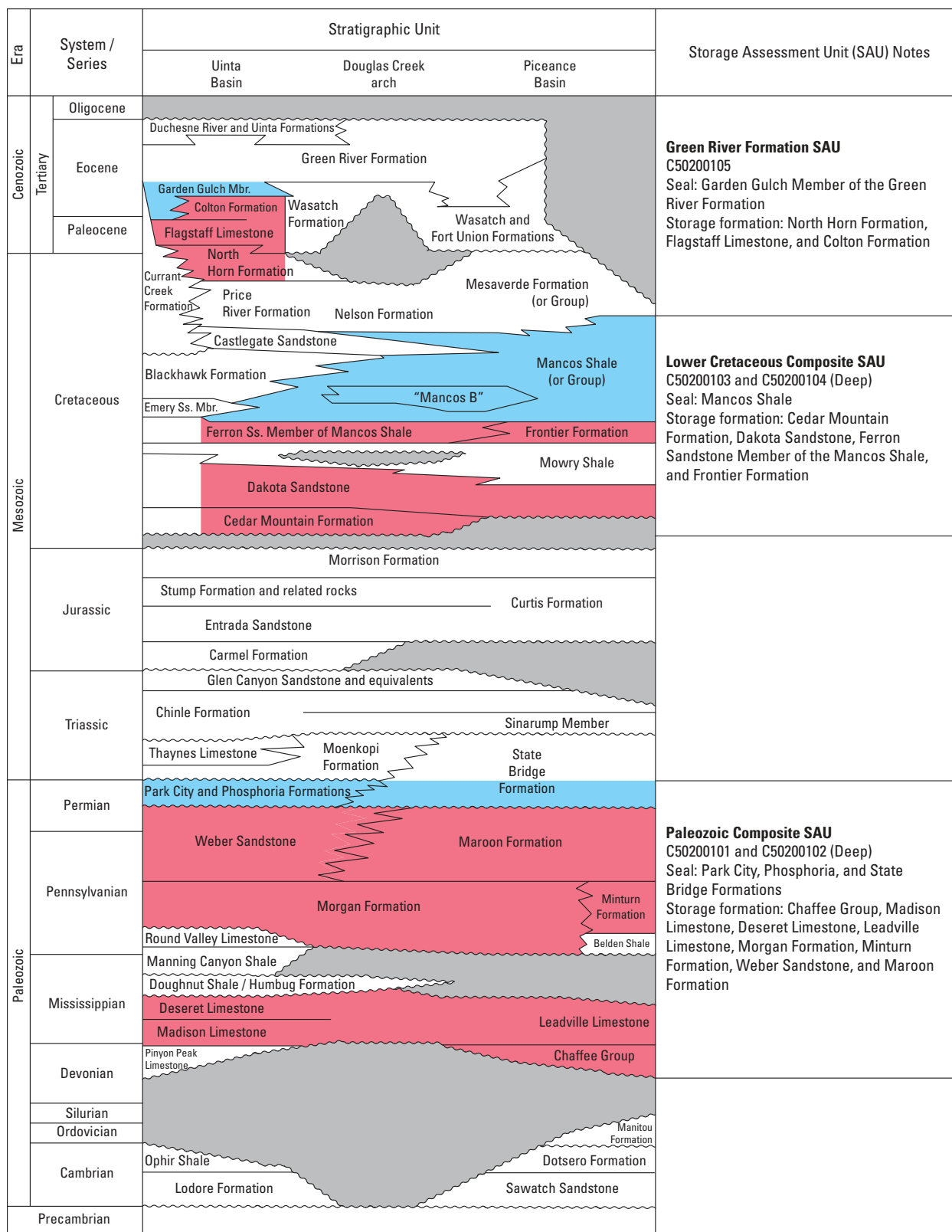


Figure 3. Generalized stratigraphic column of geologic units in the Uinta and Piceance Basins study area of Utah and Colorado (modified from U.S. Geological Survey Uinta-Piceance Assessment Team, 2003). Storage assessment units (SAUs) consist of a storage formation (red) and regional seal (blue). Wavy lines indicate unconformable contacts, and gray areas represent unconformities or hiatuses. Only significant unconformities are shown. In some cases, subdivisions of units or lesser known correlative units are not shown. Abbreviations: Mbr., Member; Ss., Sandstone.

Paleozoic Composite SAU C50200101 and Paleozoic Composite Deep SAU C50200102

By Marc L. Buursink

The Paleozoic Composite SAU and Paleozoic Composite Deep SAU include only those portions of the preserved Upper Devonian to Permian geologic section deemed suitable as storage formations for CO₂ storage. The SAUs are located beneath a regionally extensive seal in the Uinta and Piceance Basins study area (fig. 2). The suitable storage formation rocks consist of siliciclastic and carbonate lithologies and include, in ascending stratigraphic order, (1) the Chaffee Group in the Piceance Basin, (2) the Madison and Deseret Limestones in the Uinta Basin and the correlative Leadville Limestone in the Piceance Basin, and (3) the Morgan Formation and Weber Sandstone in the Uinta Basin and the Minturn and Maroon Formations in the Piceance Basin (Tremain, 1993; Johnson, 2003; Johnson and Roberts, 2003) (fig. 3). Regionally, the Phosphoria Formation black shale and its stratigraphic equivalents, the Park City and State Bridge Formations, overlie the Weber Sandstone and function as the sealing formations (Rascoe and Baars, 1972; Bowker and Jackson, 1989; Maughan, 1994; Johnson, 2003). The Devonian Pinyon Peak Limestone in the Uinta Basin consists of shaly limestone about 150 feet (ft) thick (Loughlin, 1919) and was not included as a storage formation in this composite SAU, nor were Cambrian formations included due to storage formation quality and data availability limitations. The Late Devonian Chaffee Group includes the Parting and Dyer Formations and is the basal storage formation. The Parting Formation, a highly variable transgressive unit, is generally a quartzose sandstone that coarsens to the east, suggesting a primary source in the vicinity of the northern Front Range. The Parting grades westward and southward into arenaceous shale with some dense dolostone. The Dyer Formation consists of a lower fossiliferous limestone and an upper stromatolitic dolostone (Baars, 1972).

The Mississippian Leadville Limestone consists of limestone and dolostone, probably represents a single depositional history, and was deposited during the maximum extent of the third Paleozoic marine transgression (Geldon, 2003a). The equivalent Deseret Limestone name is commonly used by industry in well logs and seismic data interpretation (Potter and others, 1991). The Morgan Formation in the Piceance Basin, a sequence of sandstones with intercalated shale and crystalline marine limestone, is likely derived from the ancestral Front Range. The Morgan is about 950 to over 1,500 ft thick, and unconformably overlies Mississippian rocks (Brill, 1944). The Minturn Formation is divided into a lower zone of conglomerate, sandstone, and discontinuous carbonate rocks; a middle zone of marine carbonate rocks; and an upper zone of widely spaced carbonate rocks separated by sandstone and conglomerate; it ranges from about 1,600 to 5,800 ft thick (Murray, 1958). The Middle Pennsylvanian through lower Permian Weber Sandstone is a prolific oil producer in the Uinta and Piceance Basins study area. The eolian sandstone is present in the subsurface throughout the northern part of the study area and is overlain by the Permian to Triassic State Bridge Formation, which acts as the storage formation's top seal (Bowker and Jackson, 1989). Along its eastern, southeastern, and southern depositional margins, the Weber interfingers with the Middle Pennsylvanian through lower Permian Maroon Formation, and toward the southwest and west the Weber includes an increasing amount of marine carbonate rocks (Johnson, 2003). The Weber thins toward the east and is about 370 ft thick near Meeker, Colorado, where it rests conformably on the Lower and Middle Pennsylvanian Morgan Formation, and is unconformably overlain by the lower Permian Phosphoria or Park City Formations (Johnson, 2003).

The Paleozoic Composite SAU and Paleozoic Composite Deep SAU boundaries are defined by the top of the uppermost storage formation and by the extent of the regional seal (fig. 4). Formation top depths reported in a commercial database (IHS Energy Group, 2010) for the Weber Sandstone helped to define the top depth of the storage interval. The Paleozoic Composite SAU occurs at depths between 3,000 and 13,000 ft with a most-likely areal extent of about 1.7 million acres; and the Paleozoic Composite Deep SAU lies at depths between 13,000 and 20,000 ft with a most-likely areal extent of about a 1.2 million acres. These interpretations are supported by field-scale structure-contours maps (Hefner and Barrow, 1992; Chidsey and Sprinkel, 2005) and are supplemented by cross sections (Hefner and Barrow, 1992; Johnson and Roberts, 2003). To assess the composite SAU gross storage formation interval, isopach maps (Mallory, 1972; Geldon, 2003a) of storage formations within the SAU were scanned, geo-referenced, and digitized. Next, the thickness values were scaled by a unique net-to-gross ratio for each formation that was derived from the literature and well logs (Bowker and Jackson, 1989; Johnson, 2003). Finally, using a geographic information system (GIS), the net-porous storage formation interval of the composite SAU was summed (Buursink and others, 2011). The Paleozoic Composite SAU gross storage formation thickness ranges from 2,500 to 4,000 ft, and the net storage formation thickness varies between 500 and 1,200 ft. The Paleozoic Composite Deep SAU gross storage formation thickness ranges from 2,500 to 4,500 ft, and the net storage formation thickness varies between 600 and 1,100 ft.

The Paleozoic interval in the Uinta and Piceance Basin is a prolific hydrocarbon producer and thus sufficient well-log and core data exist for characterizing reservoir quality. Porosity and permeability trends for individual storage formations within the composite SAUs were derived from multiple sources including Bowker and Jackson (1989) and the USGS Regional Aquifer-System Analysis work (Geldon, 2003b); average field values are extracted from Nehring Associates Inc. (2010), a commercial

oil and gas database. The Paleozoic Composite SAU porosity for the net porous interval ranges from 6 to 14 percent and permeability ranges from 0.01 to 200 millidarcys (mD). The Paleozoic Composite Deep SAU porosity ranges from 5 to 10 percent and permeability ranges from 0.0001 to 1 mD. The occurrence and distribution of these reservoir properties in the composite SAUs is generally a function of the storage formation's lithology and depth.

The storage capacity of an SAU is also affected by the formation's water quality and buoyant trapping potential. Water-quality data obtained from published databases (Breit, 2002) and maps (Geldon, 2003b) indicate areas with either fresh or saline waters in the SAU. Areas exist in each SAU where the total dissolved solids (TDS) of the groundwater is either under or above the underground sources of drinking water (USDW) maximum limit of 10,000 parts per million (ppm) defined by the U.S. Environmental Protection Agency (2009). Generally, the TDS in groundwater increases slightly with depth in the SAU.

To generate a probabilistic maximum volume for buoyant trapping for each SAU, structure contours of closure, hydrocarbon exploration and production data (including play descriptions by Hemborg, 1993, and Spencer, 1995), and the average field size from Nehring Associates Inc. (2010) were tabulated along with the mean average porosity and net porous thickness for the Paleozoic Composite SAU. For the Paleozoic Composite Deep SAU, a similar process was followed, though field areas were modelled using shallower depth analogs.

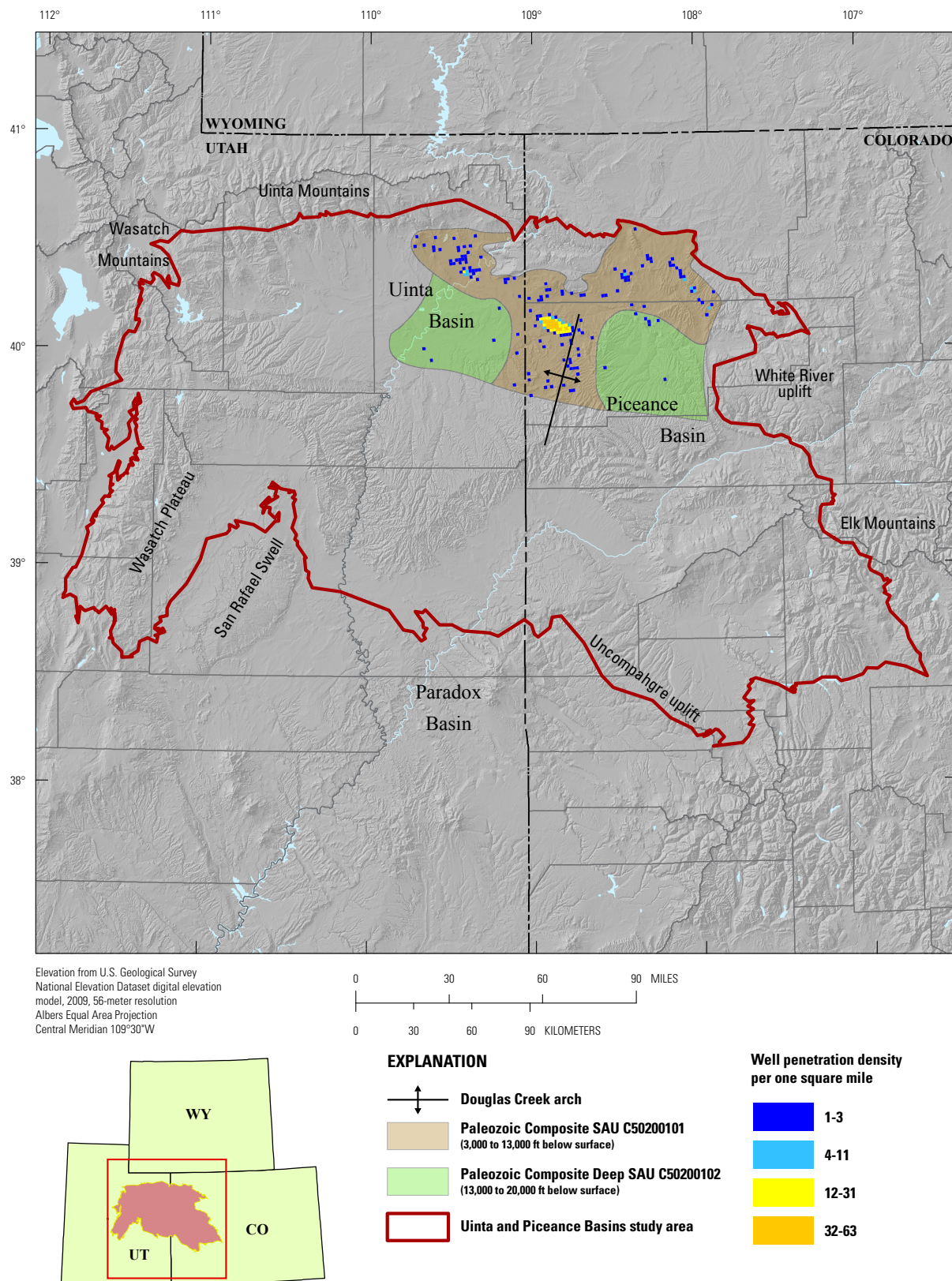


Figure 4. Map of the Paleozoic Composite C50200101 and Paleozoic Composite Deep C50200102 Storage Assessment Units (SAUs) in the Uinta and Piceance Basins. Well penetration density is the number of wells (per 1-square-mile grid cell) derived from the ENERDEQ well database (IHS Energy Group, 2011) that have penetrated the top of the storage formation. Study area boundaries were modified from the U.S. Geological Survey National Oil and Gas Assessment (U.S. Geological Survey Uinta-Piceance Assessment Team, 2002). Abbreviation: ft, feet.

Lower Cretaceous Composite SAU C50200103 and Lower Cretaceous Composite Deep SAU C50200104

By Matthew D. Merrill

The Lower Cretaceous sandstones in the Uinta and Piceance Basins are (in ascending order) the Cedar Mountain Formation, Dakota Sandstone, Ferron Sandstone Member of the Mancos Shale on the Wasatch Plateau, and Frontier Formation (fig. 3). All are included in the Lower Cretaceous Composite (C50200103) and Lower Cretaceous Composite Deep (C50200104) SAUs (fig. 5). The Cedar Mountain Formation is a minor lacustrine and fluvial sandstone, whereas the Dakota Sandstone is composed of sandstones from fluvial, shoreface, and tidally influenced environments (Kirschbaum, 2003). In the San Rafael Swell, an area in the southwest of the composite basin (fig. 2), the Dakota Sandstone consists of two major units (1) a lower amalgamated sandstone with large-scale cross stratification and numerous individual sand bodies, and (2) an upper unit of mud-encased, lenticular sandstones in bed sets that are 5 to 12 ft thick (Kirschbaum and Schenk, 2011). The depositional environment of the Ferron Sandstone Member of the Mancos Shale in the San Rafael Swell and Wasatch Plateau was described by Anderson and Ryer (2004) as a wave-dominated, fluvial deltaic setting. The Frontier Formation is of similar age as the Ferron Sandstone Member, but located in the central portion of the basin. Silts of the Frontier were deposited in a distal shoreface environment (Kirschbaum, 2003). The Mancos and Mowry Shales are thick (in excess of 3,000 ft; Roberts, 2003), dark-gray to black, calcareous and bentonitic shales deposited in the ancestral Mowry Sea of the Western Interior Seaway (Kirschbaum, 2003). The Mancos Shale is the major sealing unit for the sandstone storage formations of the two SAUs; however, the Mowry Shale could provide additional sealing potential though it is not required to seal the SAU.

Two factors determined whether a target storage formation was included in either of the Lower Cretaceous SAUs and determined their boundaries (fig. 5). The first, was whether the depth from the surface to the top of the storage formation was greater than 3,000 ft. The second, was whether the storage formation was overlain by adequate confining shale in the sealing formations. The depth to the storage formations included in the shallower Lower Cretaceous Composite SAU ranges from 3,000 to 13,000 ft, with a mean depth of 7,250 ft; the area of the SAU is approximately 7,500,000 acres. The depth to the storage formations included in the Lower Cretaceous Composite Deep SAU ranges from 13,000 to 28,000 ft, with a mean depth of 15,000 ft; the area of the SAU is 3,777,000 acres. For more information on the characteristics used to define the SAUs, refer to the preface or to Brennan and others (2010) and Blondes and others (2013).

Determining the SAU-wide storage formation thicknesses for either of the SAUs was complicated by the highly variable thicknesses of the sandstone formations, particularly where the addition of the Ferron in the southwest adds considerable thickness. A GIS-based calculation subtracting various well tops from the IHS database (IHS Energy Group, 2010), and isopach maps from Henry and Finn (2003), resulted in a range of gross thicknesses from 200 to 500 ft, and 80 to 140 ft, respectively, for the net porous thickness of the storage formation. For the deep SAU, the gross and net thicknesses were determined to be 140 to 500 ft and 28 to 100 ft, respectively. Net thickness data came from published hydrologic and geologic reports by Tripp (1989) and Freethy and Cordy (1991).

The porosity and permeability of the storage formations within the boundaries of each SAU are from published hydrocarbon fields reports and databases. The porosity for the standard SAU (Lower Cretaceous Composite SAU) ranges from 10 to 18 percent and permeability ranges from 0.01 to 100 mD, and the porosity for the deep SAU (Lower Cretaceous Composite Deep SAU) ranges from 5 to 10 percent and permeability ranges from 0.001 to 10 mD (Noe, 1993; Sprinkel, 1993; Nehring Associates Inc., 2010).

In the standard SAU, water-quality data suggest that the total dissolved solids (TDS) in the formation waters range from above to below the Environmental Protection Agency (EPA) USDW maximum limit of 10,000 ppm; approximately 50 percent of the standard SAU contains saline water that is acceptable for storage purposes (>10,000 ppm TDS) (Freethy and Cordy, 1991; Breit, 2002; Blondes and Gosai, 2011). In the deep SAU, the surface area with saline waters suitable for storage increases to 60 percent.

The boundaries, thicknesses, rock properties, and water-quality information mentioned above were applied to define the assessed areas in accordance with the USGS CO₂ sequestration assessment methodology (Brennan and others, 2010), and were used to calculate the available storage space within the Lower Cretaceous Composite (C50200103) and Lower Cretaceous Composite Deep (C50200104) SAUs.

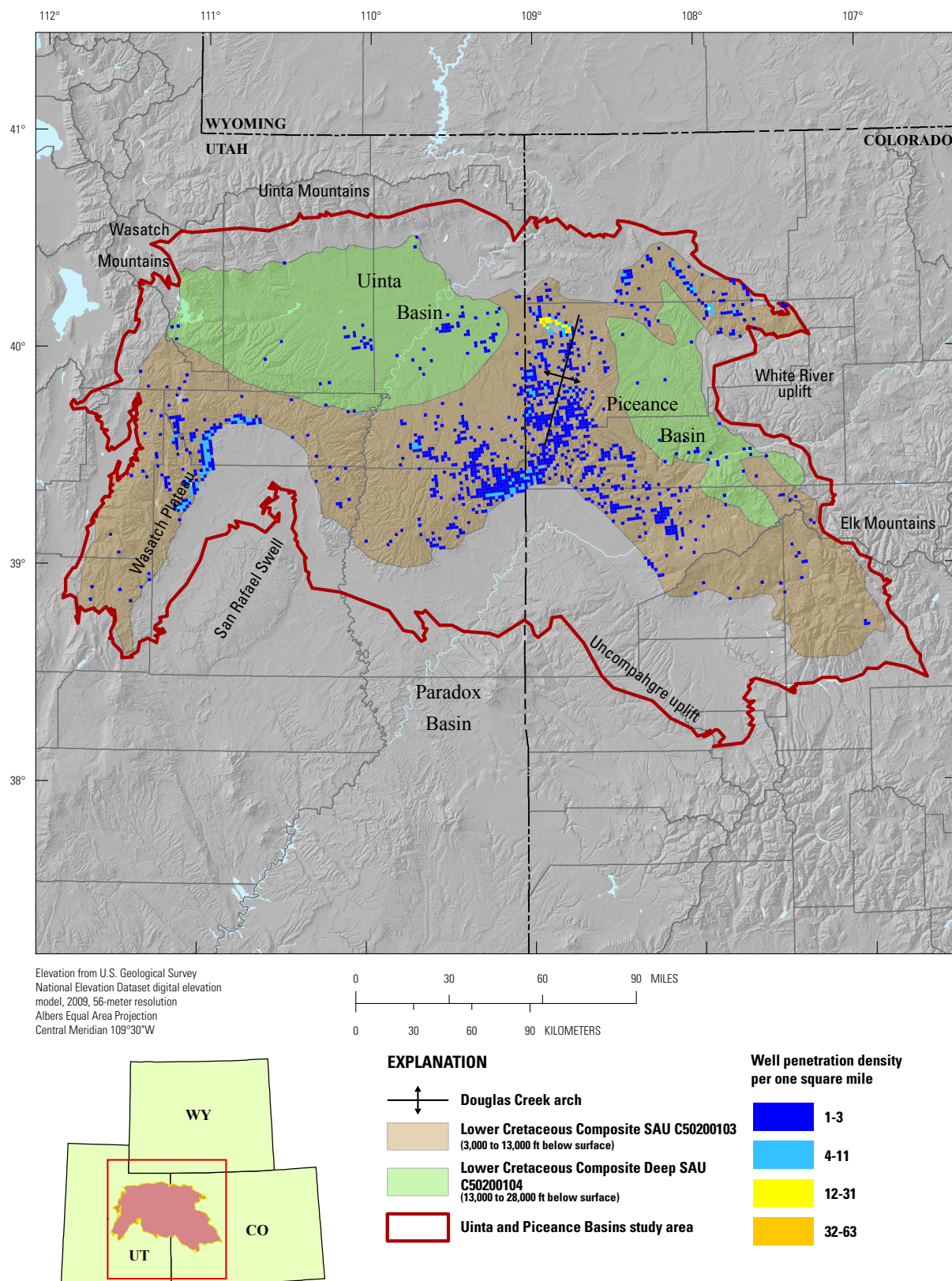


Figure 5. Map of the Lower Cretaceous Composite C50200103 and Lower Cretaceous Composite Deep C50200104 Storage Assessment Units (SAUs) in the Uinta and Piceance Basins. Well penetration density is the number of wells (per 1-square-mile grid cell) derived from the ENERDEQ well database (IHS Energy Group, 2011) that have penetrated the top of the storage formation. Study area boundaries were modified from the U.S. Geological Survey National Oil and Gas Assessment (U.S. Geological Survey Uinta-Piceance Assessment Team, 2002). Abbreviation: ft, feet.

Green River Formation SAU C50200105

By Joseph A. East

The Green River Formation SAU C50200105 is located only within the Uinta Basin portion of the Uinta and Piceance Basins study area in Utah (fig. 6). Failure to satisfy SAU minimal depth requirements established in the USGS's assessment methodology (Brennan and others, 2010) limited the SAU to the Uinta Basin where the depth to the bottom of the seal was greater than 3,000 ft. The SAU's extent was further refined using geophysical well logs to confirm the shale thickness in the sealing formation. The SAU's seal is the Eocene Garden Gulch Member of the Green River Formation and equivalent units at the base of the Green River Formation (fig. 3). The Garden Gulch is a deep-water lacustrine shale that covers much of the Uinta Basin, including all of the SAU (Johnson, 1985; Dubiel, 2003).

The Green River Formation SAU storage formation rocks are Late Cretaceous to Eocene in age. The rocks were deposited in ancestral Lake Flagstaff, a Paleocene and Eocene lake formed by changes in fluvial drainages following the waning foreland thrusting of the Sevier orogeny and, to a lesser extent, Laramide basement uplifts (Stanley and Collinson, 1979). Lake Flagstaff occupied the eastern flank of the Wasatch Plateau and extended northward and eastward into the trough of the Uinta Basin south of the Uinta Mountains. Storage formations include porous rocks in the North Horn and Colton Formations, and the intervening Flagstaff Limestone. Formation names in this report follow those used by Dubiel (2003) and the stratigraphic references therein, primarily Fouch (1975), Johnson (1985, 1989), and Fouch and others (1994).

Shifting alluvial and lacustrine depositional environments during the Paleocene and Eocene have resulted in the interfingering of formations, the occurrence of tongues, and numerous stratigraphic pinch outs in the units of this SAU (Johnson, 1989; Dubiel, 2003). The North Horn Formation was deposited in primarily fluvial and fluvial to lacustrine environments dominated by clastic sediment from the Cretaceous (Maastrichtian) to the Paleocene (Olsen, 1995). Although subdivided into different intervals by Olsen (1995), for the purpose of this report the formation can be described as a commonly sand-dominated unit with significant amounts of mudstone and carbonate rocks. The late Paleocene to early Eocene fluvial and alluvial Colton Formation includes both a sand-dominated facies in the southern Uinta Basin and a mud-dominated facies in the central and northern part of the basin (Ryder and others, 1976; Zawiskie and others, 1982). Colton sandstones were deposited in a moderate-sinuosity stream and low-sinuosity distributary setting (Zawiskie and others, 1982). The Flagstaff Limestone on the Wasatch Plateau and western Uinta Basin, includes limestone, dolostone, sandstone, chert, and gypsum deposited in a lacustrine setting; the formation was further divided by Stanley and Collinson (1979), but those specific members are not described here.

Basal depths of sand-free shales that are thicker than 50 ft and are at depths from the surface greater than 3,000 ft, were determined from formation tops data and used as an initial step in defining the SAU's boundary. The depth of the SAU from the surface ranges from 3,000 ft to a maximum of 10,000 ft, with a mean depth of 5,500 ft. The areal extent of the SAU is 1,137,000 acres (fig. 6). Isopach maps of the SAU were calculated from formation tops data in a proprietary internal database (IHS Energy Group, 2010). The mean SAU gross thickness is estimated to be 5,500 ft, with a maximum thickness of 6,000 ft and a minimum of 5,000 ft. The net porous thickness of the SAU for storage was calculated by determining the percentage of sand within the SAU storage formation interval. Geophysical logs from Dubiel (2003) for wells that penetrated the SAU were digitized and the percentage of sand and the thickness were extracted from the total volume. The average calculated porous sand content was 36 percent and that ratio was applied to the SAU gross thicknesses to determine the average net porous thickness of 1,980 ft, with a minimum porous thickness of 1,800 ft and a maximum of 2,160 ft. Sandstone porosity values from a proprietary database suggest that storage formations in the SAU exhibit an average of 9 percent porosity, with a minimum of 5 percent and a maximum of 12 percent (Nehring Associates Inc., 2010). Data from the 2003 USGS NOGA in the Uinta and Piceance Basins indicate that the porosity in the SAU's storage formations averages 5 percent and ranges from 3 to 10 percent. Permeability data for the SAU from the Nehring Associates Inc. (2010) database are limited to 3 data points ranging from 0.1 to 28 mD. The 2003 USGS assessment of the Green River Formation TPS observed that the sands of the SAU's storage formations have core-derived matrix permeability values near and commonly below 0.1 mD (Dubiel 2003). Permeability for the assessment was calculated at 0.1 mD as the most likely, 0.001 mD as the minimum, and 28 mD as the maximum. Water-quality measurements in the SAU were both above and below 10,000 ppm TDS (Breit, 2002). Approximately 35 percent of the areal extent of the SAU contains storage formation rocks with groundwater above the EPA's (2009) 10,000 ppm TDS threshold, but this could range from a maximum of 80 percent to a minimum of 20 percent of the SAU. The boundaries, thicknesses, rock properties, and water-quality information mentioned above were used in accordance with the USGS geologic CO₂ storage assessment methodology (Brennan and others, 2010) to calculate the available storage space within the Green River Formation SAU C50200105.

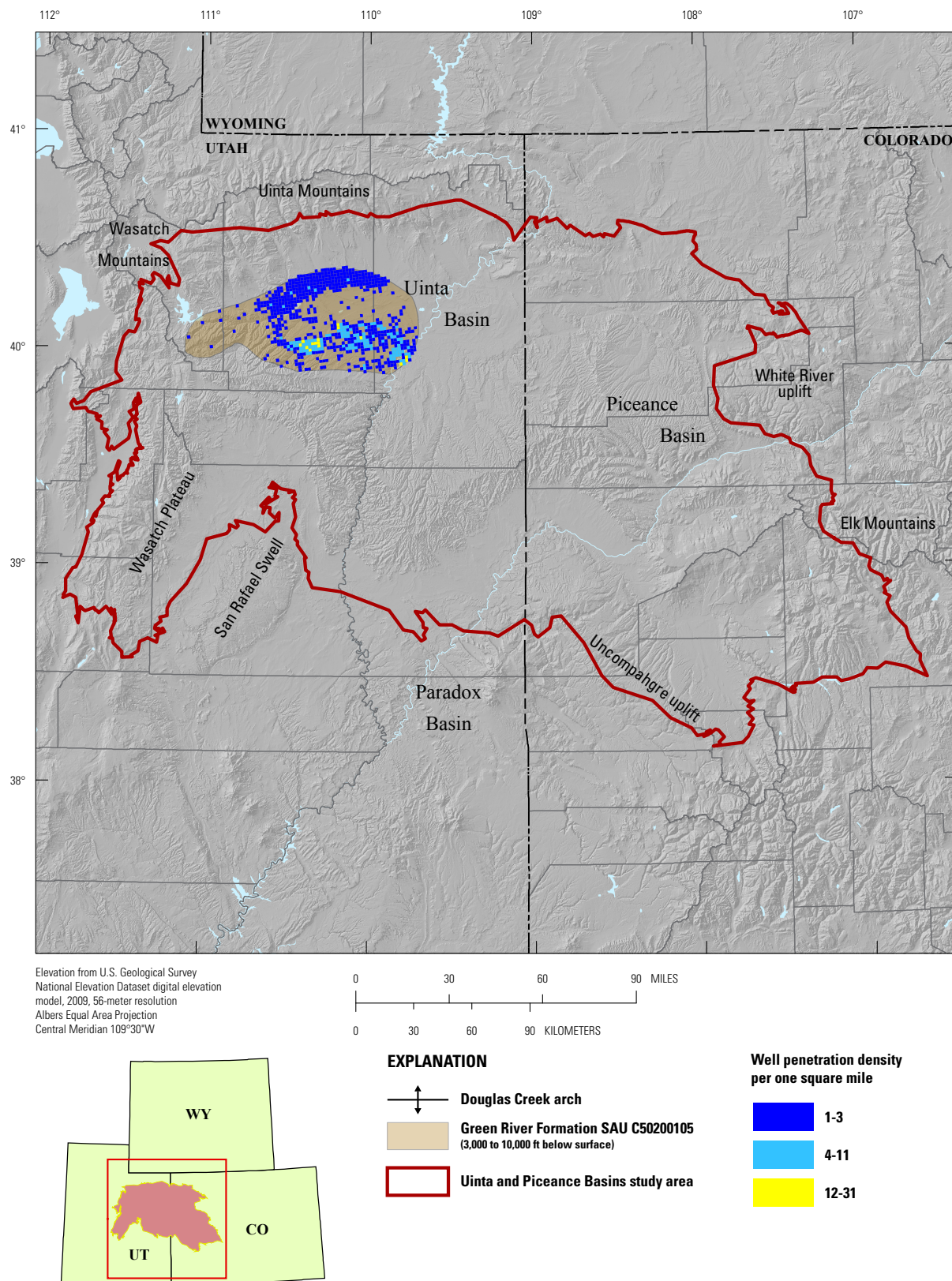


Figure 6. Map of the Green River Formation C50200105 Storage Assessment Unit (SAU) in the Uinta and Piceance Basins. Well penetration density is the number of wells (per 1-square-mile grid cell) derived from the ENERDEQ well database (IHS Energy Group, 2011) that have penetrated the top of the storage formation. Study area boundaries were modified from the U.S. Geological Survey National Oil and Gas Assessment (U.S. Geological Survey Uinta-Piceance Assessment Team, 2002). Abbreviations: ft, feet.

Paradox Basin

By Marc L. Buursink

Introduction

The Paradox Basin study area is located in southeastern and south-central Utah and southwestern Colorado (fig. 7). The study area boundary has been generally defined by the geographic extent of evaporite rocks within the Middle Pennsylvanian Paradox Formation (Nuccio and Condon, 1996; Huntoon and others, 2002), not by the USGS NOGA Paradox Basin Province boundary, which follows State and county lines and river channels (Huffman, 1995a). The basin has a northwest-to-southeast length of about 190 miles (mi), and a northeast-to-southwest width of about 95 mi (Nuccio and Condon, 1996). The region surrounding the study area includes the Paradox fold and fault belt, the Blanding Basin, and the Four Corners platform (fig. 7). It is bounded to the northeast by the Uncompahgre Plateau, to the southwest by the Monument upwarp, and to the northwest by the San Rafael Swell, although the southern and southwestern border of the Paradox Basin is poorly defined topographically and structurally (Nuccio and Condon, 1996). The far northern end of the basin merges with the southern part of Uinta Basin, the San Juan Basin is located to the southeast, and the Henry Mountains Basin is located to the west (fig. 7).

The Paradox fold and fault belt in the northern part of the study area consists of a series of roughly parallel, northwest-trending faults, anticlines, and synclines (Kelley, 1958; Nuccio and Condon, 1996) (fig. 7). The basin is asymmetric, with the deepest portion along this northeastern border adjacent to the modern Uncompahgre Plateau in Utah and Colorado; the plateau represents a present-day Laramide structure occupying the location of the Middle Pennsylvanian Uncompahgre uplift, a broad anticline cored by Precambrian rocks in the Ancestral Rocky Mountains that was completely eroded by Cretaceous time (Huntoon and others, 2002). The Blanding Basin and the Four Corners platform are located south of the fold and fault belt (fig. 7); the Blanding Basin is a generally undeformed area with Jurassic and Cretaceous rock outcrops, and the Four Corners platform is a structural high separating the Paradox and San Juan Basins with Cretaceous rock outcrops (Nuccio and Condon, 1996). The Monument upwarp southwest of the Paradox Basin is a broad, generally north-trending anticline consisting of deep canyons and high mesas. Within or around the Paradox Basin are Late Cretaceous to Tertiary intrusive rocks of the La Sal, Abajo, and Sleeping Ute Mountains (Nuccio and Condon, 1996).

Geologic History

The Paradox Basin and the Uncompahgre Plateau originated in the late Paleozoic from intraplate stresses caused by the collision of the ancestral continents Gondwana and Laurentia (Barbeau, 2003; Kluth and DuChene, 2009). The basin subsided rapidly and accumulated as much as 9,000 ft of Middle and Upper Pennsylvanian evaporites, clastic rocks (mainly shale), and carbonate rocks (which unconformably overlie the basement throughout much of the basin) and then accumulated about 6,000 ft of Permian marine and continental sediments (Nuccio and Condon, 1996; Huntoon and others, 2002) (fig. 8). Specifically, the interbedded shale and salt were eroded from the Uncompahgre uplift and were deposited along the northern basin margin, whereas gypsum and marine carbonate rocks precipitated from hypersaline waters along the gently dipping southwestern basin margin and interfingered with the shale and salt deposits (Huntoon and others, 2002; Whidden, 2012). Marine waters that replenished the salt supply entered the Paradox Basin from several structural sags to the south, including the paleo-San Juan Basin, where carbonate rocks of Pennsylvanian age are thick (Baars and Stevenson, 1981).

During the Triassic and Jurassic, continental deposition in mainly lacustrine, fluvial, and eolian environments dominated in the Paradox Basin study area (Huntoon and others, 2002). Deposition on alluvial fans and other clastic environments resulted in differential loading of the Pennsylvanian salt accumulation and initiated the formation of salt anticlines. The Paradox Basin study area lay near the west coast of the ancestral continent Pangea from the Pennsylvanian to the Jurassic, which was a critical location that recorded a sedimentary record of an evolving tropical and monsoonal climate (Dubiel and others, 1996). Some Cretaceous rocks are present in the southeastern part of the basin, whereas Tertiary rocks have been completely eroded except for the igneous intrusive centers (Nuccio and Condon, 1996). Later tectonics, including the Laramide orogeny, have modified and covered areas of the oval-shaped basin; and the relatively recent uplift of the Colorado Plateau and erosion by the Colorado and Green Rivers have dissected the basin (Nuccio and Condon, 1996). Nevertheless, data are complete enough to construct isopach maps for the Cambrian through Jurassic units in the basin. For additional details on Paradox Basin geology, the reader is referred to Peterson (1989) and Huffman and others (1996).

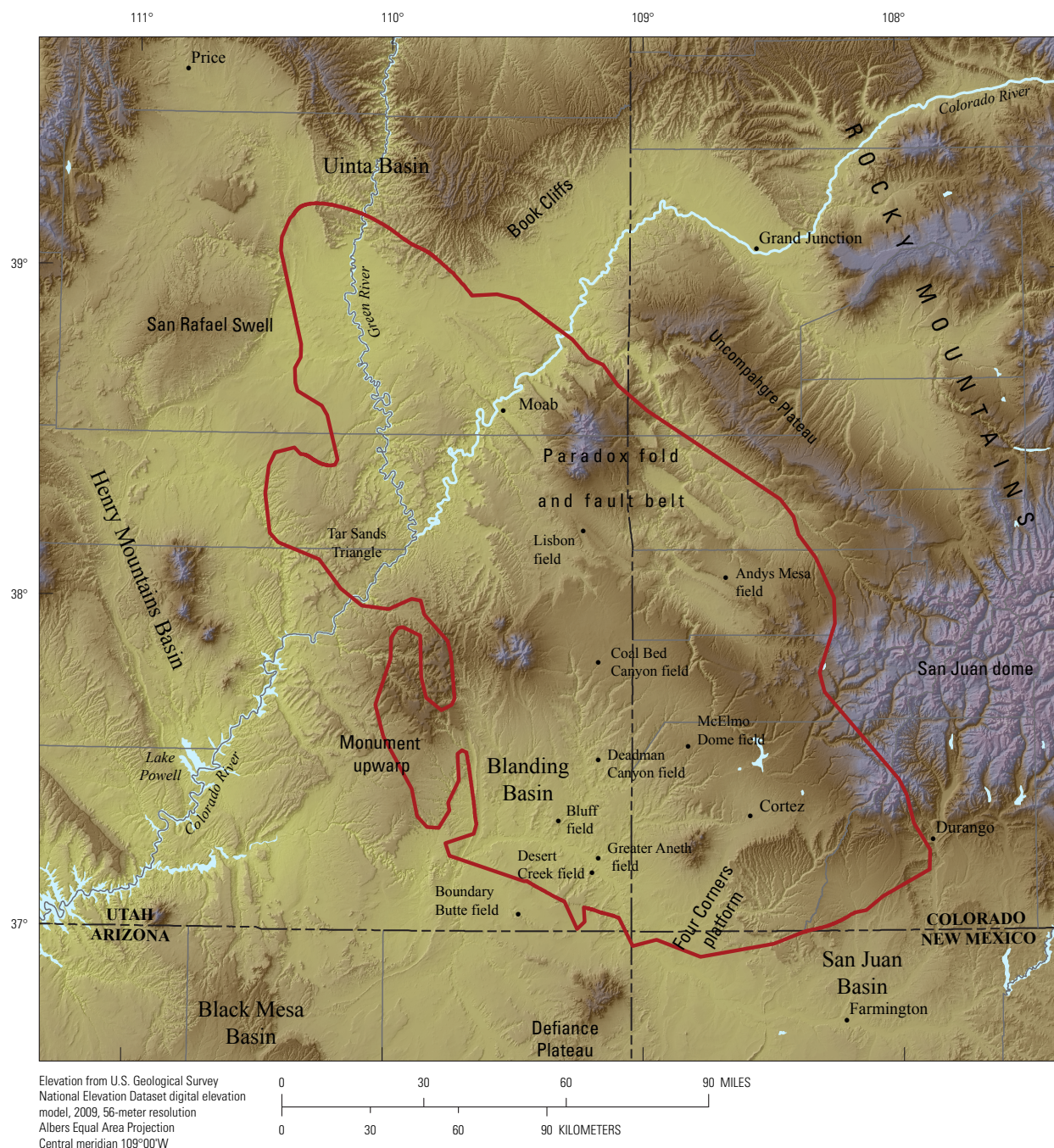


Figure 7. Map showing the Paradox Basin study area, including major structural features (modified from Kelley, 1958; Nuccio and Condon, 1996; Huntoon and others, 2002; and Davatzes and Aydin, 2005). Study area boundaries were modified from Nuccio and Condon (1996) and Huntoon and others (2002).

Hydrocarbon and Carbon Dioxide Production and Exploration

Hydrocarbon exploration drilling and seismic surveying increased in the Paradox Basin in the early 1970s, although by 1978 only a few exploration wells had been drilled down to Paleozoic formations in the area from Farmington, New Mexico, to Price, Utah (Stevenson, 1983). Historically, the hydrocarbon production in the basin has mostly been from porous carbonate buildups of the southwestern shelf margin of the evaporite basin (Huffman, 1995a). Currently, the Paradox Basin contains about 100 oil fields that produce primarily from the informal Ismay and Desert Creek horizons in the Pennsylvanian Paradox Formation (Goldhammer and others, 1991; Huntoon and others, 2002). Morgan (1993) identified eight reservoirs in the Paradox Formation play and five in the Leadville Limestone play in the Lisbon field. Hydrocarbons in the Paradox Formation are internally derived from black organic shales, with a cyclic deposition of carbonate sediments, shales, and evaporites into the basin contributing to the source rock, reservoir rock, and cap rock (Huntoon and others, 2002).

The Greater Aneth field, with in-place resources of more than 1,000 million barrels of oil (MMBO), accounts for up to two-thirds of the proven resources in the basin, and other fields in this primarily stratigraphic play account for the rest (Huffman, 1995a). The field, discovered in 1956, includes four production units and occupies an area of approximately 47,000 acres in southeastern Utah. Infill drilling at Aneth field dominated most activity in the basin from 1974 to 1980 (Stevenson, 1983). In addition, six hydrocarbon accumulations produce from pre-Pennsylvanian pre-salt structural blocks; the largest of these is the Leadville Limestone in the Lisbon field, which has resources of approximately 43 MMBO and 250 billion cubic feet of gas (BCFG) (Huffman, 1995a). The Andys Mesa gas field has had cumulative production through 1993 of 18 BCFG and 11,000 barrels of condensate from a Permian to Pennsylvanian reservoir along the flanks of northwest-trending salt anticlines in the axial area of the Paradox salt basin (Huffman, 1995a). Furthermore, more viscous hydrocarbons are found in the Permian White Rim Sandstone exposed along the western bank of the Colorado River near its confluence with the Green River in the locally named “Tar Sand Triangle” (Sanford, 1995). This area of the White Rim may hold an estimated 6.3 billion barrels of heavy oil (Huntoon and others, 2002).

In addition to hydrocarbon resources, the Paradox Basin also holds significant quantities of natural CO₂ as low-Btu (British thermal unit) gas, most notably in the McElmo Dome field. These carbon dioxide reservoirs are similar to conventional natural gas fields, where gas collects in structures or stratigraphic traps. About 10 natural CO₂ fields have been exploited in the Colorado Plateau and Southern Rocky Mountains area, although many more reservoirs with high CO₂ concentrations have been found by exploration drilling (Allis and others, 2001). Typically, these CO₂ fields have multiple, stacked reservoirs, which indicates vertical movement of CO₂ up through the rocks. Five of these fields are still producing CO₂ mostly to assist oil production through EOR (enhanced oil recovery). Of the total 33 megatons per year (Mt/y) of CO₂ produced, 25 Mt/y is piped about 500 mi from the McElmo Dome field (Paradox Basin) to western Texas (Allis and others, 2001). The McElmo Dome field has an area of 310 square miles with an average depth of about 6900 ft, and has a gas composition of 98.2 percent CO₂, 1.6 percent nitrogen (N₂), and 0.2 percent methane (CH₄) with a total reserve of 17 TCFG (Tremain, 1993). Several low-Btu, high-CO₂ fields exist in the Utah portion of the Paradox Basin including the Bluff, Boundary Butte, Coal Bed Canyon, Deadman Canyon, and Desert Creek fields (Chidsey and Morgan, 1993). This trend is underlain by thick Paleozoic carbonate rocks that generated CO₂ when metamorphosed by igneous intrusions or deep burial (Chidsey and Morgan, 1993).

Carbon Dioxide Storage Assessment

The USGS regional CO₂ storage resource assessment of the Paradox Basin includes just one SAU, the Paleozoic Composite C50210101, so named because the SAU includes multiple formations from the Paleozoic Era considered for storage (fig. 8). No other SAUs were assessed in this study area because the assessment geologists found that potential SAUs in the Mesozoic strata were too shallow in the Paradox Basin. Mesozoic strata that included both a storage formation and regional seal were found to the north; however, these strata are under the Wasatch Plateau and are included in the Uinta and Piceance Basins study area, also described in this report. At the field scale, Chidsey and others (2010) investigated the CO₂ storage potential of the Greater Aneth field.






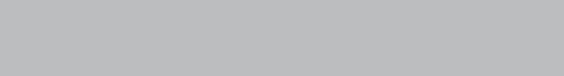

Era	System	Stratigraphic unit			Storage Assessment Unit (SAU) notes
Mesozoic	Cretaceous	Mesaverde Group (Ferron Sandstone Member)			
		Mancos Shale			
		Dakota Sandstone Burro Canyon Formation Morrison Formation			
	Jurassic	San Rafael Group			
					
	Triassic	Glen Canyon Group			
		Chinle Formation Shinarump Member			
		Moenkopi Formation Timpoweap Member			
Paleozoic	Permian	Cutler Formation	Kaibab Ls. / White Rim Ss. / De Chelly Ss.	Paleozoic Composite SAU C50210101 Seal: Paradox Formation anhydrites and shales of the Hermosa Group Storage formation: Aneth Formation, McCracken Member of the Elbert Formation, Ouray Limestone, Redwall and Leadville Limestones, and the middle Hermosa Group (lower part of the Paradox Formation)	
			Organ Rock Tongue		
			Cedar Mesa Sandstone		
			Halgaito Tongue		
	Pennsylvanian	Hermosa Group	Honaker Trail Formation		
					
			Paradox Formation		
					
			Pinkerton Trail Formation		
			Molas Formation		
	Mississippian		Redwall and Leadville Limestones		
					
	Devonian		Ouray Limestone		
			Elbert Formation		
			McCracken Member		
			Aneth Formation		
	Silurian				
	Ordovician				
	Cambrian		Lynch Dolomite		
			Muav Limestone		
			Bright Angel Shale		
			Tapeats Sandstone / Ignacio Quartzite		
					
Precambrian		Igneous and metamorphic rocks			

Figure 8. Generalized stratigraphic column of geologic units in the Paradox Basin study area, Utah, Colorado, Arizona, and New Mexico (modified from Huffman, 1995a). Storage assessment units (SAUs) consist of a storage formation (red) and regional seal (blue). Wavy lines indicate unconformable contacts, and gray areas represent unconformities or hiatuses. Only significant unconformities are shown. In some cases, subdivisions of units or lesser known correlative units are not shown. Abbreviations: Ls., Limestone; Ss., Sandstone.

Paleozoic Composite SAU C50210101

By Marc L. Buursink

The Paleozoic Composite SAU includes only those portions of the preserved Devonian to Middle Pennsylvanian geologic section deemed suitable as storage formations for CO₂ storage and that are located beneath a regionally extensive seal in the Paradox Basin (fig. 9). The suitable storage formation rocks consist of siliciclastic and carbonate lithologies and include, in ascending stratigraphic order, the Aneth Formation, the McCracken Member of the Elbert Formation, the Ouray Limestone, the Redwall Limestone, the Leadville Limestone, and the carbonate strata in the lower part of the Paradox Formation (Stevenson and Baars, 1988; Huffman and others, 1996) (fig. 8). Regionally, evaporites and black shales in the middle of the Paradox Formation function as the sealing rocks (Stevenson and Baars, 1988; Geldon, 2003a).

In the Paradox Basin, erosional unconformities separate Devonian and Mississippian rocks from Cambrian carbonate formations (fig. 8) (Huffman, 1995a; Geldon, 2003a). These Cambrian formations were not included in this composite SAU due to reservoir quality and data availability limitations. The Aneth Formation, which is the oldest Devonian rocks in the SAU, is located mostly in the Blanding Basin (fig. 7) and consists of very dense dolostones (Stevenson and Baars, 1988). The McCracken Member of the Elbert Formation is a basal sandstone extending discontinuously from the Defiance Plateau to the Uncompahgre Plateau and from the mountains of the San Juan dome to the area west of the Colorado and Green Rivers (fig. 9). It ranges from less than 5 to about 125 ft thick; consists predominantly of poorly sorted, commonly glauconitic sandstone and quartzite; and produces oil in the Lisbon field area (Stevenson and Baars, 1988; Geldon, 2003a). Quartzite of the Elbert Formation in southwestern Colorado, southeastern Utah, and northeastern Arizona is overlain conformably to gradationally by the Upper Devonian Ouray Limestone (Geldon, 2003a) and was not considered as a storage formation. The Ouray Limestone is typically micritic and is unconformably overlain by the Redwall Limestone (Stevenson and Baars, 1988). The Mississippian Redwall and Leadville Limestones consist of limestone and dolostone, and, as discussed in the Uinta-Piceance Basin section of this report, probably represent a single depositional unit that was deposited during the maximum extent of the third Paleozoic marine transgression (Geldon, 2003a). The Lower Pennsylvanian Molas Formation, a ferruginous paleosol that cuts progressively deeper into the Redwall and Leadville Limestones from west to east (Stevenson and Baars, 1988), was not included as a storage formation.

From the Uinta Basin to the Kaibab Plateau (not shown), the Molas Formation is gradationally overlain by the Pinkerton Trail Formation, which is the lower member of the Pennsylvanian Hermosa Group, and generally consists of a relatively thin succession of marine carbonate rocks and dark-gray to black shale (Stevenson and Baars, 1988; Geldon, 2003a). The Pinkerton Trail Formation was not included as a storage formation even though it is overlain conformably or gradationally by the Paradox Formation (part of which is a storage formation for this SAU) and by the upper members of the Hermosa Group. The Paradox Formation of the middle Hermosa Group consists of chemical, biogenic, and clastic sediments that accumulated during multiple cycles of sea-level fluctuation in a barred trough adjacent to the ancestral Uncompahgre uplift (Stevenson and Baars, 1988; Geldon, 2003a). On the northeastern edge of the basin, the Paradox Formation is in gradational contact with both the lower and upper members of the Hermosa Group, and the Pinkerton Trail and Honaker Trail Formations (fig. 8), both of which include clastic sediments eroded from the ancestral Uncompahgre uplift that interfinger with evaporite facies of the Paradox. As a result, the Paradox Formation consists of micaceous to arkosic sandstone and conglomerate; sandy shale; and carbonaceous and micaceous, fossiliferous limestone and dolomite with thin gypsum beds (Geldon, 2003a). At the southwestern edge of the basin, the Paradox Formation consists of carbonate sediments accumulated under relatively shallow marine conditions. Near the center of the Paradox Basin, certain anticlines are cored with salt (about 70 to 80 percent of the formation) that generally ranges from 2,500 to 15,000 ft thick (Stevenson and Baars, 1988; Geldon, 2003a).

The Paleozoic Composite SAU boundaries are defined by the top of the uppermost storage formation and by the extent of the regional seal. Formation top depths reported in a commercial database (IHS Energy Group, 2010) for the Leadville Limestone or the correlative Redwall Limestone helped to define the top of the storage interval. The Paleozoic Composite SAU, which lies between 3,000 and 12,500 ft deep, covers a mean storage area of about 6.1 million acres (fig. 9). The extent of the SAU is supported by structure-contour maps from Peterson (1989) and McClure and others (2003a) and by supplemental data on cross sections from Peterson (1989) and McClure and others (2003b). To assess the composite SAU gross storage formation thickness interval, isopach maps (Mallory, 1972; Stevenson and Baars, 1988; Peterson, 1989; Geldon, 2003a) of storage formations within the SAU were scanned, geo-referenced, and digitized. Next, the thickness values were scaled by a unique net-to-gross ratio for each formation derived from the literature and well logs (Stevenson and Baars, 1988; McClure and others, 2003b; Scott, 2003). Finally, using a GIS, the net-porous storage formation interval of the composite SAU was summed (for example, see Buursink and others, 2011). The Paleozoic Composite SAU gross storage formation thickness ranges from 1,000 to 4,000 ft and the net storage formation thickness varies between 100 and 600 ft.

Prolific hydrocarbon production from Paleozoic formations has resulted in a large number of available well log and core data that were accessed to characterize storage formation quality. Porosity and permeability trends for individual storage formations within the composite SAUs were derived from multiple sources, including Peterson (1989), Morgan (1993), and Geldon (2003b). Average field values were extracted from Nehring Associates Inc. (2010), a commercial oil and gas database. Porosity of the more porous units within the Paleozoic Composite SAU conducive to storage ranges from 6 to 14 percent for the net interval and permeability ranges from 0.1 to 100 mD. Distribution of these reservoir properties in the SAU was generally a function of the storage formation depth and relative abundances of different storage formation lithologies.

Water-quality data obtained from published databases (Breit, 2002) and maps (Geldon, 2003b) for the SAU area indicate both fresh and saline waters. Groundwater TDS at various locations in the SAU is both above and below the EPA's (2009) USDW maximum limit of 10,000 ppm. Storage-formation areas with groundwater TDS below the 10,000 ppm maximum limit were identified and removed from the SAU. A probabilistic maximum volume for buoyant trapping in the SAU was determined using hydrocarbon exploration and production data from Morgan (1993), play descriptions from Huffman (1995a), and average field size from Nehring Associates Inc. (2010) using a method similar to that described for the Paleozoic Composite SAU in the Uinta and Piceance Basins study area.

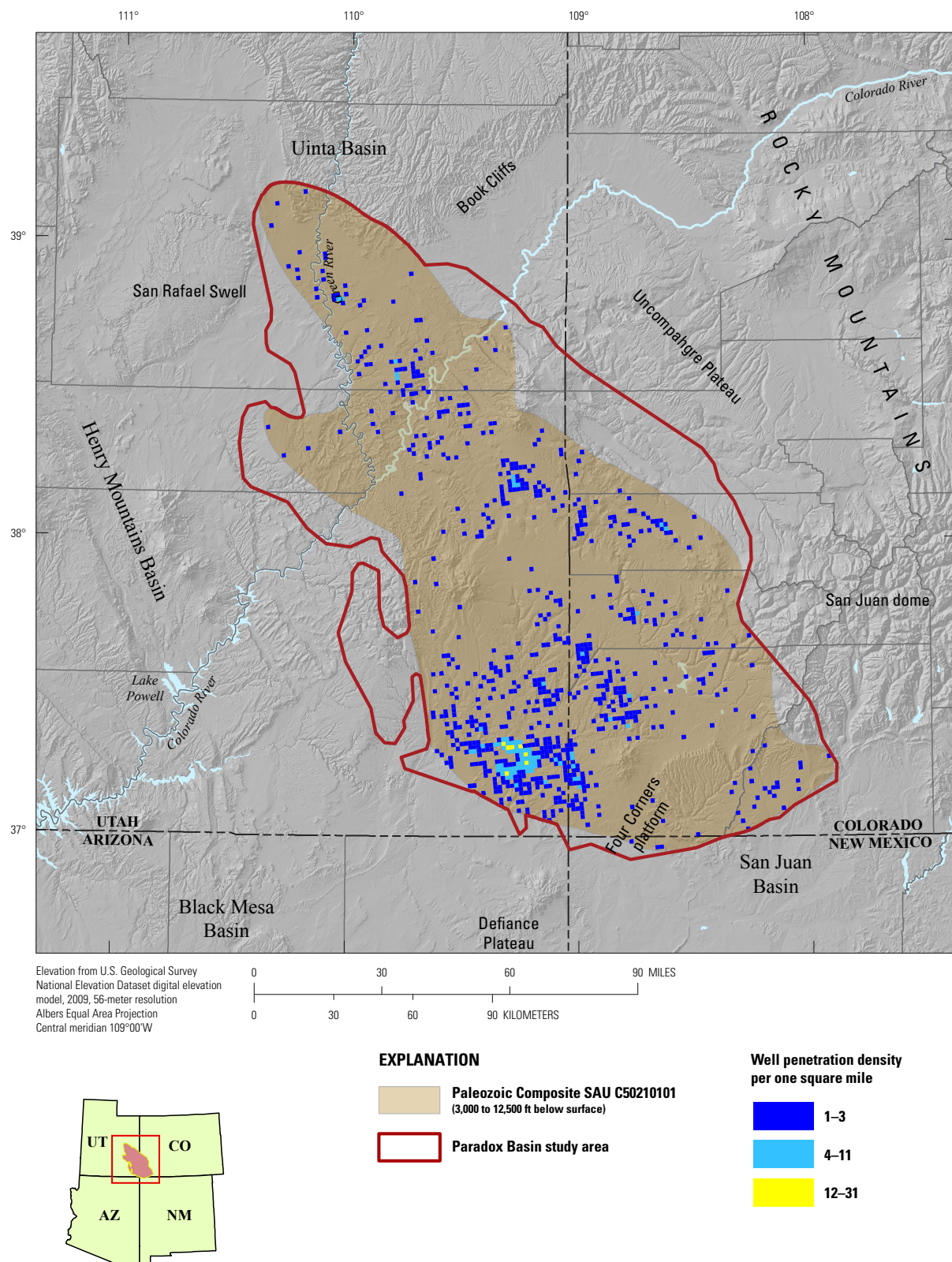


Figure 9. Map of the Paleozoic Composite C50210101 Storage Assessment Unit (SAU) in the Paradox Basin. Well penetration density is the number of wells (per 1-square-mile grid cell) derived from the ENERDEQ well database (IHS Energy Group, 2011) that have penetrated the top of the storage formation. Study area boundaries were modified from Nuccio and Condon (1996) and Huntoon and others (2002). Abbreviation: ft, feet.

San Juan Basin

By Ronald M. Drake II

Introduction

The San Juan Basin lies primarily within the northwestern corner of New Mexico but also lies in the southwestern corner of Colorado. The asymmetrical structural basin is bounded on the west by the Defiance uplift, on the northwest by the Four Corners platform, on the northeast by the Archuleta arch, on the east by the Nacimiento uplift, on the southeast by the Puerco platform, and on the southwest by the Zuni Uplift (fig. 10). The basin study area is about 120 mi from east to west, and about 150 mi from north to south. The basin dips gently toward the northeast and is sharply upturned along its northwestern, northern, northeastern, and eastern boundaries. Maximum depth to basement is more than 14,400 ft (Craig, 2001); its deepest point is in the northeastern portion of the basin. The basin contains a thick interval of Mesozoic strata and lesser amounts of Paleozoic and Cenozoic strata (fig. 11). The following descriptions of the basin's stratigraphy provide only a general context for both the basin and the SAUs within. Readers seeking greater detail on the stratigraphy should refer to Beaumont and Read (1950), Jentgen (1977), Stevenson and Baars (1977), Huffman and Condon (1993), and the other references in the following section.

Geologic History

The San Juan Basin contains Precambrian to Cenozoic rocks with notable unconformities representing missing early and middle Paleozoic strata. Basement rocks include Precambrian quartzite to schist and granite (Stevenson and Baars, 1977); they are overlain by Cambrian quartzite, quartzose sandstone, and friable sandstone with some local shale lenses deposited by an eastward-transgressing sea (Stevenson and Baars, 1977). There are no known Ordovician or Silurian rocks in the San Juan Basin. Devonian rocks in the basin record a transgression that resulted in the deposition of marine limestone and dolomite (Beaumont and Read, 1950; Stevenson and Baars, 1977). Mississippian limestones represent a shallow sea environment, and they were not uniformly deposited within the basin due to topographic highs like the Zuni uplift (Armstrong and Holcomb, 1989). Partial post depositional erosion of the Mississippian and older Paleozoic rocks occurred across the San Juan Basin area as shallow seas receded (Beaumont and Read, 1950).

The late Paleozoic in the region was defined by cyclic sedimentation in an established San Juan trough that alternated between alluvial clastic sediments derived from the north, transgressive carbonates derived from the south, and arid and eolian deposits forming in between (Huffman and Condon, 1993). The uplift of the Uncompahgre and San Luis highlands in the Ancestral Rocky Mountains region to the north and northeast (and the presence of stable highlands in the south) created a depositional center in the modern San Juan Basin area called the San Juan trough. Clastic sediments derived from the Ancestral Rockies to the northeast and carbonate sediments deposited in seas to the southwest produced interbedded continental and marine deposits that thicken to the southeastern portion of the basin. In general, the transition from the Late Pennsylvanian to the Permian marks a shift from carbonate-shelf marine deposition to continental redbed and sabkha-type deposition (Huffman and Condon, 1993). However, deviations from these trends did occur; detailed stratigraphy and paleogeography of the late Paleozoic is available in Jentgen (1977) and Huffman and Condon (1993), and the references therein.

Upper Triassic deposits in the San Juan Basin consist of sandstones of terrigenous origin that represent the last clastic pulses from a waning uplift in the southern Ancestral Rocky Mountains (Kurtz and Anderson, 1980). Deposited in fluvial, marshland, and lacustrine environments, Upper Triassic rocks vary from conglomerates at the base to pink and red shales (O'Sullivan, 1977; Kurtz and Anderson, 1980).

Redbeds, eolian sandstones, mudstones, limestones, and evaporites from sabkha and eolian environments, and then from littoral and shallow seas, dominate the rock record of the Lower Jurassic in the basin (Beaumont and Read, 1950; Condon and Peterson, 1986). A Late Jurassic regression of the shallow sea ushered in a period of terrestrial deposition with fluvial, alluvial, and lacustrine environments that lasted until the Late Cretaceous. Interpretations suggest that the Lower Cretaceous rocks were deposited in high-energy, braided and meandering fluvial settings; they contain sandstone and conglomerate intervals indicating deposition in point-bar, channel-bar, and channel-fill environments (Ridgley, 1977). The Late Cretaceous in the basin was marked by repeated transgressions and regressions with a shallow sea to the northeast and sediment source to the southwest (Molenaar, 1977). Rocks in the stratigraphic record represent mainly regressive phases where deltaic and interdeltic sediments were deposited. For more information regarding the Cretaceous and younger stratigraphy of the San Juan Basin, see Ridgley and Hatch (2013).

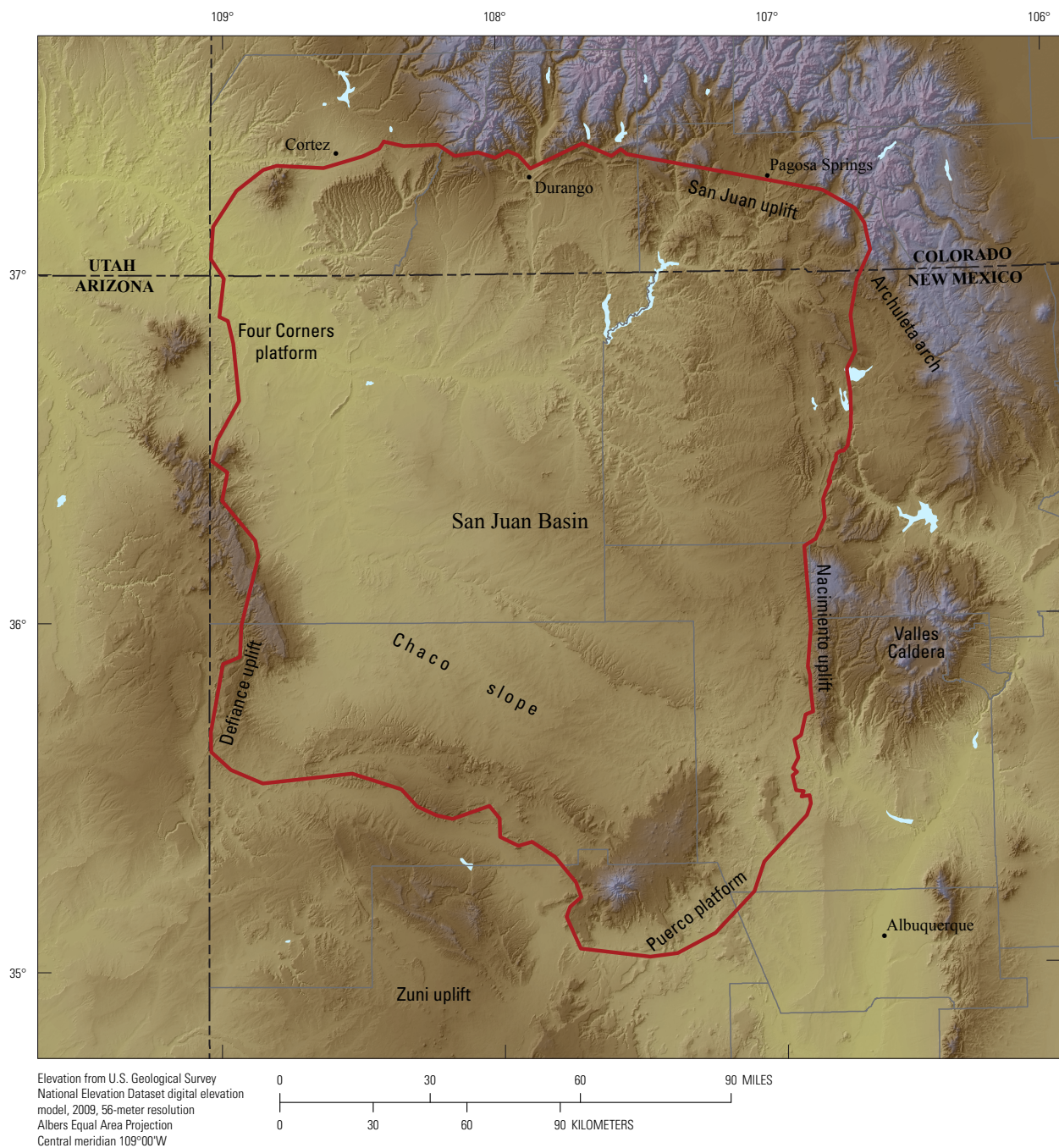
The Laramide orogeny began in the latest Cretaceous through early Tertiary with uplift occurring from Mexico to Canada (English and Johnston, 2004), including uplift along the eastern edge of the San Juan Basin. During the earliest stages of the orogeny, the ancestral Western Interior Seaway regressed, marking the end of marine deposition in the San Juan Basin.

Hydrocarbon Exploration and Production

Through 2009, the San Juan Basin has produced 42.6 TCFG and 381 MMBO (Fassett, 2010). Most of the oil and gas has been produced from Cretaceous rocks in the basin with significant oil production coming from the Tooto Sandstone fields (Fassett, 2010). The Todilto Limestone is the source of the oil produced from the Entrada Sandstone reservoir in the basin (Huffman, 1995b). Most recently, coal-bed methane production has increased dramatically from the Fruitland Formation (Fassett, 2010). According to Fassett (2010), oil production includes almost 100 MMBO of condensate from fractured sandstone reservoirs. For more details on production data and undiscovered resources assessment results in the San Juan Basin, please see Fassett (2010) and the U.S. Geological Survey San Juan Basin Assessment Team (2013).

Carbon Dioxide Storage Assessment

The USGS National Carbon Dioxide Storage Resources Assessment Team investigated and ultimately assessed four SAUs. Storage formations assessed for CO₂ storage in the San Juan Basin include in ascending stratigraphic order (1) the Entrada Sandstone; (2) the Dakota Sandstone; (3) the Tooto Sandstone Lenticle, El Vado Sandstone Member in the upper part of the Mancos Shale, and the Gallup Sandstone; and (4) sandstones of the Mesaverde Group and the “Chacra sands” of the Lewis Shale (fig. 11). The following sections describe each of the SAUs in the San Juan Basin.



EXPLANATION

San Juan Basin study area

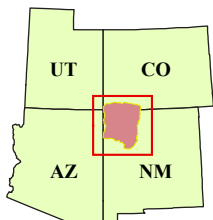


Figure 10. Map showing the San Juan Basin study area, including major structural features (modified from Craigg, 2001). Study area boundaries were modified from the U.S. Geological Survey National Oil and Gas Assessment (U.S. Geological Survey San Juan Basin Assessment Team, 2002).

Era	System/Series		Stratigraphic unit	Storage Assessment Unit (SAU) notes
Cenozoic	Tertiary		San Jose Formation	
			Nacimiento Formation	
Mesozoic	Cretaceous	Upper	Ojo Alamo Sandstone	
			Kirtland Shale	
			Fruitland Formation	
			Pictured Cliffs Sandstone	
			Lewis Shale	
			Cliff House Sandstone	
			Menefee Formation	
			Point Lookout Sandstone	
			upper Mancos Shale	
			Gallup Sandstone	
			Tocito Sandstone Lentil	
			El Vado	
			Juana Lopez Member	
			Greenhorn Limestone Member	
			Graneros Member	
			Dakota Sandstone	
	Jurassic	Lower	Burro Canyon Formation	
			Morrison Formation	
			Bushy Basin Member	
		Upper	Westwater Canyon Member	
			Recapture Member	
			Cow Springs Sandstone	
			San Rafael Group	
			Wanakah Formation	
			Beclabito Member	
			Todilto Limestone Member (with anhydrite bed)	
			Entrada Sandstone	
			Chinle Formation	
Paleozoic	Permian	Cutler Group	De Chelley Sandstone	
			Organ Rock Shale	
			Cedar Mesa Formation	
			Halgaito Formation	
	Pennsylvanian	Hermosa Group	Rico Formation	
			Honaker Trail Formation	
			Paradox Formation	
			Pinkerton Trail Formation	
	Mississippian		Molas Formation	
			Leadville Limestone	
	Devonian		Ouray Limestone	
			Elbert Formation	
	Cambrian		Ignacio Quartzite	
	Precambrian			

Lewis Shale and Mesaverde Group SAU

C50220104
Seal: Lewis Shale
Storage formation: Point Lookout Sandstone, Menefee Formation, Cliff House Sandstone, and "Chacra sands" of the Lewis Shale

Gallup Sandstone SAU

C50220103
Seal: upper Mancos Shale
Storage formation: Gallup Sandstone, Tocito Sandstone Lentil, and El Vado Sandstone

Dakota Sandstone SAU

C50220102
Seal: lower Mancos Shale and the Graneros Member of the lower Mancos Shale
Storage formation: Dakota Sandstone

Entrada Sandstone SAU

C50220101
Seal: Wanakah Formation and Todilto Limestone Member (with anhydrite bed) of the Wanakah Formation
Storage formation: Entrada Sandstone

Figure 11. Generalized stratigraphic column of geologic units in the San Juan Basin study area of New Mexico and Colorado (modified from Huffman, 1995b). Storage assessment units (SAUs) consist of a storage formation (red) and regional seal (blue). Wavy lines indicate unconformable contacts, and gray areas represent unconformities or hiatuses. Only significant unconformities are shown. In some cases, subdivisions of units or lesser known correlative units are not shown.

Entrada Sandstone SAU C50220101

By Peter D. Warwick and Sean T. Brennan

The storage formation interval for the Entrada Sandstone SAU in the San Juan Basin is composed of porous, silty, and sandy eolian (dune and interdune) deposits of the Middle Jurassic Entrada Sandstone (fig. 11) (Condon and Peterson, 1986; Ridgley and Hatch, 2013). The regional seal overlying the Entrada Sandstone is the upper gypsum and anhydrite unit of the Middle Jurassic Todilto Limestone Member of the Wanakah Formation (fig. 11). The upper gypsum to anhydrite unit overlies a lower laminated to massive limestone unit of the Todilto Limestone Member (Condon and Peterson, 1986; Ridgley and Hatch, 2013). Depths from the surface to the base of the seal and top of the storage formation range from 3,000 to 10,100 ft with an average depth of approximately 6,000 ft (IHS Energy Group, 2010, 2011).

The thickness of the Entrada Sandstone in the San Juan Basin ranges from 60 to 330 ft (Green and Pierson, 1977; Condon and Peterson, 1986; Huffman, 1995b; IHS Energy Group, 2010, 2011). The variable thickness is related in part to a relict dune topography that was inundated by the marine waters associated with deposition of the overlying Todilto Limestone Member (Vincelette and Chittum, 1981; Ridgley and Hatch, 2013). Potential storage formation rocks are confined to the eolian sandstone facies of the Entrada Sandstone. Sandstones in the interdune deposits are commonly finer grained than in the dune sandstones and, where present, they may be locally interbedded with siltstones and mudstones (Ridgley and Hatch, 2013). The mean total thickness of the Entrada Sandstone SAU was estimated to range from 200 to 325 ft, with a most likely total thickness of 250 ft. The four storage formation types found in the Entrada Sandstone are influenced by the following features: (1) stratigraphic traps related to the relict dune topography; (2) structural traps related to syndepositional movement along basement faults; (3) rocks of the Entrada and overlying Todilto that dip regionally to the northeast, which tends to limit the area of closure of the dune ridges; and (4) local and regional porosity changes within the Entrada Sandstone (Ridgley and Hatch, 2013). The mean thickness of the net porous interval for storage formations in the Entrada Sandstone SAU was estimated to range from 100 to 150 ft, with a most likely thickness of 125 ft.

The Todilto Limestone Member includes a basal, organic-rich limestone that ranges from not present to 30 ft thick and is the source bed for oil that is produced from the Entrada Sandstone (Ridgley and Hatch, 2013). Overlying the limestone is an upper anhydrite unit that varies in thickness from absent over dune crests to about 120 ft in interdune areas of the underlying Entrada Sandstone (Condon and Peterson, 1986; Massé and Ray, 1995). Vincelette and Chittum (1981) mapped the geographic extent of the upper anhydrite facies of the Todilto Limestone Member and showed that it is limited to the central part of the San Juan Basin. The depth to the top of the Todilto Limestone Member and the lateral extent of the upper anhydrite facies are the limiting factors defining the boundaries of the Entrada Sandstone SAU (fig. 12). The area of the Entrada Sandstone SAU was also defined by formation-top data in the IHS Energy Group (2010, 2011) commercial database.

Water-quality data from Breit (2002) and a saline aquifer database provided to the U.S. Geological Survey (USGS) by the New Mexico Bureau of Geology and Mineral Resources suggest that the Entrada Sandstone SAU interval is dominated by fresh water (<10,000 ppm TDS) with only limited occurrence of saline water (>10,000 ppm TDS) within the SAU area. Approximately 10 percent (with a minimum of 5 percent and maximum of 25 percent) of the potential storage space in the storage formation may contain saline water suitable for subsurface storage of CO₂. Data from Massé and Ray (1995), Huffman (1995b), Nehring Associates Inc. (2010), and Ridgley and Hatch (2013) suggest that porosity of the net porous interval of the Entrada Sandstone SAU ranges from 20 to 26 percent, with a most likely estimate of 23 percent. Permeability of the Entrada Sandstone SAU is estimated to range from 10 to 1,200 mD, with 370 mD as the most likely estimate (Nehring Associates Inc., 2010). Structural and stratigraphic closures for buoyant trapping of CO₂ within the Entrada Sandstone were estimated from existing reservoir areas and thicknesses reported in the Nehring Associates Inc. (2010) database.

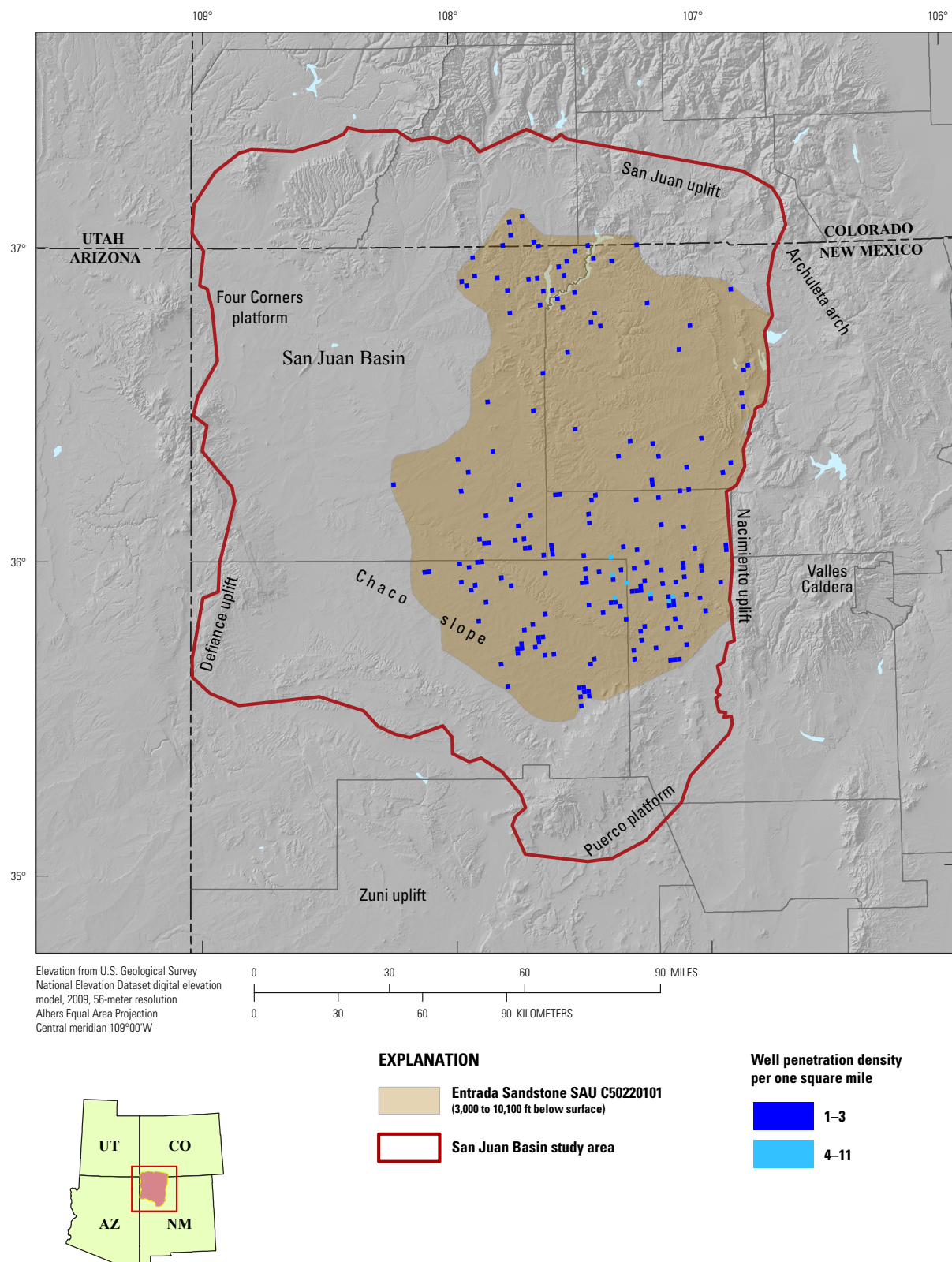


Figure 12. Map of the Entrada Sandstone C50220101 Storage Assessment Unit (SAU) in the San Juan Basin. Well penetration density is the number of wells (per 1-square-mile grid cell) derived from the ENERDEQ well database (IHS Energy Group, 2011) that have penetrated the top of the storage formation. Study area boundaries were modified from the U.S. Geological Survey National Oil and Gas Assessment (U.S. Geological Survey San Juan Basin Assessment Team, 2002). Abbreviation: ft, feet.

Dakota Sandstone SAU C50220102

By Ronald M. Drake II

The storage formation for the Dakota Sandstone SAU is composed of marine and nonmarine clastic rock deposited during the Cretaceous in response to a regional transgression of the ancestral Western Interior Seaway (fig. 11) (Owen, 1973; Grant and Owen, 1974). The Dakota Sandstone lies above a regional unconformity and is described as a shoreface deposit (Fassett, 2006). Within the northwestern part of the basin, the Dakota Sandstone consists of mostly nonmarine channel deposits with interbedded coal and conglomerates. To the southeast, the Dakota grades into a shallow-marine deposit (Huffman, 1995b). The Dakota Sandstone ranges in thickness from 175 to 275 ft (Umbach, 1950) and includes the Encinal Canyon Member, Oak Canyon Member, Cubero Tongue, Paguate Tongue, and Twowells Tongue (Molenaar, 1977; Ridgley and Hatch, 2013). The regional seal overlying the Dakota Sandstone is the Mancos Shale, which includes the Graneros Shale Member (fig. 11) that lies directly on top of the Dakota Sandstone. Maximum thickness of the Mancos Shale is 2,400 ft (Fassett, 2006).

At depths greater than 3,000 ft below the surface, the Dakota Sandstone SAU is a potential storage formation for CO₂ storage in the San Juan Basin. More than 8,000 well penetrations (IHS Energy Group, 2011) were used to define the SAU boundary where the Dakota Sandstone is at least 3,000 ft below the surface, and the overlying sealing unit being at least 75 ft thick. No Dakota Sandstone lies below 13,000 ft; therefore, no deep Dakota SAU has been defined. The area of the Dakota Sandstone SAU is about 5,829,000 acres (fig. 13). The mean total thickness of the Dakota Sandstone in the San Juan Basin ranges from 175 to 275 ft, with the most likely total thickness being 225 ft (Umbach, 1950; Fassett, 1974; Stone and others, 1983; IHS Energy Group, 2011). The storage formation thickness was calculated from boreholes penetrating both the top of the Dakota Sandstone and the top of the underlying unit (either the Burro Canyon Formation or the equivalent Morrison Formation). In some cases, the Burro Canyon or Morrison Formation were not stratigraphically separated from the Dakota (IHS Energy Group, 2011) and therefore their thickness (or thicknesses) were included as part of the Dakota Sandstone thickness; but this was not a common problem and the impact is assumed to be minimal. The thickness of the Dakota Sandstone was also determined using the isopach map from Stone and others (1983). The mean thickness of the net porous interval for storage formations in the Dakota Sandstone SAU was estimated to range from 30 to 60 ft, with the most likely thickness being 45 ft.

Water-quality data from Breit (2002) and a saline aquifer database provided to the USGS by the New Mexico Bureau of Geology and Mineral Resources suggest that the Dakota Sandstone SAU interval consists of both fresh water (<10,000 ppm TDS) and saline water (>10,000 ppm TDS) within the area of the SAU. Approximately 35 percent (with a minimum of 20 percent and maximum of 50 percent) of the potential storage space may contain saline water suitable for subsurface storage of CO₂. Data from Franklin and Tieh (1989), Huffman (1995b), and Nehring Associates Inc. (2010) suggest that the porosity of the net porous interval of the Dakota Sandstone SAU ranges from 5 to 15 percent, with the most likely estimate being 10 percent. Permeability of the Dakota Sandstone SAU is estimated to range from 0.001 to 100 mD, with 0.25 mD as the most likely estimate (Huffman, 1995b; Nehring Associates Inc., 2010). The maximum buoyant trapping volumes were calculated using existing data from producing fields and the Dakota Sandstone SAU thicknesses and storage formation properties described above.

Overall, the above storage formation characteristics were used to calculate available storage space for CO₂ within the Dakota Sandstone SAU in accordance with the USGS carbon sequestration assessment methodology (Brennan and others, 2010; Blondes and others, 2013). The results of the assessment have been reported and are available from the USGS Geologic Carbon Dioxide Storage Resources Assessment Team (2013a,b,c).

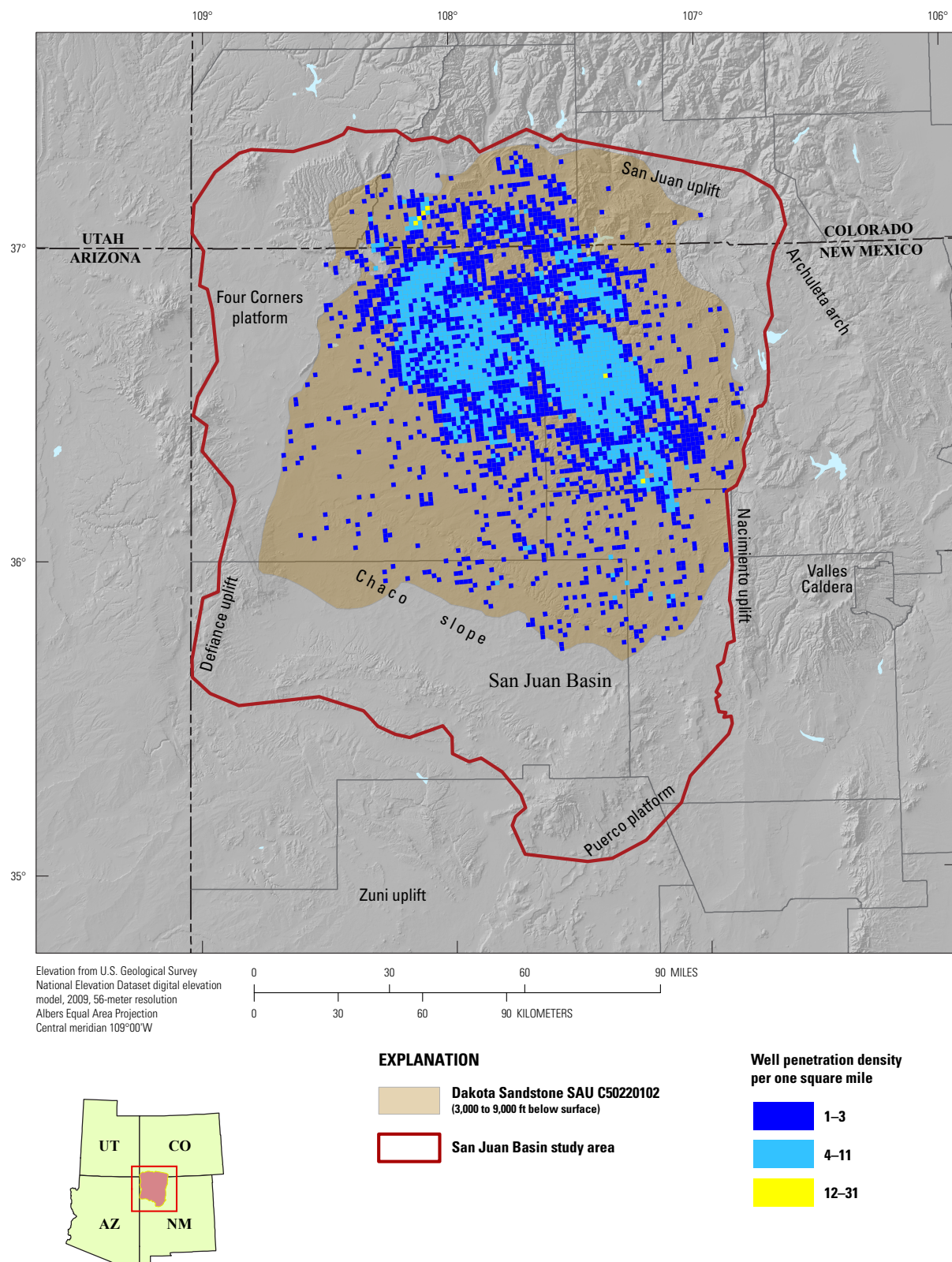


Figure 13. Map of the Dakota Sandstone C50220102 Storage Assessment Unit (SAU) in the San Juan Basin. Well penetration density is the number of wells (per 1-square-mile grid cell) derived from ENERDEQ well database (IHS Energy Group, 2011) that have penetrated the top of the storage formation. Study area boundaries were modified from the U.S. Geological Survey National Oil and Gas Assessment (U.S. Geological Survey San Juan Basin Assessment Team, 2002). Abbreviation: ft, feet.

Gallup Sandstone SAU C50220103

By Ronald M. Drake II

The Gallup Sandstone SAU is composed of the porous strata of the Gallup Sandstone, the Tociito Sandstone Lentil, and the El Vado Sandstone Member of the Mancos Shale (fig. 11). The Gallup Sandstone has been described as a northeastward-prograding marine and coastal sandstone deposit within the Mancos Shale (Nummedal and Molenaar, 1995). The regional seal is the thick marine upper part of the Mancos Shale (fig. 11), which lies directly on top of the Gallup Sandstone. The upper part of the Mancos Shale is as much as 2,400 ft thick (Fassett, 2006). According to Molenaar (1974), the massive regressive Gallup Sandstone only extends to the northeast about halfway across the San Juan Basin; however, IHS data report the presence of “Gallup” Sandstone northeast of Molenaar’s extent for Gallup Sandstone. This discrepancy is probably due to industry and IHS reporting the Tociito Sandstone Lentil and the El Vado Sandstone Member as the Gallup Sandstone instead (Molenaar and others, 2002; and Ridgley and others, 2013).

The Gallup Sandstone is a potential storage formation unit for CO₂ storage in the San Juan Basin at depths greater than 3,000 ft below the surface. Almost 9,300 well penetrations (IHS Energy Group, 2011) were used to define the SAU boundary, which is based on (1) the top of the Gallup Sandstone or Tociito Sandstone Lentil at a depth of at least 3,000 ft below the surface, and (2) the overlying sealing unit being at least 75 ft thick. Within the San Juan Basin, there are no Gallup or equivalent strata below 13,000 ft; therefore, no deep Gallup SAU has been defined. The area of the Gallup Sandstone SAU is about 4,670,000 acres (fig. 14). The mean total thickness of the Gallup Sandstone in the San Juan Basin ranges from 275 to 425 ft, with the most likely total thickness being 350 ft (Stone and others, 1983). The Gallup Sandstone thickness data from Stone and others (1983) were digitized and contoured within the SAU boundary. The mean thickness of the net porous interval for storage formations in the Gallup Sandstone SAU was estimated to range from 15 to 105 ft, with the most likely thickness being 45 ft.

Water-quality data from Breit (2002) and a saline aquifer database provided to the USGS by the New Mexico Bureau of Geology and Mineral Resources suggest that the Gallup Sandstone SAU interval consists of both fresh water (<10,000 ppm TDS) and saline water (>10,000 ppm TDS) within the area of the SAU. Approximately 40 percent (with a minimum of 25 percent and a maximum of 65 percent) of the potential storage space may contain saline water suitable for subsurface storage of CO₂. Data from Devlin and Tomkins (1957), Huffman (1995b), Nehring Associates Inc. (2010), and Ridgley and others (2013) suggest that porosity of the net porous interval of the Gallup Sandstone SAU ranges from 6 to 18 percent, with the most likely estimate being 12 percent. The permeability of the Gallup Sandstone SAU is estimated to range from 0.4 to 400 mD, with 50 mD as the most likely estimate (Huffman, 1995b; Nehring Associates Inc., 2010; Ridgley and others, 2013). The maximum buoyant trapping volumes were calculated using existing data from producing fields and the Gallup Sandstone SAU thicknesses and storage formation properties described above.

The characteristics described here were used to calculate available storage space for CO₂ within the Gallup Sandstone SAU in accordance with the USGS carbon sequestration assessment methodology (Brennan and others, 2010; Blondes and others, 2013). The results of the assessment have been reported and are available from the USGS Geologic Carbon Dioxide Storage Resources Assessment Team (2013a,b,c).

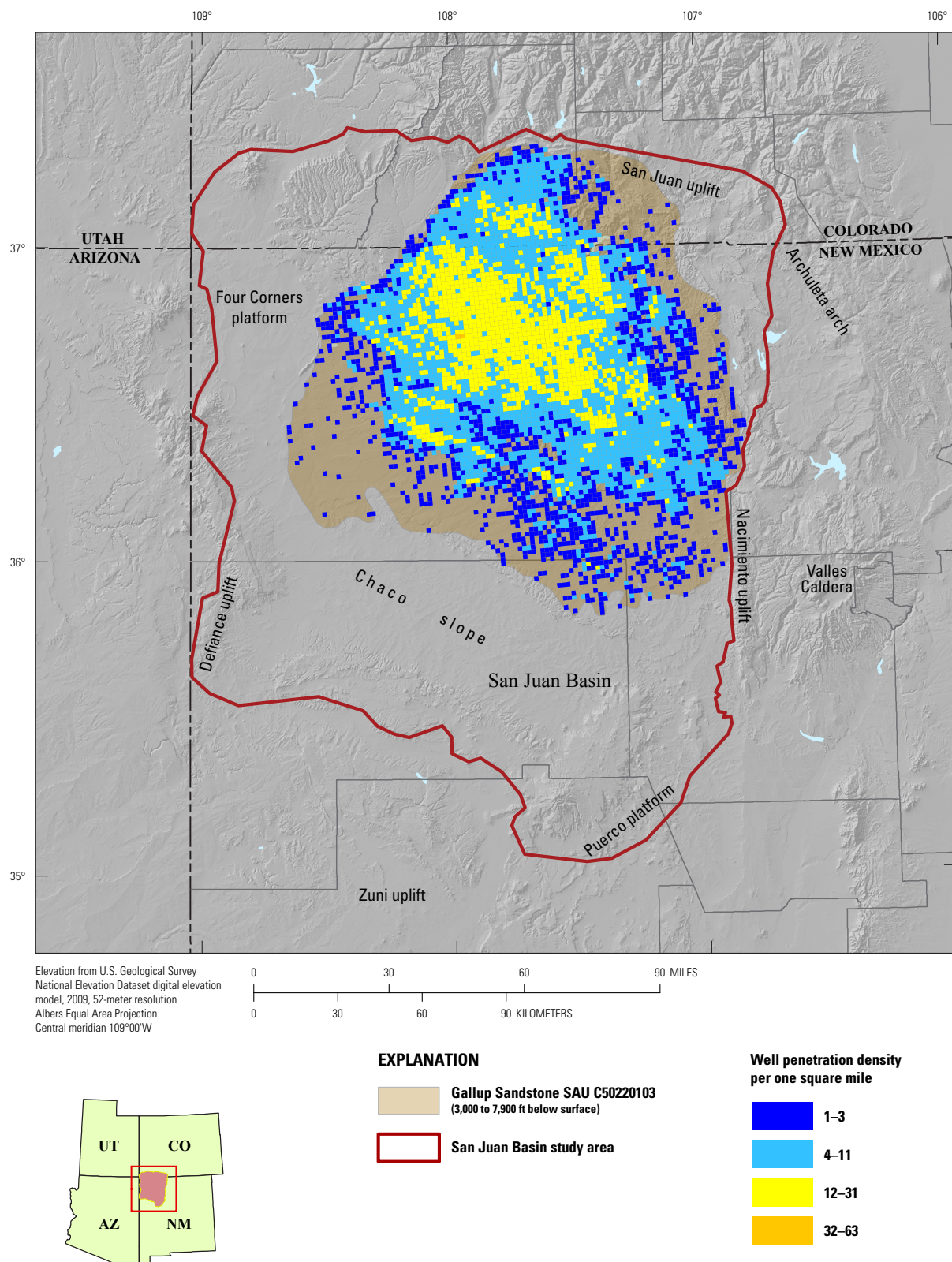


Figure 14. Map of the Gallup Sandstone C50220103 Storage Assessment Unit (SAU) in the San Juan Basin. Well penetration density is the number of wells (per 1-square-mile grid cell) derived from the ENERDEQ well database (IHS Energy Group, 2011) that have penetrated the top of the storage formation. Study area boundaries were modified from the U.S. Geological Survey National Oil and Gas Assessment (U.S. Geological Survey San Juan Basin Assessment Team, 2002). Abbreviation: ft, feet.

Lewis Shale and Mesaverde Group SAU C50220104

By Ernie R. Slucher

The Upper Cretaceous Lewis Shale and Mesaverde Group SAU consists mostly of the Mesaverde Group, a diachronous, northeastwardly thinning, regressive to transgressive wedge of siliciclastic rocks deposited in marine, marginal-marine, and nonmarine environments (Aubrey, 1991; Molenaar and others, 2002). The basal Mesaverde is gradational with the underlying marine Mancos Shale, whereas the upper contact intertongues with the overlying marine Lewis Shale (fig. 11) (Molenaar and Baird, 1992). Potential storage units within the Mesaverde Group include, in ascending stratigraphic order, the Point Lookout Sandstone, sandstones of the Menefee Formation, and the Cliff House Sandstone. In general, the Point Lookout Sandstone represents regressive coastal deposits that migrated northeastward and stratigraphically upward with time (Engler and others, 2001). Conversely, the Cliff House Sandstone is a less persistent shoreface deposit that formed mainly during regressive back-step and stand-still phases of an otherwise southwestward transgressive event (Donselaar, 1989; Whitehead, 1993; Engler and others, 2001). The Menefee Formation, a sequence of coal-bearing deltaic and fluvial sediments with some estuarine facies, was deposited landward (southwesterly) of the Point Lookout and Cliff House Sandstones (Donselaar, 1989; Whitehead, 1993). The Lewis Shale, a regionally extensive deposit hundreds to thousands of feet thick, functions as the sealing unit of the SAU.

The low permeability “Chacra sands” (an industry term defined in New Mexico) also are included as potential storage formations in the SAU (Engler and others, 2001; Fassett, 2010). The term “Chacra” is applied to a multitude of producing off-shore marine sandstones encased within the Lewis Shale in a 750-ft-thick interval beneath the Huerfanito Bentonite Bed of the Lewis Shale and southwest of the “Chacra line” (illustrations are available in Whitehead, 1993; Engler and others, 2001; and Fassett, 2006). Regionally, these sands are distal basinward equivalents of the La Ventana Tongue of the Cliff House Sandstone (Fassett, 2006, 2010). Northeast of the “Chacra line,” similar sandstones within the Lewis Shale are included within the Mesaverde Group production reservoir as defined in New Mexico (Engler and others, 2001). The Huerfanito Bentonite Bed is an important isochronous Campanian marker bed in the upper half of the Lewis Shale that is commonly used for stratigraphic analyses of Upper Cretaceous rocks in the basin (Fassett, 2000). For assessment purposes, the Huerfanito Bentonite Bed delineates the top of the SAU so to include the Chacra sands production interval even though the majority of the potential storage formations within the SAU are more than 1,000 ft below the Huerfanito.

The Lewis Shale and Mesaverde Group SAU covers approximately 1,760,000 acres and is located from 3,000 to 5,400 ft below the surface, with the most likely depth to the top of the SAU being approximately 4,000 ft (fig. 15). The depth to the Huerfanito Bentonite Bed at the top of the SAU was based on IHS Energy Group (2010) data, augmented by the structure-contour map of the Huerfanito in Ayers and others (1994). IHS Energy Group (2010) data indicate the most likely range of the total thickness of the SAU is from 1,800 to 2,200 ft, with 2,000 ft being the regional mean thickness. Data of Reneau and Harris (1957), Arnold (1974), Molenaar and Baird (1992), and Whitehead (1993) were employed for net-to-gross ratio determination of the thickness of potential storage formation intervals within the SAU. The resulting 0.08 net-to-gross ratio proportion was applied to the gross thickness values, yielding minimum, maximum, and most likely net-porous thicknesses of 120, 200, and 160 ft, respectively. Petrophysical data (Reneau and Harris, 1957; Arnold, 1974; Huffman, 1987; Whitehead, 1993; Byrnes, 1997; Teufel and others, 2004; Fassett, 2010; Phil Nelson, U.S. Geological Survey, written commun., 2011) on potential storage units within the basin indicate minimum and maximum mean porosity values of 4 and 14 percent, with 9 percent being most likely. However, permeability values are generally low, ranging between 0.0004 and 160 mD, with the higher values associated with sandstones deposited in onshore and coastal to shoreface environments. The most likely permeability of all units within the SAU, however, is 2 mD. The methodology defined by Brennan and others (2010) and Blondes and others (2013) was used to determine the minimum and central tendency buoyant-trapping pore volumes. The maximum buoyant-trapping pore volume is based on (1) the maximum net-porous interval thickness, (2) the maximum mean porosity value, and (3) reported and projected continuous oil reserve volumes (Huffman, 1987; Whitehead, 1993; Fassett, 2010). Traditionally, gas production from the SAU interval has been considered to be basin-centered gas in continuous reservoirs (Huffman, 1995b; U.S. Geological Survey San Juan Basin Assessment Team, 2002; Teufel and others, 2004). More recently, Fassett and Boyce (2005) and Fassett (2010) defined the gas traps as conventional stratigraphic pinch-out reservoirs. For this assessment, gas production was deemed to be from continuous reservoirs and not used in the maximum buoyant-trapping determination. Groundwater salinity data within the Lewis Shale and Mesaverde Group SAU indicate a mixed fresh to saline groundwater system (Levings and others, 1990; Thorn and others, 1990; Breit, 2002). Saline groundwater in excess of 10,000 ppm TDS is present over 30 to 70 percent of the total SAU acreage and is therefore available as potential storage areas.

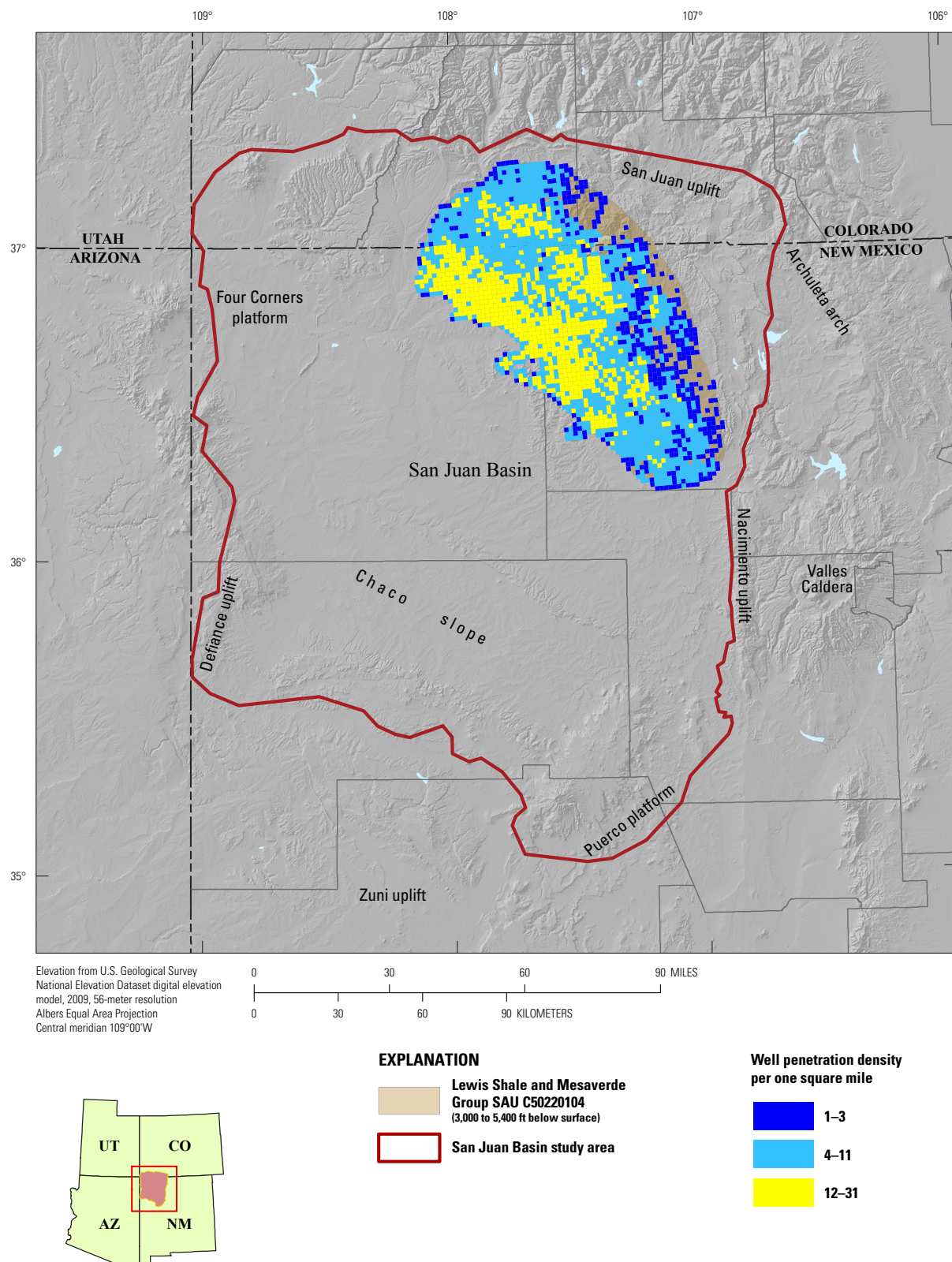


Figure 15. Map of the Lewis Shale and Mesaverde Group C50220104 Storage Assessment Unit (SAU) in the San Juan Basin. Well penetration density is the number of wells (per 1-square-mile grid cell) derived from the ENERDEQ well database (IHS Energy Group, 2011) that have penetrated the top of the storage formation. Study area boundaries were modified from the U.S. Geological Survey National Oil and Gas Assessment (U.S. Geological Survey San Juan Basin Assessment Team, 2002). Abbreviation: ft, feet.

Eastern Great Basin

By Matthew D. Merrill

Introduction

The Great Basin of the southwestern United States is the northernmost and widest manifestation of the Basin and Range physiographic region of the North American continent and exhibits a repeating pattern of linear, normal-fault-bounded mountain ranges flanked by alluvium-filled valleys that developed in an extensional tectonic environment. In the 1995 National Oil and Gas Assessments (NOGA), the USGS investigated the potential undiscovered hydrocarbons in the Great Basin, but divided it into two separate assessment provinces, the Western and Eastern Great Basin (fig. 16). The Western Great Basin includes areas of western Nevada, northeastern California, and southeastern and south-central Oregon (Barker and others, 1995). The Eastern Great Basin includes central and eastern Nevada, western Utah, and a small part of southeastern Oregon and eastern California (Peterson and Grow, 1995). The Western Great Basin underwent compressive orogenic events in the late Paleozoic to early Mesozoic that resulted in widespread igneous intrusion and metamorphism and Neogene extensional tectonics that resulted in volcanism, alteration, faulting, and high heat flow (Barker and others, 1995). The destructive impact of these events on source rocks has been shown by low success rates of hydrocarbon production in the Western Great Basin. Similar thermal events occurred in the Eastern Great Basin, but to a lesser degree, and this area has produced some hydrocarbons. Therefore, this CO₂ storage assessment evaluates only the Eastern Great Basin of western Utah and eastern Nevada. The boundaries of the Eastern Great Basin study area to the west, south, and north are the same as those used during the 1995 NOGA by Peterson and Grow (1995). Those boundaries are described as extending from the Snake River Plain on the north, the 117° longitude line on the west, and the California State boundary on the south. However, the eastern boundary of the study area differs from that of the 1995 NOGA. Due to limited hydrocarbon production in the Eastern Great Basin, the eastern boundary was created from the more clearly defined boundaries to the east, including the western edges of the Wyoming Thrust Belt TPSs (U.S. Geological Survey Wyoming Thrust Belt Province Assessment Team, 2003), the Uinta-Piceance Basin TPSs (U.S. Geological Survey Uinta-Piceance Assessment Team, 2002), and the assessment province boundary of the Paradox Basin (Whidden, 2012) (fig. 1).

Geologic History

The geologic evolution of the Great Basin has been, and continues to be, a thoroughly studied geologic topic and a bibliography documenting these investigations would be well populated. Cook (1989) mentions no less than 60 publications in the introduction of his review paper on the Great Basin. The reader is referred to the following publications and the extensive references therein to learn more about the basin: Cook (1988, 1989) for its general geology, Parsons (1995) for its geophysical characteristics, and Anna and others (2007) for a review of its hydrocarbon exploration. A generalized stratigraphic column for the basin is provided in figure 17.

This summary of the geologic history of the Great Basin leans heavily on the stages of basin evolution outlined by Cook (1989), which provides a short and clear narrative to the basin's history. As mentioned briefly above, the Great Basin has been affected by a significant number of both collisional tectonic events and, more recently, by extensional rifting events. However, there have also been periods that were relatively quiet in terms of tectonic activity. Precambrian basement rocks of the Great Basin are not well understood, but appear to be a collage of collided continental magmatic arcs and oceanic island arcs (Cook, 1989). Deposited on this basement lies thousands of meters of Belt Supergroup siliciclastic sediments ranging in age from about 1,200 to 900 Ma (Cook, 1989). Fragmentation and rifting began at about 900 to 800 Ma, culminating around 650 Ma with the creation of a passive margin on the western side of the North American craton. Late Proterozoic and Early Cambrian shallow-marine and terrestrial siliciclastic sediments were deposited along the margin and formed a broad continental shelf that, by the Late Cambrian, had shallowed to a shelf-carbonate depositional environment (Cook, 1989). From the Cambrian to Devonian the modern Great Basin area occupied a passive continental margin that accumulated 9,840 to 16,400 ft of shallow-water, shoal, platform, and deep-water carbonates.

After 200 million years of relative stability dominated by carbonate sediment deposition, the third episode of Great Basin evolution was one of tectonic collisions. First, the Late Devonian to Early Mississippian Antler orogeny resulted in the landward thrusting of 60 to 90 mi of the Roberts Mountains allochthon (fig. 16). The Antler orogenic highlands and a foreland basin to the east were formed from the collision. The foreland basin drowned the early Paleozoic carbonate platform during the Mississippian, depositing thousands of feet of siliciclastic sediments on top of the carbonate sediments. Carbonate deposition returned to the margin again in the Pennsylvanian and Permian, paused during the Permian to Triassic Sonoma orogeny, and then

reestablished itself in the Middle to Late Triassic (Cook, 1988, 1989). The Permian through Triassic Sonoma orogeny produced less structural shortening than the Antler orogeny and no foreland basin; however, the thrusting of 40 to 60 mi of the Golconda allochthon was similar to the Antler event. Marine deposition ended in the Jurassic with the beginning of Andean-type subduction tectonics on the western side of Great Basin.

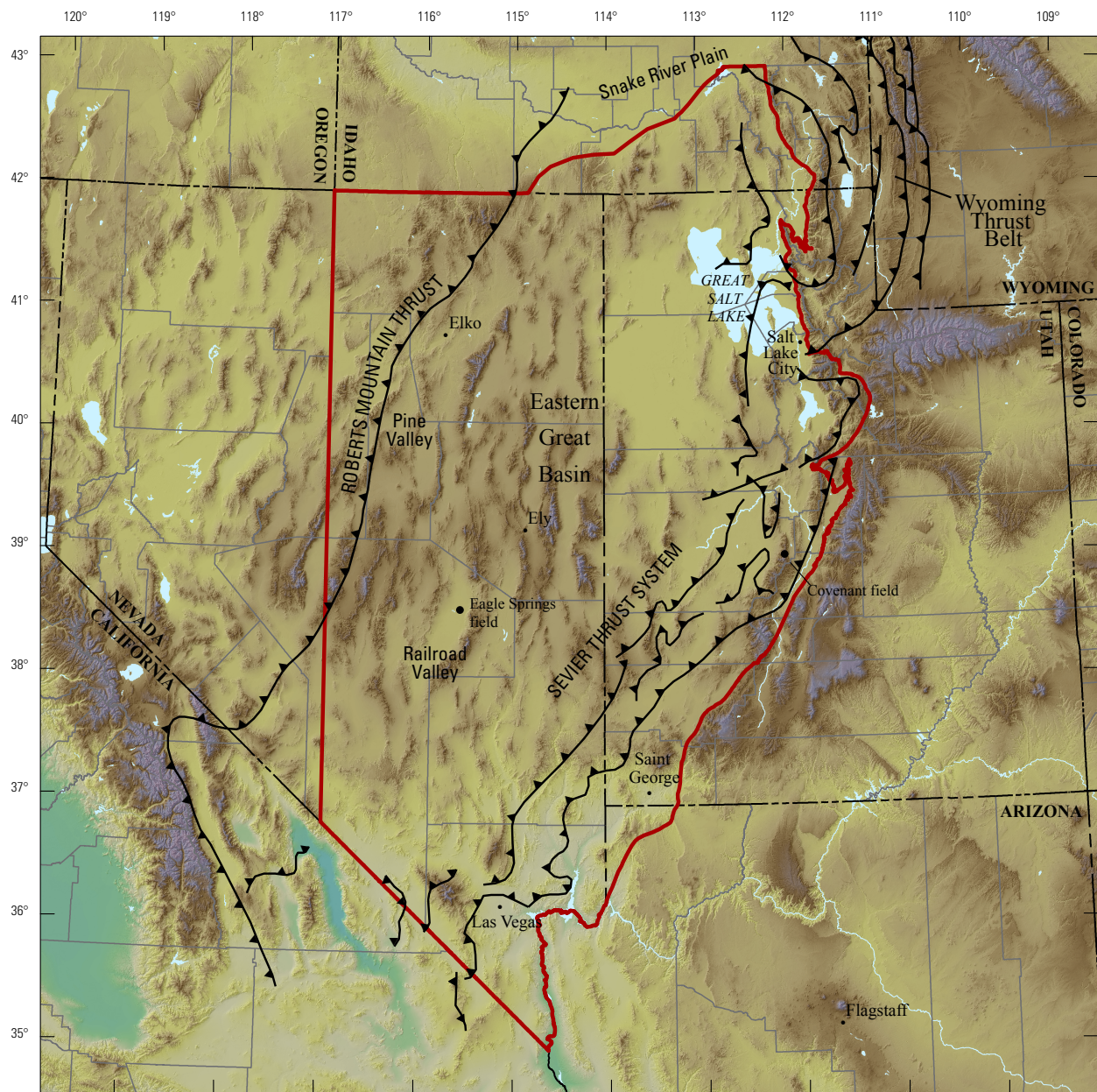
Cretaceous to Eocene subduction of the Pacific plate beneath the North American plate marked the fourth episode of basin evolution. The Andean-type subduction in California produced magmatic arcs and led to the emplacement of batholiths. Although subduction-related magmatism occurred to the west, the Great Basin experienced minor volcanic activity; fluvial, alluvial, and lacustrine accumulation were more common (Cook, 1988). The subduction also created large thrust faults such as the Sevier thrust system with 60 mi of crustal shortening, a feature that dominates the structure of the eastern edge of the Great Basin. The final phase in the formation of today's Great Basin was Oligocene to Holocene crustal extension. Intracontinental rifting and block faulting produced regularly spaced mountains bounded by normal faults and separated by alluvium-filled valleys. Extension and faulting also brought volcanic material to the surface in the form of ignimbrites or ash-flow tuffs.

Hydrocarbon Exploration and Production

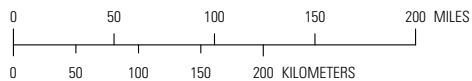
Natural gas in the Great Basin was first discovered on the eastern shore of the Great Salt Lake in the late 1800s during water-well drilling; the gas was subsequently piped to Salt Lake City (Anna and others, 2007). Oil was also discovered during the same period from natural seeps on the eastern shore of Great Salt Lake. Production began at a nearby location, but was eventually shut in because of low production and poor marketability (Anna and others, 2007). Drilling continued near seeps and on anticlines until the first major commercial production began in 1954 in the western half of the Eastern Great Basin at the Eagle Springs field in Railroad Valley, Nye County, Nevada (Peterson and Grow, 1995). Railroad Valley has produced 44 MMBO from nine fields and is the largest producer in the study area; the second largest producing area is Covenant field, Sevier County, Utah, which since its discovery has produced over 15 MMBO through 2011. The third largest producing area is the Pine Valley with four fields yielding a total of 5 MMBO (Anna and others, 2007). Anna and others (2007) list a number of factors to explain the difficulties of past exploration and the relatively low production from this basin; they include (1) complex structures that resulted from massive compressional events followed by more recent extensional tectonics; (2) stacked, structurally segregated carbonate sequences that were difficult to characterize; (3) deposition and differential erosion that lead to complex burial histories; (4) seismic-data acquisition that was complicated by thick, unconsolidated basin fills mixed with volcanic units; (5) remote locations and access issues; and (6) the absence of pipeline infrastructure.

Carbon Dioxide Storage Assessment

Echoing the low potential for hydrocarbon production in the Great Basin, Price and others (2005) concluded in their preliminary assessment of CO₂ sequestration in Nevada that there does not appear to be significant potential for CO₂ sequestration in deep saline aquifers in numerous deep alluvial valleys in Nevada. In addition, LaPointe and others (2007) concluded that the relatively small size of Nevada's oil and gas fields and their generally high thermal gradients suggest that the potential for CO₂ sequestration by enhanced oil recovery (EOR) is low. Investigations by the USGS assessment team focused on two potential SAUs in the Eastern Great Basin: (1) a nonquantitative assessment of the Joana Limestone (C50190101) over much of the study area, and (2) a full quantitative assessment of the Navajo Sandstone (C50190102) in the easternmost Sevier thrust system of the Eastern Great Basin. More detailed descriptions of the two SAUs are provided in the following sections.



Elevation from U.S. Geological Survey
National Elevation Dataset digital elevation
model, 2009, 56-meter resolution
Albers Equal Area Projection
Central meridian 114°30'W



EXPLANATION

▲▲▲ Thrust fault — Sawteeth on upper plate

Eastern Great Basin study area

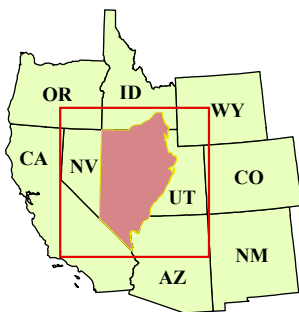


Figure 16. Map showing the Eastern Great Basin study area, including major structural features (modified from Cook and Corboy, 2004; and Anna and others, 2007). Study area boundaries were modified from the U.S. Geological Survey National Oil and Gas Assessment (U.S. Geological Survey Eastern Great Basin Assessment Team, 2005).

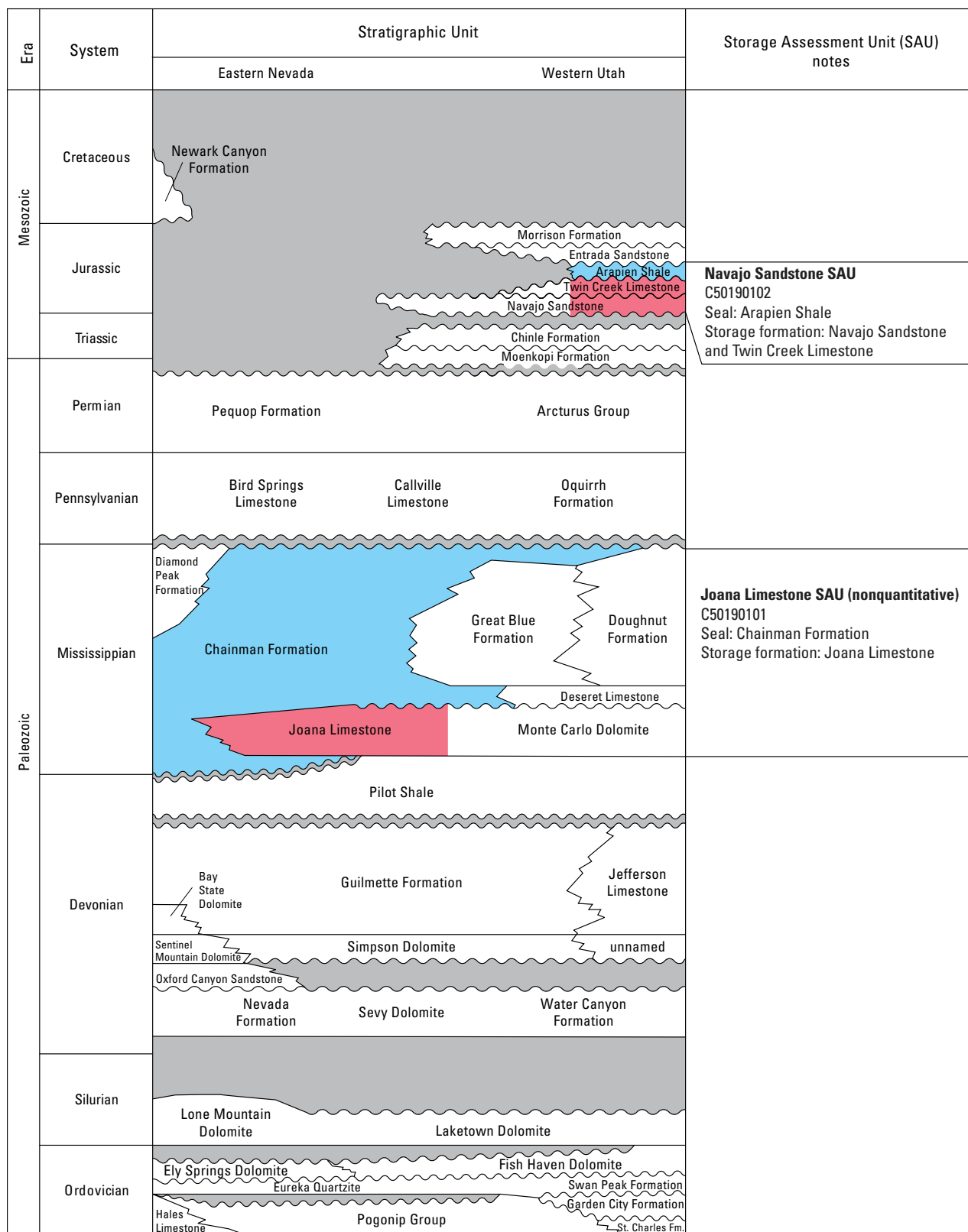


Figure 17. Generalized stratigraphic column of geologic units in the Eastern Great Basin study area of Nevada, Utah, Arizona, and Idaho (modified from Anna and others, 2007). Storage assessment units (SAUs) consist of a storage formation (red) and regional seal (blue). Wavy lines indicate unconformable contacts, and gray areas represent unconformities or hiatuses. Only significant unconformities are shown. In some cases, subdivisions of units or lesser known correlative units are not shown. Abbreviation: Fm., Formation.

Joana Limestone SAU C50190101

By William H. Craddock

The Joana Limestone was deposited on a broad carbonate shelf that formed the western margin of North America during the Mississippian (Poole and Claypool, 1984; Trexler and others, 1996). The continental shelf extended across much of modern Utah and eastern Nevada, and it extended into adjoining regions of Idaho and Montana to the north and Arizona and California to the south (Trexler and others, 1996). The carbonate shelf was separated from the island arc (formed during the Antler orogeny) by a broad ocean basin during the Mississippian (Poole and Claypool, 1984), and open-marine shales accumulated in the intervening ocean basin (Anna and others, 2007). As the Antler arc encroached eastward during the Mississippian, carbonate deposition across the continental shelf gave way to siliciclastic sedimentation (Poole and Claypool, 1984). The Chainman Shale (or Formation) is a regionally extensive shale that overlaps the Joana Limestone across much of eastern Nevada and western Utah. The Chainman may serve as a good caprock for potential CO₂ sequestration storage formations (fig. 17). Significant structural deformation makes it difficult to evaluate the depositional thickness of the Chainman shales, but it may be either as thick as 6,000 ft in the Oquirrh Basin of northwestern Utah or as thin as a few hundred feet in the southern Utah-Nevada border region (Anna and others, 2007). In either case, the depositional thickness appears to be sufficient to contain a relatively large column of CO₂ in the subsurface, although significant fracturing during Mesozoic and Cenozoic tectonism may compromise the quality of the Chainman as a caprock (Anderson and others, 1983).

The area that may be suitable for CO₂ storage in the Joana Limestone is herein defined by the region of probable overlap by the overlying Chainman Formation. Geologic mapping (Hintze, 1974; Nevada Bureau of Mines and Geology, 1999) and stratigraphic information from about 110 boreholes (IHS Energy Group, 2010) suggest that this suitable area occurs in eastern Nevada and western Utah. Across much of this, the Joana appears to be sufficiently deep for supercritical CO₂ storage (fig. 18). However, in many of the narrow, elongate mountain ranges that transect the area, particularly those in eastern Nevada, the rocks may outcrop in fault-bounded blocks. Moreover, there is a structural high along the north-central Nevada-Utah border, above which the entire Phanerozoic sedimentary veneer of the Great Basin region has been eroded (Miller and Gans, 1983).

Complex Mesozoic and Cenozoic structural deformation (Allmendinger and others, 1983) makes it difficult to infer regional patterns in the thickness of the Joana Limestone. However, six measured sections in east-central Nevada exhibit thicknesses ranging from 230 to 830 ft (Gillmore, 1990), and several measured sections to the west exhibit composite thicknesses ranging from 80 to 440 ft (Giles, 1996). Depositional facies within the SAU boundary are likely to include (1) platform shallow-to moderate-water-depth grainstones, packstones, and mudstones; (2) platform-margin high-energy reefs and bioclastic buildup deposits; (3) slope turbidites, debris flows, and mudstone; and (4) deepwater, calcareous mudstones, cherts, shales, and pelagic chalks (Anna and others, 2007). Although it is difficult to generalize about the net thickness of porous rocks within the Joana on a basinwide scale, the platform and platform-margin reef deposits are thought to be the most porous strata (Anna and others, 2007). Moreover, the formation can be subdivided into seven parasequences, and a possible subaerial exposure near the termination of these depositional sequences may have facilitated karstification and the development of zones of high porosity (Giles, 1996; Anna and others, 2007).

Well-log-derived measurements of porosity suggest that, in general, the Paleozoic carbonate shelf and slope rocks in Utah and Nevada exhibit porosities ranging from 0 to 7 percent with a central tendency of approximately 3 percent (Anna and others, 2007). Potential zones of karst porosity (or cavernous pores) may be characterized by high porosity (Choquette and Pray, 1970; Lucia, 1995; Giles, 1996; Anna and others, 2007). Indeed, high karst porosity (10 to 40 percent) has been identified within underlying Silurian carbonates along the Nevada-Utah border (Cook and Corboy, 2004). Devonian carbonate reservoirs in the region, such as the Ghost Ranch field and Blackburn field (LaPointe and others, 2007), exhibit significant fracture porosity, suggesting that there may also be significant fracture porosity in the Joana Limestone in addition to primary or secondary porosity (Anna and others, 2007; LaPointe and others, 2007). Direct measurements of permeability are lacking within the Joana Limestone and (or) other Paleozoic carbonate reservoirs within the Great Basin. However, global analogs of carbonate reservoirs suggest that the permeability may be highly variable across the basin, ranging over several orders of magnitude, from ≤ 0.1 mD to $\geq 1,000$ mD (Lucia, 1995). The rocks with generally low matrix porosity are also likely to be characterized by relatively low permeability, perhaps 10 mD or less (Lucia, 1995). Zones of fracture porosity are likely to exhibit corresponding high permeability.

At a regional scale, the quality of the formation waters within the Joana Limestone is poorly defined. However, concentration measurements of total dissolved solids (TDS) from fractured Devonian carbonate reservoirs suggest the potential for relatively fresh and potentially potable formation waters (approximately 1,000 to 5,000 ppm TDS), as well as waters that are too saline to serve as a drinking water supply ($>15,000$ ppm TDS) (LaPointe and others, 2007).

Although the basic qualities of the Joana Limestone (a moderately porous reservoir rock overlain by thousands of feet of shale) appear to be favorable to CO₂ storage, it should be emphasized that the unit is unproven. A compilation of oil and gas

production data from the State of Nevada suggests that none of the oil fields in the State are sufficiently large to accommodate all of the CO₂ emissions from a large coal-fired power plant (LaPointe and others, 2007), and the porosity, permeability, and seal quality of the Joana in any one location may be unfavorable for CO₂ containment. New and detailed site characterization would be required to develop a potential CO₂ disposal site.

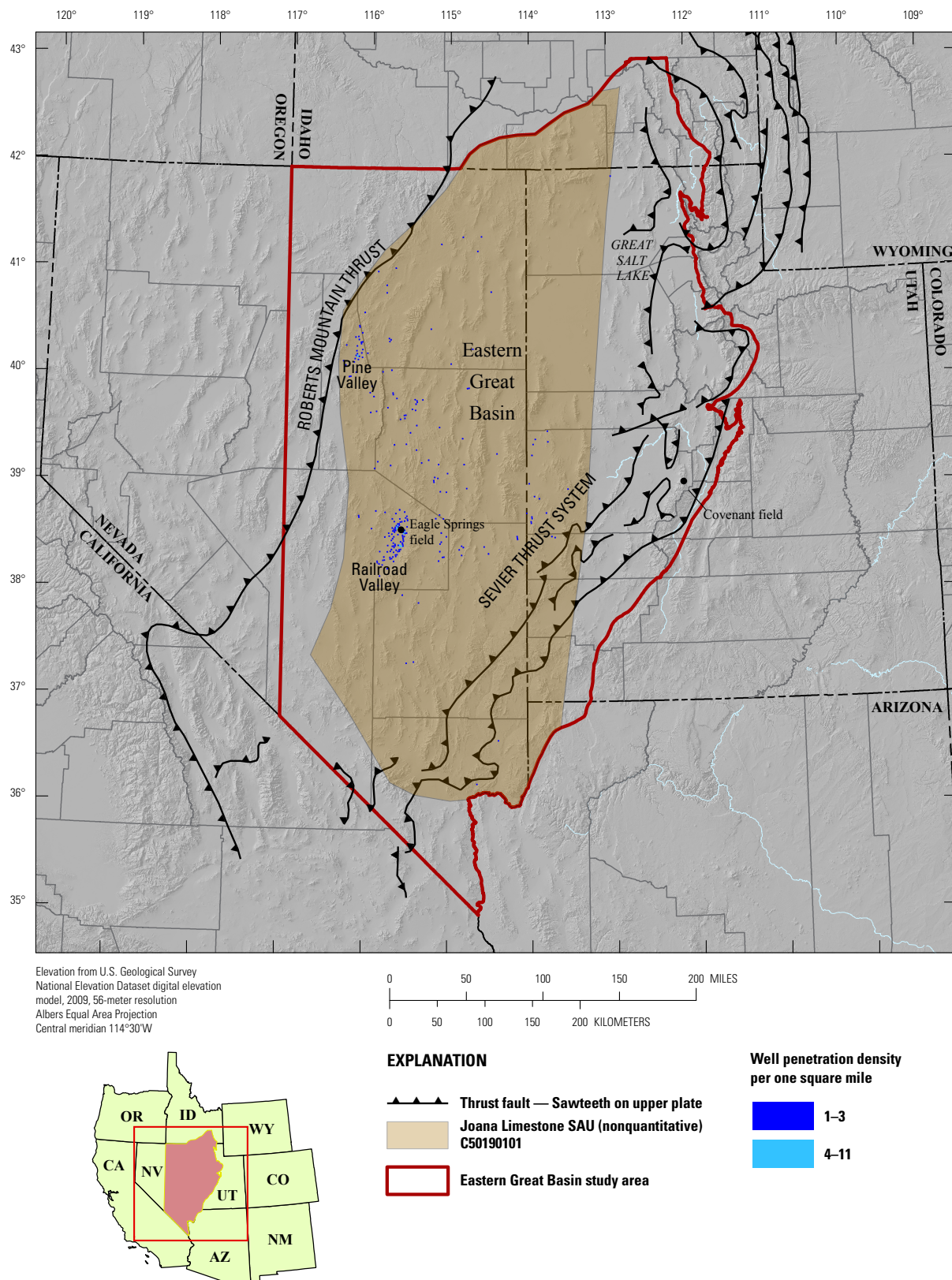


Figure 18. Map of the Joana Limestone nonquantitative C50190101 Storage Assessment Unit (SAU) in the Eastern Great Basin. Well penetration density is the number of wells (per 1-square-mile grid cell) derived from the ENERDEQ well database (IHS Energy Group, 2011) that have penetrated the top of the storage formation. Study area boundaries were modified from the U.S. Geological Survey National Oil and Gas Assessment (U.S. Geological Survey Eastern Great Basin Assessment Team, 2005). Abbreviation: ft, feet.

Navajo Sandstone SAU C50190102

By Ronald M. Drake II and Matthew D. Merrill

The Navajo Sandstone SAU is limited to the eastern edge of the Eastern Great Basin study area along the boundary between the Basin and Range physiographic province and the Colorado Plateau (fig. 19). This boundary region corresponds to the Sevier thrust system area in Utah has been referred to as the Utah hingeline by Chidsey and Sprinkel (2007) and authors cited therein. Although the storage formations in the SAU extend over large portions of the Eastern Great Basin study area, the SAU is restricted to the known mapped geographic extent of the sealing formation, the Middle Jurassic Arapien Shale. The Arapien was deposited on the western side of a shallow epicontinental ancestral sea known as the Carmel-Twin Creek Seaway, which covered most of Utah and parts of Wyoming and Montana (de Gibert and Ekdale, 2002) (fig. 17). The Arapien is roughly 2,000 to 10,000 ft thick and is composed of calcareous mudstones, gypsiferous shaly siltstone, fine-grained sandstone, arenaceous limestone, and evaporites (Sprinkel, 1982). Within the SAU at the Covenant field, the Arapien is 4,800 ft thick due to intraformational thrusting and salt diapirism (Chidsey and others, 2007) (fig. 19). As in many basins, the stratigraphic nomenclature has evolved over time; for an explanation see Sprinkel (1982). The Arapien Shale lies on top of the Twin Creek Limestone, which in turn overlies the Navajo Sandstone. Anna and others (2007) note that lithologic descriptions of the Arapien Shale in central Utah from Sprinkel (1982) did not identify it as a hydrocarbon source rock, but indicated it to be an excellent seal to oil leaking from underlying reservoirs.

The Arapien Shale acts as the confining layer for two Jurassic storage formations, the Navajo Sandstone and Twin Creek Limestone (fig. 17). Located throughout Utah, the Navajo Sandstone is equivalent to the Nugget Sandstone to the north in Wyoming and Idaho and equivalent to the Aztec Sandstone in southern Nevada (Baker and others, 1936; Peterson, 1972). Noted for its curved, cliff-forming, and crossbedded outcrops throughout the southwest, the Navajo Sandstone is an eolian sand dune deposit from an environment similar to today's Sahara Desert (Chidsey and Sprinkel, 2007). The Twin Creek Limestone extends over much of the thrust belt region of north-central Utah and western Wyoming and is characterized by gray limestones with minor red siltstone, sandstone, gypsum, and anhydrite (Sprinkel, 1982). Although the formation has been subdivided into multiple members, such level of detail is not necessary for a review of this scale; see Sprinkel (1982) for more details.

Boundaries for the Navajo Sandstone SAU encompass approximately 850,000 acres and are limited to the extent of the Arapien Shale as determined using well-based formation-top information from a proprietary database by IHS Energy Group (2011) (fig. 19). Depth to the top of the shallowest storage formation (the Twin Creek Limestone) ranges from 4,000 to 13,000 ft, with an average depth from the surface across the SAU of about 7,000 ft (IHS Energy Group, 2011). A combination of well-based thicknesses from the Covenant field and an interpolation of thickness across the SAU from other well records yields combined thicknesses for the two storage formations ranging from 1,200 to 1,600 ft (Chidsey and others, 2007; IHS Energy Group, 2011). Only 300 to 500 ft (with the most likely being 400 ft) of that total thickness consists of porous sandstones that could be used to store CO₂ (Chidsey and others, 2007). Reservoir properties such as porosity and permeability determine the availability of the pore space in the rock for storage and the potential for movement of the CO₂ once injected, respectively. Chidsey and others (2007) indicated that, across six different lithofacies in the Navajo Sandstone, average porosity ranged from 5 to 13 percent, with a central value of 8 percent. The same dataset revealed that Navajo permeability has a minimum value of 0.01 mD, a most likely value of 1 mD, and a maximum of 300 mD. Water-quality information was not available for the Twin Creek Limestone; however, limited data for the Navajo Sandstone indicate that the formation water is both above and below the EPA's USDW maximum limit of 10,000 ppm TDS. It is estimated that 70 percent of the SAU's area contains saline water ($\geq 10,000$ ppm TDS); however, this area could be as small as 20 percent or as large as 100 percent of the SAU (Breit, 2002; Chidsey and others, 2007).

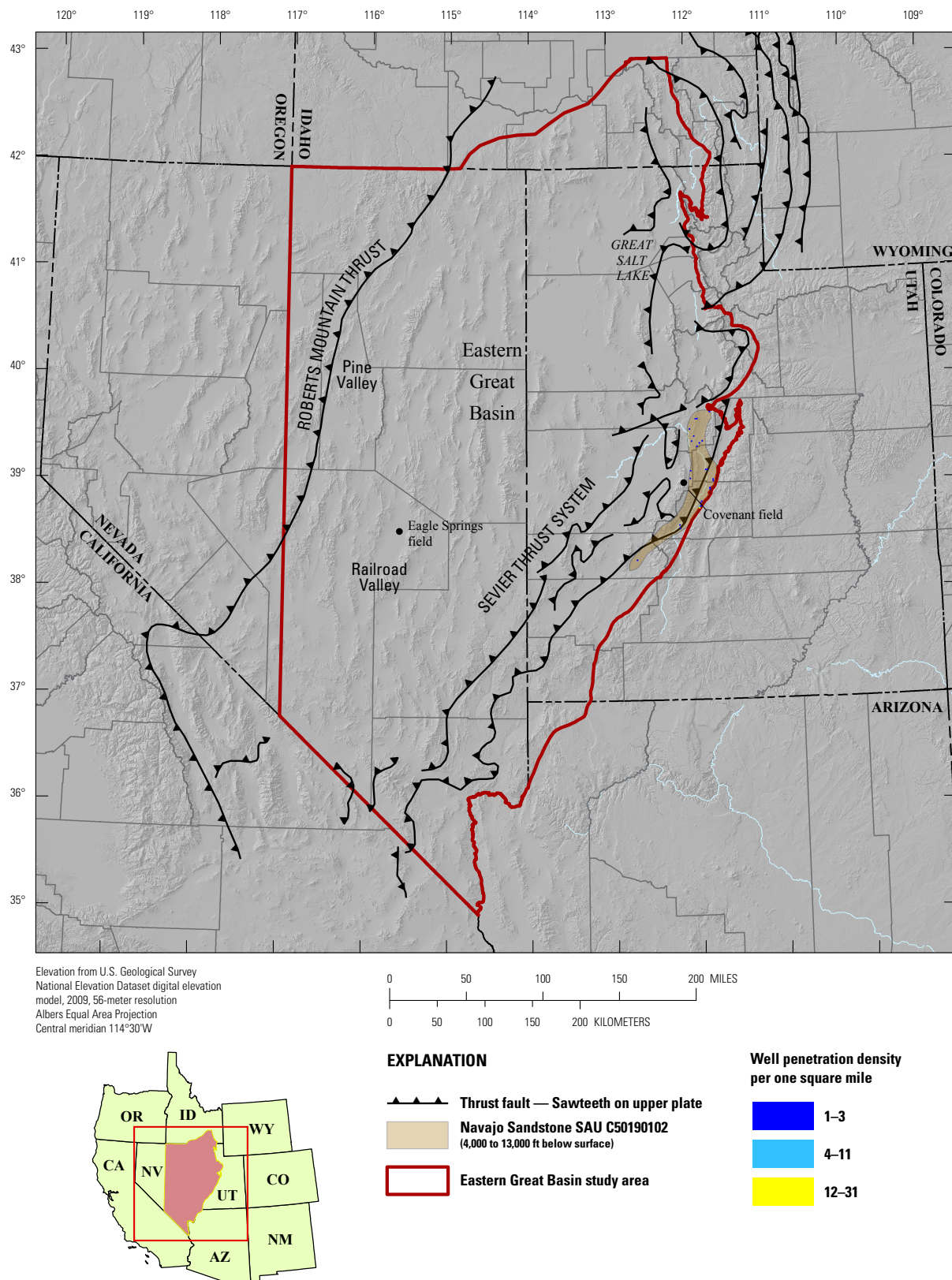


Figure 19. Map of the Navajo Sandstone C50190102 Storage Assessment Unit (SAU) in the Eastern Great Basin. Well penetration density is the number of wells (per 1-square-mile grid cell) derived from the ENERDEQ well database (IHS Energy Group, 2011) that have penetrated the top of the storage formation. Study area boundaries were modified from the U.S. Geological Survey National Oil and Gas Assessment (U.S. Geological Survey Eastern Great Basin Assessment Team, 2005). Abbreviation: ft, feet.

Raton Basin

By Matthew D. Merrill

Introduction and Geologic History

The Raton Basin is an asymmetrical basin that formed during the Laramide orogeny (Late Cretaceous through Eocene) in the Southern Rocky Mountains. Its northern half is in Colorado and southern half in New Mexico, and it is bounded on the west by the Sangre de Cristo Mountains, on the north by the Wet Mountains and Apishapa arch, on the east by the Las Animas arch, Sierra Grande arch, and on the southwest by the Cimarron uplift. The basin includes a study area of approximately 2,913,000 acres (fig. 20). The geology and resource potential of the Raton Basin is thoroughly discussed by various authors (Shaw, 1958; Baltz, 1965; Woodward, 1983; Higley, 2007) and is not restated here with the exception of the following brief summary.

Like many Laramide orogenic basins in the Rocky Mountains, the Raton was formed by crustal movement on preexisting structural elements established during the Pennsylvanian Period during the uplift of the Ancestral Rocky Mountains (Baltz, 1965). Devonian through Tertiary sedimentary units are present in the Raton Basin with crystalline basement rock below these sediments (fig. 21). In general, the stratigraphy and depositional environments of the Raton Basin are similar to those of other southern Rocky Mountain and southwestern interior basins. A thin discontinuous interval of Mississippian carbonate strata is presumed to be present in the Raton Basin on the basis of its discontinuous presence in the Sangre de Cristo Mountains to the west (Woodward, 1983). During the Pennsylvanian, the area of the Raton Basin was part of a much larger feature called the central Colorado trough, which received sediments from transgressing and regressing Pennsylvanian seas (Shaw, 1958). Permian deposits are similar to those in adjacent basins and include arid marginal-marine sandstones, shales, and limestones of the Yeso Formation, Glorieta Sandstone, and San Andreas Limestone. The Jurassic interval consists of mainly claystones, mudstones, siltstones, and sandstones deposited in alluvial and flood-plain environments (Baltz, 1965; Woodward, 1983). Cretaceous rocks in the Raton Basin were deposited along the southwestern margin of the Western Interior Seaway and range from fluvial and coastal sandstones to shallow carbonates and deeper-water shales. Late Cretaceous and early Tertiary strata have been identified by various authors as documenting the initial stages of the Laramide orogeny in the Raton Basin (Higley, 2007). Thrusting and uplifting changed the topography of the region, and the retro-arc foreland depositional environment of the Cretaceous was replaced by a more fluvial and lacustrine dominated environment with multiple sources of sediments from the newly uplifted mountains (Dolly and Meissner, 1977).

Hydrocarbon and Carbon Dioxide Exploration and Production

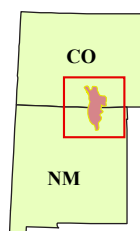
Woodward (1983) cites early gas shows in the Cretaceous Dakota Sandstone from the late 1970s; however, production was considered to be disappointing early on. The dominance of terrigenous rocks over generally more productive marine sandstones and a lack of deeper tests have been mentioned as possible explanations for poor hydrocarbon productivity. The majority of hydrocarbon production comes from coalbed methane in the Vermejo and Raton Formations of the Upper Cretaceous to middle Paleocene age (Higley, 2007). Production in the Raton Basin oil and gas province totaled approximately 4,325 barrels of oil, 300 BCFG, and 3,570 billion cubic feet of CO₂ cumulatively by 2003 (Higley, 2007). Sheep Mountain and Little Sheep Mountain are laccoliths that intruded into the sedimentary sequence during the Eocene; these mountains host fields that produce CO₂ from the Dakota and Entrada Sandstones below the intrusion, which is used for enhanced oil recovery in western Texas fields (Roth, 1983). The Oakdale field, approximately 12 mi to the south of Gardner, Colorado, also contains CO₂ in the Dakota and Entrada as well as in igneous rock reservoirs (Worrall, 2004). Higley (2007) stated that more than 635 wells in the northwestern part of the basin produce CO₂ from strata ranging from the Pennsylvanian to Permian Sangre de Cristo Formation to the Lower Cretaceous Dakota Sandstone.

Carbon Dioxide Storage Assessment

The USGS Geologic Carbon Dioxide Storage Resources Assessment Team investigated and ultimately assessed one storage assessment unit (SAU), the Dakota Sandstone SAU. However, the assessment geologist and panel determined that, although the SAU contained great potential for storage, the groundwater in the potential storage formation did not meet EPA requirements for injecting CO₂ because it is potentially potable (<10,000 ppm TDS). Therefore, the Dakota Sandstone SAU in the Raton Basin is a nonquantitatively (rather than quantitatively) assessed unit. Details of the Dakota Sandstone SAU are provided in the following section.



EXPLANATION



Raton Basin study area

Figure 20. Map showing the Raton Basin study area, including major structural features (modified from Higley, 2007). Study area boundaries were modified from the U.S. Geological Survey National Oil and Gas Assessment (U.S. Geological Survey Raton Basin-Sierra Grande Uplift Province Assessment Team, 2005).

Era	System/Series	Stratigraphic unit	Storage Assessment Unit (SAU) notes	
Cenozoic	Holocene	alluvium, dunes, landslides, soil zones	<div>Dakota Sandstone SAU (nonquantitative) C50410101 Seal: Graneros Shale, Greenhorn Limestone and Carlile Shale Storage formation: Dakota Sandstone</div>	
	Pleistocene	Ogallala Formation		
	Pliocene			
	Miocene	Devils Hole Fm. volcanic intrusions, plugs, dikes, and sills intrude entire section		
	Oligocene	Farasita Formation		
	Eocene	Huerfano Formation		
		Cuchara Formation		
	Paleocene	Poison Canyon Formation		
		Raton Formation		
	Mesozoic	Cretaceous		Vermejo Formation
Trinidad Sandstone				
Pierre Shale				
Niobrara				Smoky Hill Marl
				Fort Hayes Limestone
				Codell Sandstone
Benton				Carlile Shale
				Greenhorn Limestone
				Graneros Shale
Dakota Sandstone				
Jurassic		Morrison Formation Wanakah Formation Entrada Sandstone		
Triassic		Dockum Group		
Paleozoic	Permian	Bernal Formation		
		San Andres Limestone		
		Glorieta Sandstone		
		Yeso Formation		
		Sangre de Cristo Formation		
	Pennsylvanian	Magdalena Group		
	Mississippian	Tererro Formation		
Devonian	Espiritu Santo Formation			
Precambrian		mafic gneiss metaquartzite group granite and granite gneiss		

Figure 21. Generalized stratigraphic column of geologic units in the Raton Basin study area of Colorado and New Mexico (modified from Higley, 2007). Storage assessment units (SAUs) consist of a storage formation (red) and regional seal (blue). Wavy lines indicate unconformable contacts, and gray areas represent unconformities or hiatuses. Only significant unconformities are shown. In some cases, subdivisions of units or lesser known correlative units are not shown. Abbreviation: Fm., Formation.

Dakota Sandstone SAU C50410101

By William H. Craddock

The Dakota Sandstone of the Raton Basin was deposited in the earliest part of the Cretaceous (fig. 21), in the west-central portion of the ancestral Western Interior Seaway during the Sevier orogeny (McGookey, 1972). The unit consists of fluvial-floodplain and marine deltaic strata (Baltz, 1965) derived from the Sevier hinterland to the west (McGookey, 1972). The Dakota Sandstone conformably overlies the Cretaceous Purgatoire Formation, a relatively fine-grained deposit (Baltz, 1965) that appears to be similar in origin to the Dakota Sandstone; in many regional subsurface studies, the Dakota Sandstone and the Purgatoire Formation are undifferentiated (Clark, 1977; Broadhead, 2008). The unit is overlain by several hundred feet of Cretaceous shale and marl and minor amounts of sandstone (from oldest to youngest) of the Graneros Shale, Greenhorn Limestone, Carlile Shale, and the Codell Sandstone (Baltz, 1965; Clark, 1977) (fig. 21). These overlying units are generally open-marine shales and limestones that were deposited during a time of shoreline transgression in the Western Interior Seaway (Baltz, 1965; Higley, 2007). All of these rocks are ultimately overlain by the Pierre Shale, which is in excess of 2,000 ft thick in parts of Raton Basin and was also deposited in an open-marine environment (Baltz, 1965; Higley, 2007). Given the great thickness of fine-grained units overlying the Dakota Sandstone, reservoirs within the Dakota should have a robust top seal. Naturally occurring CO₂ is produced from the Dakota Sandstone in the Sheep Mountain field (Higley, 2007) along the northwest flank of the basin, further attesting to the quality of the top seal of the Lower Cretaceous strata overlying the Dakota Sandstone (fig. 20).

Although there is little information on the quality of Dakota Sandstone reservoirs in the Raton Basin, rock property measurements from similar nearby basins (Piceance and San Juan Basins on fig. 1; and also the Denver Basin) indicate that the Dakota Sandstone may have favorable storage formation porosity and permeability for CO₂ injection and storage (IHS Energy Group, 2010) (fig. 22). Approximately 500 reservoir-averaged porosity measurements suggest that a reasonable average porosity for the Dakota is between 8 and 16 percent. Similar field-averaged measurements suggest that permeability ranges from 0.1 to 300 mD and that a reasonable average formation porosity is approximately 50 mD. Moreover, based on a regional network of 15 geophysical logs that extends across most of Raton Basin, the Dakota Sandstone has an estimated regional average gross thickness of about 200 ft and an average net sandstone thickness of about 150 ft in the depth range most appropriate for subsurface CO₂ storage (approximately 3,000 to 13,000 ft; Brennan and others, 2010) (Baltz, 1965; Clark, 1977; Broadhead, 2008). Notably, these thickness measurements include both the Dakota Sandstone and the Purgatoire Formation because they are generally undifferentiated in regional subsurface studies (Clark, 1977; Broadhead, 2008). There may be potential for additional storage formation intervals of 10 to 100 ft locally within the overlying Greenhorn Limestone and (or) the Codell Sandstone (both of which underlie the Pierre Shale).

The Dakota Sandstone of Raton Basin, however, appears to contain formation waters with concentrations <10,000 ppm TDS, which is below the USDW maximum limit of 10,000 ppm, and therefore considered potentially potable (U.S. Environmental Protection Agency, 2009). One measurement from a groundwater-quality database (Breit, 2002) for the Dakota Sandstone indicates the presence of fresh formation waters, with a TDS concentration of 3,055 ppm. A regional aquifer study of Lower Cretaceous sandstones indicates that the most likely TDS concentration is approximately 800 ppm (Miller and others, 2010), with the middle 50th percentile of formation waters in the Dakota Sandstone ranging from approximately 400 ppm to 1,500 ppm TDS. There is no proven saline groundwater in the Dakota Sandstone in the Raton Basin; therefore, it is not clear if it is a permissible CO₂ injection target. For this reason, quantifying the pore volume within the Dakota Sandstone SAU that may be accessible for CO₂ storage was not attempted during this assessment (fig. 22); however, the natural accumulations of CO₂ in the formation, as well as the favorable storage formation properties and high sandstone thickness within the Dakota Formation of the Raton Basin (Higley, 2007), do suggest the potential for this unit to be a target for CO₂ storage.

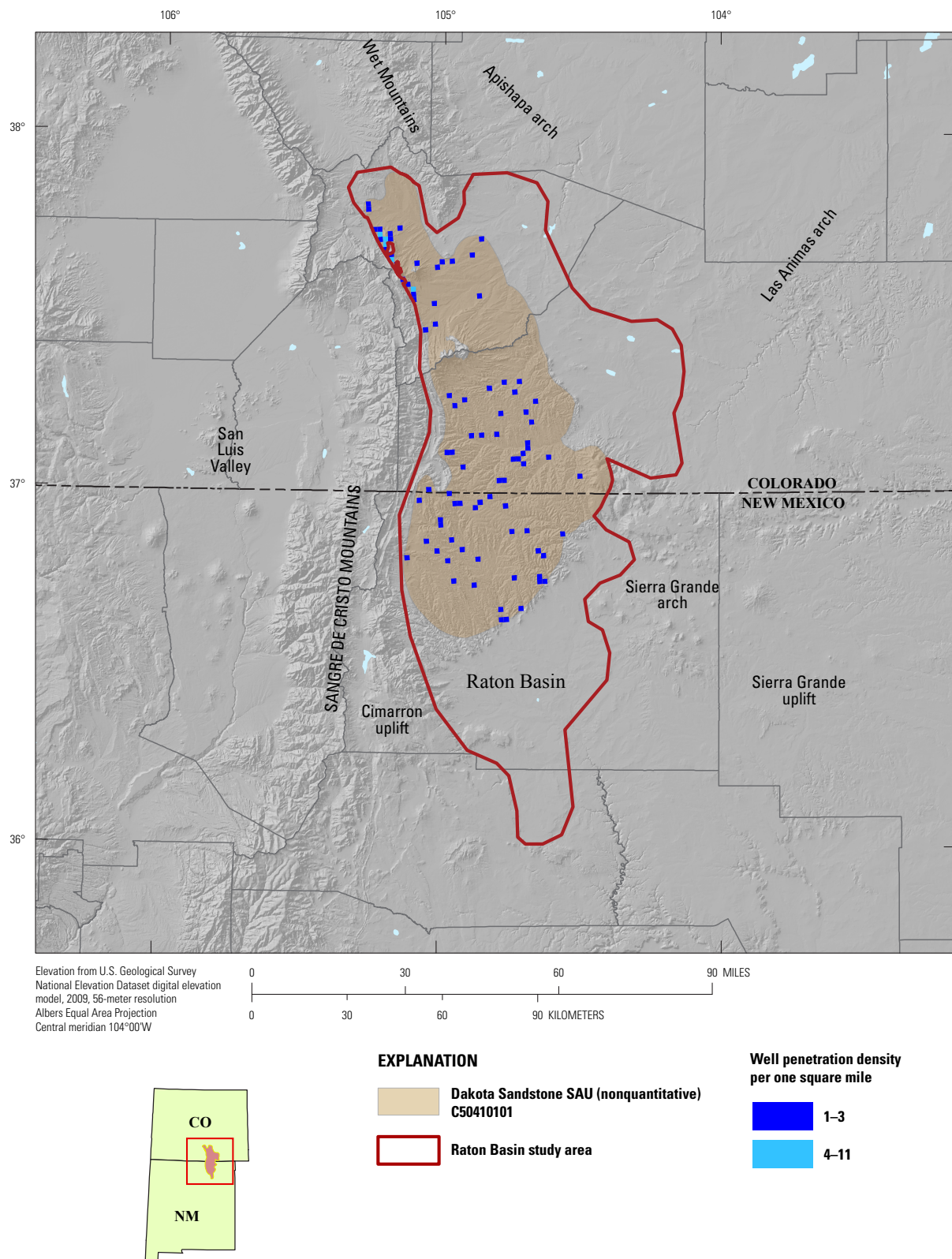


Figure 22. Map of the Dakota Sandstone C50410101 Storage Assessment Unit (SAU) in the Raton Basin. Well penetration density is the number of wells (per 1-square-mile grid cell) derived from the ENERDEQ well database (IHS Energy Group, 2011) that have penetrated the top of the storage formation. Study area boundaries were modified from the U.S. Geological Survey National Oil and Gas Assessment (Higley, 2007). Abbreviation: ft., feet.

Black Mesa Basin

By Peter D. Warwick, Ronald M. Drake II, Sean T. Brennan, and Matthew D. Merrill

The Black Mesa Basin of northeastern Arizona (fig. 1) is located in the southwestern part of the Colorado Plateau and contains gently dipping to slightly folded Paleozoic and Mesozoic sedimentary rocks that overlie a Precambrian basement composed of metasedimentary, metamorphic, and igneous rocks (Lessentine, 1965; Butler, 1995; Rauzi and Spencer, 2012, 2014). Rauzi and Spencer (2012, 2014) evaluated the basin to identify potential CO₂ storage formations. They identified four Paleozoic sandstone units as having potential for CO₂ storage: the Cambrian Tapeats Sandstone, Devonian McCracken Sandstone, and Permian De Chelly Sandstone in their 2012 report, and the Permian Cedar Mesa Sandstone in their 2014 report. The Black Mesa Basin was evaluated during this assessment for potential storage assessment units (SAUs) following the criteria outlined in Brennan and others (2010) and Blondes and others (2013). The three formations identified by Rauzi and Spencer (2012) and accompanying seal formations did not meet the assessment criteria used by the USGS Geologic Carbon Dioxide Storage Resources Assessment Team. The oldest potential SAU, the Tapeats Sandstone (storage) and overlying Bright Angel Shale (seal), did not meet the criteria because of the extremely low porosity of 1.2 to 2.4 percent for the Tapeats (Rauzi and Spencer, 2012). The next potential SAU consisting of the McCracken Sandstone (storage) and the Elbert Formation and Ouray Limestone (seal) was not assessed because units composed of mixed carbonate rock, sandstone, and shale (Elbert Formation), and units composed of carbonate rock (Ouray Limestone), were not typically identified as sealing units by the USGS assessment geologists. The third potential SAU from Rauzi and Spencer's 2012 report, the De Chelly Sandstone (storage) and Moenkopi and Chinle Formations (seal) was not assessed because these seal formations were not considered to be adequate seals in any portion of the Colorado Plateau, according to the assessment criteria.

Following completion and publication of the USGS National Assessment of Geologic Carbon Dioxide Storage Resources (U.S. Geological Survey Geologic Carbon Dioxide Storage Resources Assessment Team, 2013), Rauzi and Spencer (2014) reported the results of a new evaluation of the Black Mesa Basin, which focused on the Permian Cedar Mesa Sandstone (storage) and the overlying Organ Rock Formation (seal). The Organ Rock Formation is predominantly a tight, orange to brown, very argillaceous, very fine grained, sandy siltstone interbedded with thin shale (Rauzi and Spencer, 2014). Following the methodology established by Brennan and others (2010), siltstone is not a recommended lithology for a sealing formation; however, if rock properties suggest that vertical and horizontal permeabilities are within the ranges required to properly contain CO₂, then such a seal would be a viable part of an SAU. Rauzi and Spencer (2014) did not include evidence of the confining properties of the Organ Rock Formation; therefore, although this assessment recognized that geologic storage of CO₂ may be possible in some areas of the Black Mesa Basin, additional data describing the permeability of the seal and regarding the extent of both the seal and storage formation across the potential storage area mapped by Rauzi and Spencer (2014) are still required to satisfy the specific guidelines for inclusion in the USGS assessment. Based on currently available data, no other potential storage formations were identified in the Black Mesa Basin.

Acknowledgments

State cooperative agreements (principal investigators in parenthesis) with Arizona (Jon Spencer and Steven Rauzi), Colorado (Chris Carroll), Idaho (John Kauffman), New Mexico (Ronald Broadhead and Dana Ulmer-Scholle), and Utah (David Tabet) provided valuable data and knowledge towards the assessments of these basins. We thank Joe East for administering the USGS State cooperative agreements. The content and presentation of this report benefited greatly from the technical reviews by Ronald C. Johnson and David Tabet.

References Cited

Allis, R.G., Chidsey, T.C., Gwynn, W., Morgan, C., White, S., Adams, M., and Moore, J., 2001, Natural CO₂ reservoirs on the Colorado Plateau and Southern Rocky Mountains—Candidates for CO₂ sequestration, *in* Proceedings of the First National Conference on Carbon Sequestration: National Energy Technology Laboratory, Washington, D.C., U.S.A., May 15–17, 2001, 19 p., accessed December 23, 2015, at http://www.netl.doe.gov/publications/proceedings/01/carbon_seq/6a2.pdf.

- Allmendinger, R.W., Sharp, J.W., Von Tish, D., Serpa, L., Brown, L., Kaufman, S., Oliver, J., and Smith, R.B., 1983, Cenozoic and Mesozoic structure of the eastern Basin and Range province, Utah, from COCORP seismic-reflection data: *Geology*, v. 11, no. 9, p. 532–536.
- Anderson, P.B., and Ryer, T.A., 2004, Regional stratigraphy of the Ferron Sandstone, *in* Chidsey, T.C.J., Adams, R.D., and Morris, T.H., eds., *Analog for fluvial-deltaic reservoir modeling—Ferron Sandstone of Utah*: American Association of Petroleum Geologists, *Studies in Geology* 50, p. 211–224.
- Anderson, R.E., Zoback, M.L., and Thompson, G.A., 1983, Implications of selected subsurface data on the structural form and evolution of some basins in the northern Basin and Range province, Nevada and Utah: *Geological Society of America Bulletin*, v. 94, no. 9, p. 1055–1072.
- Anna, L.O., Roberts, L.N., and Potter, C.J., 2007, Geologic assessment of undiscovered oil and gas in the Paleozoic–Tertiary composite total petroleum system of the eastern Great Basin, Nevada and Utah, chap. 2 *of* U.S. Geological Survey Eastern Great Basin Assessment Team, comps., *Geologic assessment of undiscovered oil and gas resources of the Eastern Great Basin Province, Nevada, Utah, Idaho, and Arizona*: U.S. Geological Survey Digital Data Series DDS–69–L, 55 p., accessed June 26, 2012, at http://pubs.usgs.gov/dds/dds-069/dds-069-1/REPORTS/69_L_CH_2.pdf.
- Armstrong, A.K., and Holcomb, L.D., 1989, Stratigraphy, facies, and paleotectonic history of Mississippian rocks in the San Juan Basin of northwestern New Mexico and adjacent areas, *in* *Evolution of sedimentary basins, San Juan Basin*: U.S. Geological Survey Bulletin 1808–D, p. D1–D21. [Also available at <http://pubs.usgs.gov/bul/1808b-d/report.pdf>.]
- Arnold, E.C., 1974, Oil and gas development and production, eastern San Juan Basin, *in* Siemers, C.T., Woodward, L.A., and Callender, J.F., eds., *Ghost Ranch: New Mexico Geological Society 25th Annual Fall Field Conference Guidebook*, p. 323–328.
- Aubrey, W.M., 1991, Geologic framework of Cretaceous and Tertiary rocks in the Southern Ute Indian Reservation and adjacent areas in the northern San Juan Basin, southwestern Colorado, *in* Zech, R.S., ed., *Geology and mineral resources of the Southern Ute Indian Reservation*: U.S. Geological Survey Professional Paper 1505–B, p. B1–B24. [Also available at <https://pubs.er.usgs.gov/publication/pp1505A>.]
- Ayers, W.B., Ambrose, W.A., and Yeh, J.S., 1994, Coalbed methane in the Fruitland Formation, San Juan Basin—Depositional and structural controls on occurrence and resources, *in* Ayers, W.B., and Kaiser, W.R., eds., *Coalbed methane in the Upper Cretaceous Fruitland Formation, San Juan Basin, New Mexico and Colorado*: New Mexico Bureau of Mines and Mineral Resources Bulletin 146, p. 13–40.
- Baars, D.L., 1972, Devonian System, *in* Mallory, W.W., ed., *Geologic atlas of the Rocky Mountain region*: Denver, Colo., Rocky Mountain Association of Geologists, p. 90–99.
- Baars, D.L., and Stevenson, G.M., 1981, Tectonic evolution of the Paradox Basin, Utah and Colorado, *in* Wiegand, D.L., ed., *Geology of the Paradox Basin*: Denver, Colo., Rocky Mountain Association of Geologists, p. 23–31.
- Baker, A.A., Dane, C.H., and Reeside, J.B., Jr., 1936, Correlation of the Jurassic formations of parts of Utah, Arizona, New Mexico and Colorado: U.S. Geological Survey Professional Paper 183, 66 p., 26 pls., accessed December 23, 2015, at <http://pubs.usgs.gov/pp/0183/report.pdf>.
- Baltz, E.H., 1965, Stratigraphy and history of Raton Basin and notes on San Luis Basin, Colorado–New Mexico: *American Association of Petroleum Geologists Bulletin*, v. 49, no. 11, p. 2041–2075.
- Barbeau, D.L., 2003, A flexural model for the Paradox Basin—Implications for the tectonics of the Ancestral Rocky Mountains: *Basin Research*, v. 15, no. 1, p. 97–115.
- Barker, C.E., Fouch, T.D., Grow, J.A., and Peterson, J.A., 1995, Western Great Basin Province (018), *in* Gautier, D.L., Dolton, G.L., Takahashi, K.I., and Varnes, K.L., eds., *1995 National assessment of United States oil and gas resources—Results, methodology, and supporting data*: U.S. Geological Survey Digital Data Series DDS–30, 13 p.
- Beaumont, E.C., and Read, C.B., 1950, Geologic history of the San Juan Basin area, New Mexico and Colorado, *in* Kelley, V.C., Beaumont, E.C., and Silver, C., eds., *San Juan Basin, New Mexico and Colorado*: New Mexico Geological Society 1st Annual Fall Field Conference Guidebook, p. 49–54.

- Blondes, M.S., Brennan, S.T., Merrill, M.D., Buursink, M.L., Warwick, P.D., Cahan, S.M., Cook, T.A., Corum, M.D., Craddock, W.H., DeVera, C.A., Drake, R.M., II, Drew, L.J., Freeman, P.A., Lohr, C.D., Olea, R.A., Roberts-Ashby, T.L., Slucher, E.R., and Varela, B.A., 2013, National assessment of geologic carbon dioxide storage resources—Methodology implementation: U.S. Geological Survey Open-File Report 2013–1055, 26 p., accessed May 29, 2013, at <http://pubs.usgs.gov/of/2013/1055/>.
- Blondes, M.S., and Gosai, M.A., 2011, An expanded Wyoming water quality database [abs.]: American Association of Petroleum Geologists Rocky Mountain Section, Annual Meeting, Cheyenne, Wyo., June 25–29, at http://www.searchanddiscovery.com/abstracts/pdf/2011/rocky/abstracts/ndx_blondes.pdf.
- Bowker, K.A., and Jackson, W.D., 1989, The Weber Sandstone at Rangely field, Colorado, *in* Coalson, E.B., and others, eds., Petrogenesis and petrophysics of selected sandstone reservoirs of the Rocky Mountain region: Denver, Colo., Rocky Mountain Association of Geologists, p. 65–80.
- Breit, G.N., 2002, Produced waters database: U.S. Geological Survey database accessed May 20, 2011, at <http://energy.cr.usgs.gov/prov/prodwat/>.
- Brennan, S.T., Burruss, R.C., Merrill, M.D., Freeman, P.A., and Ruppert, L.F., 2010, A probabilistic assessment methodology for the evaluation of geologic carbon dioxide storage: U.S. Geological Survey Open-File Report 2010–1127, 31 p., accessed September 22, 2013, at <http://pubs.usgs.gov/of/2010/1127/>.
- Brill, K.G., Jr., 1944, Late Paleozoic stratigraphy, west-central and northwestern Colorado: Geological Society of America Bulletin, v. 55, no. 5, p. 621–656.
- Broadhead, R.F., 2008, The natural gas potential of north-central New Mexico; Colfax, Mora and Taos Counties: New Mexico Bureau of Geology and Mineral Resources, Open-File Report No. 510, 145 p., accessed October 3, 2011, at <http://geoinfo.nmt.edu/publications/openfile/details.cfm?Volume=510>.
- Butler, W.C., 1995, Northern Arizona province (024), *in* Gautier, D.L., Dolton, G.L., Takahashi, K.I., and Varnes, K.L., eds., 1995 National assessment of United States oil and gas resources—Results, methodology, and supporting data: U.S. Geological Survey Digital Data Series DDS–30, release 2, 28 p., accessed February 21, 2014, at <http://certmapper.cr.usgs.gov/data/noga95/prov24/text/prov24.pdf>.
- Buursink, M.L., Slucher, E.R., Merrill, M.D., and Warwick, P.D., 2011, Assessing composite storage formations for geologic carbon sequestration [abs.]: American Association of Petroleum Geologists Eastern Section Meeting, Washington, D.C., U.S.A., September 25–27, 2011, American Association of Petroleum Geologists Search and Discovery Article 90131, accessed May 29, 2013, at http://www.searchanddiscovery.com/abstracts/pdf/2011/eastern/abstracts/ndx_buursink.pdf.
- Byrnes, A.P., 1997, Reservoir characteristics of low-permeability sandstones in the Rocky Mountains: The Mountain Geologist, v. 34, no. 1, p. 39–51.
- Chidsey, T.C., Jr., Carney, S.M., and Morgan, C.D., 2010, Geological site characterization of the Aneth unit, Greater Aneth field, southeastern Utah, for sequestration of carbon dioxide—A project summary [abs.]: American Association of Petroleum Geologists Rocky Mountain Section, Durango, Colo., June 13–16, 2010, American Association of Petroleum Geologists Search and Discovery Article 90106, at http://www.searchanddiscovery.com/abstracts/pdf/2010/rms/abstracts/ndx_chidsey.pdf.
- Chidsey, T.C., Jr., Laine, M.D., Sprinkel, D.A., Vrona, J.P., and Strickland, D.K., 2007, Covenant oil field, central Utah thrust belt—Possible harbinger of future discoveries: American Association of Petroleum Geologists Search and Discovery Article 10130, accessed December 21, 2015, at <http://www.searchanddiscovery.com/documents/2007/07070chidsey/>.
- Chidsey, T.C., Jr., and Morgan, C.D., 1993, Low-BTU gas in Utah, *in* Robertson, R.F., and Broadhead, J.M., eds., Atlas of major Rocky Mountain gas reservoirs: Socorro, N. Mex., New Mexico Bureau of Mines and Mineral Resources, 171 p.
- Chidsey, T.C., Jr., and Sprinkel, D.A., 2005, Petroleum geology of Ashley Valley oil field and hydrocarbon potential of the surrounding area, Uintah County, Utah, *in* Dehler, C.M., Pederson, J.L., Sprinkel, D.A., and Kowallis, B.J., eds., Uinta Mountain geology: Utah Geological Association Publication 33, p. 347–368, accessed October 19, 2015, at <http://archives.datapages.com/data/uga/data/076/076001/pdfs/347.pdf>.
- Chidsey, T.C., Jr., and Sprinkel, D.A., 2007, Major oil plays in Utah and vicinity—Quarterly technical progress report: Utah Geological Survey, Department of Natural Resources, U.S. Department of Energy Contract No. DE–FC26–02NT15133, 41 p.

- Choquette, P.W., and Pray, L.C., 1970, Geologic nomenclature and classification of porosity in sedimentary carbonates: American Association of Petroleum Geologists Bulletin, v. 54, no. 2, p. 207–250.
- Clark, W.R., 1977, Raton Basin, *in* Bortz, L.C., and Irwin, D., eds., Subsurface cross sections of Colorado: Denver, Colo., Rocky Mountain Association of Geologists Special Publication, no. 2, p. 25–26, 2 pls.
- Condon, S.M., and Peterson, F., 1986, Stratigraphy of Middle and Upper Jurassic rocks of the San Juan Basin—Historical perspective, current ideas, and remaining problems, *in* Turner-Peterson, C.E., Satos, E.S., and Fishman, N.S., eds., A basin analysis case study—The Morrison Formation, Grants uranium region, New Mexico: American Association of Petroleum Geologists Studies in Geology 22, p. 7–26.
- Cook, H.E., 1988, Overview—Geologic history and carbonate petroleum reservoirs of the Basin and Range Province, western United States, *in* Goolsby, S.M., and Longman, M.W., eds., Occurrence and petrophysical properties of carbonate reservoirs in the Rocky Mountain region: Denver, Colo., Rocky Mountain Association of Geologists, p. 213–228.
- Cook, H.E., 1989, Geology of the Basin and Range Province, western United States—An overview, chap. 2 *of* Taylor, M.E., ed., Cambrian and Early Ordovician stratigraphy and paleontology of the Basin and Range Province, western United States, Las Vegas, Nevada, to Salt Lake City, Utah, July 1–7, 1989: American Geophysical Union, Field Trip Guidebook, v. T125, p. 6–13.
- Cook, H.E., and Corboy, J.J., 2004, Great Basin Paleozoic carbonate platform—Facies, facies transitions, depositional models, platform architecture, sequence stratigraphy, and predictive mineral host models: U.S. Geological Survey Open-File Report 2004–1078, 129 p. [Also available at <https://pubs.er.usgs.gov/publication/ofr20041078>.]
- Craig, S.D., 2001, Geologic framework of the San Juan structural basin of New Mexico, Colorado, Arizona, and Utah, with emphasis on Triassic through Tertiary rocks: U.S. Geological Survey Professional Paper 1420, 70 p. [Also available at <https://pubs.er.usgs.gov/publication/pp1420>.]
- Davatzes, N.C., and Aydin, A., 2005, Distribution and nature of fault architecture in a layered sandstone and shale sequence—An example from the Moab fault, Utah, *in* Sorkhabi, R., and Tsuji, Y., eds., Faults, fluid flow, and petroleum traps: American Association of Petroleum Geologists Memoir 85, p. 153–180.
- de Gibert, J.M., and Ekdale, A.A., 2002, Ichnology of a restricted epicontinental sea, Arapien Shale, Middle Jurassic, Utah, USA: Palaeogeography, Palaeoclimatology, Palaeoecology, v. 183, nos. 3–4, p. 275–286. [Also available at <http://www.sciencedirect.com/science/article/pii/S0031018201004916>.]
- Devlin, F.J., and Tomkins, J.Q., 1957, The Bisti area, San Juan County, New Mexico, *in* Little, C.J., Gill, J.J., Bourn, O.B., Pritchett, F.L., and Smith, K.G., eds., Geology of southwestern San Juan Basin: Durango, Colo., Four Corners Geological Society Guidebook, 2nd Field Conference, p. 152–154.
- Dolly, E.D., and Meissner, F.F., 1977, Geology and gas exploration potential, Upper Cretaceous and lower Tertiary strata, northern Raton Basin, Colorado, *in* Veal, H.K., ed., Exploration frontiers of the central and southern Rockies, Rocky Mountain Association of Geologists Guidebook: Denver, Colo., Rocky Mountain Association of Geologists, p. 247–270.
- Donselaar, M.E., 1989, The Cliff House Sandstone, San Juan Basin, New Mexico—Model for the stacking of ‘transgressive’ barrier complexes: Journal of Sedimentary Petrology, v. 59, no. 1, p. 13–27.
- Dubiel, R.F., 2003, Geology, depositional models, and oil and gas assessment of the Green River total petroleum system, Uinta-Piceance Province, eastern Utah and western Colorado, chap. 5 *of* U.S. Geological Survey Uinta-Piceance Assessment Team, comps., Petroleum systems and geologic assessment of oil and gas in the Uinta-Piceance Province, Utah and Colorado: U.S. Geological Survey Digital Data Series 69–B, 41 p., accessed May 30, 2013, at http://pubs.usgs.gov/dds/dds-069/dds-069-b/REPORTS/Chapter_5.pdf.
- Dubiel, R.F., Huntoon, J.E., Stanescu, J.D., Condon, S.M., and Mickelson, D.L., 1996, Permian-Triassic depositional systems, paleogeography, paleoclimate, and hydrocarbon resources in Canyonlands, Utah: Colorado Geological Survey Open-File Report 96–4, Field Trip No. 5, 23 p.
- Engler, T.W., Brister, B.S., Chen, Her-Yuan, and Teufel, L.W., 2001, Oil and gas resource development for San Juan Basin, New Mexico: New Mexico Bureau of Geology and Mineral Resources Open-File Report 463, 125 p., accessed September 14, 2015, at <http://geoinfo.nmt.edu/publications/openfile/details.cfm?Volume=463>.

- English, J.M., and Johnston, S.T., 2004, The Laramide orogeny—What were the driving forces?: *International Geology Review*, v. 46, no. 9, p. 833–838.
- Fassett, J.E., 1974, Cretaceous and Tertiary rocks of the eastern San Juan Basin, New Mexico and Colorado: New Mexico Geological Society 25th Annual Fall Field Conference Guidebook: p. 225–230.
- Fassett, J.E., 2000, Geology and coal resources of the Upper Cretaceous Fruitland Formation, San Juan Basin, New Mexico and Colorado, chap. Q of Kirschbaum, M.A., Roberts, L.N.R., and Biewick, L.R.H., eds., *Geologic assessment of coal in the Colorado Plateau—Arizona, Colorado, New Mexico, and Utah*: U.S. Geological Survey Professional Paper 1625–B, version 1.0, p. Q1–Q131, accessed September 22, 2011, at http://pubs.usgs.gov/pp/p1625b/Reports/Chapters/Chapter_Q.pdf.
- Fassett, J.E., 2006, The San Juan Basin—A complex giant gas field, New Mexico and Colorado: *The Mountain Geologist*, v. 43, no. 3, p. 225–230.
- Fassett, J.E., 2010, Oil and gas resources of the San Juan Basin, New Mexico and Colorado, in Fassett, J.E., Zeigler, K.E., and Lueth, V.W., eds., *Geology of the four corners country: New Mexico Geological Society 61st Annual Fall Field Conference Guidebook*, p. 181–196.
- Fassett, J.E., and Boyce, B.C., 2005, Fractured-sandstone reservoirs, San Juan Basin, New Mexico and Colorado; Stratigraphic traps, not basin-centered gas deposits—With an overview of Fruitland Formation coal-bed methane, in Bishop, M.G., Cumella, S.P., Robinson, J.W., and Silverman, M.R., eds., *Gas in low permeability reservoirs of the Rocky Mountain region*, Rocky Mountain Association of Geologists Guidebook: Denver, Colo., Rocky Mountain Association of Geologists, p. 109–185, 1 CD-ROM.
- Fouch, T.D., 1975, Lithofacies and related hydrocarbon accumulations in Tertiary strata of the western and central Uinta Basin, Utah, in Bolyard, D.W., ed., *Symposium on deep drilling frontiers of the central Rocky Mountains*: Denver, Colo., Rocky Mountain Association of Geologists, p. 163–173.
- Fouch, T.D., Nuccio, V.F., Anders, D.E., Rice, D.D., Pitman, J.K., and Mast, R.F., 1994, Green River (!) petroleum system, Uinta Basin, Utah, U.S.A., in Magoon, L.B., and Dow, W.G., eds., *The petroleum system—From source to trap*: American Association of Petroleum Geologists Memoir 60, p. 399–421.
- Franklin, S.P., and Tieh, T.T., 1989, Petrography, diagenesis, and reservoir properties of the Dakota Sandstone of West Lindrith field, Rio Arriba County, New Mexico, in Coalson, E.B., ed., *Petrogenesis and petrophysics of selected sandstone reservoirs of the Rocky Mountain region*: Denver, Colo., Rocky Mountain Association of Geologists, p. 117–133.
- Freethy, G.W., and Cordy, G.E., 1991, Geohydrology of Mesozoic rocks in the upper Colorado River Basin in Arizona, Colorado, New Mexico, Utah, and Wyoming, excluding the San Juan Basin—Regional aquifer-system analysis: U.S. Geological Survey Professional Paper 1411–C, 118 p., accessed December 10, 2010, at <http://pubs.usgs.gov/pp/1411c/report.pdf>.
- Geldon, A.L., 2003a, Geology of Paleozoic rocks in the upper Colorado River Basin in Arizona, Colorado, New Mexico, Utah, and Wyoming, excluding the San Juan Basin—Regional aquifer-system analysis: U.S. Geological Survey Professional Paper 1411–A, 112 p., 18 pls., accessed December 10, 2010, at <http://pubs.usgs.gov/pp/1411a/report.pdf>.
- Geldon, A.L., 2003b, Hydrologic properties and ground-water flow systems of the Paleozoic rocks in the upper Colorado River Basin in Arizona, Colorado, New Mexico, Utah, and Wyoming, excluding the San Juan Basin—Regional aquifer-system analysis: U.S. Geological Survey Professional Paper 1411–B, 153 p., 13 pls., accessed December 10, 2010, at <http://pubs.usgs.gov/pp/1411b/report.pdf>.
- Giles, K.A., 1996, Tectonically forced retrogradation of the Lower Mississippian Joana Limestone, Nevada and Utah, in Longman, M.W., and Sonnenfeld, M.D., eds., *Paleozoic systems of the Rocky Mountain region*, Rocky Mountain section: Denver, Colo., SEPM (Society for Sedimentary Geology), p. 145–164.
- Gilmore, T.J., 1990, Stratigraphy and depositional environments of the Lower Mississippian Joana Limestone in southern White Pine and northern Lincoln Counties, Nevada: *The Mountain Geologist*, v. 27, no. 2, p. 69–76.
- Goebel, K.A., 1991, Paleogeographic setting of Late Devonian to Early Mississippian transition from passive to collisional margin, Antler foreland, eastern Nevada and western Utah, in Cooper, J.D., and Stevens, C.H., eds., *Paleozoic paleogeography of the western United States II*: Los Angeles, Calif., SEPM (Society for Sedimentary Geology), Pacific Section, v. 67, p. 401–418.

- Goldhammer, R.K., Oswald, E.J., and Dunn, P.A., 1991, Hierarchy of stratigraphic forcing—Example from Middle Pennsylvanian shelf carbonates of the Paradox Basin: Kansas Geological Survey Bulletin 233, p. 361–413, accessed February 10, 2014, at <http://www.kgs.ku.edu/Publications/Bulletins/233/Goldhammer/goldhammer.pdf>.
- Grant, K., and Owen, D.E., 1974, The Dakota Sandstone (Cretaceous) of the southern part of the Chama Basin, New Mexico—A preliminary report on its stratigraphy, paleontology, and sedimentology, *in* Siemers, C.T., Woodward, L.A., and Callender, J.F., eds., Ghost Ranch: New Mexico Geological Society 25th Annual Fall Field Conference Guidebook, p. 239–249.
- Green, M.W., and Pierson, C.T., 1977, A summary of the stratigraphy and depositional environments of Jurassic and related rocks in the San Juan Basin, Arizona, Colorado, and New Mexico, *in* Fassett, J.E., James, H.L., and Hodgson, H.E., eds., San Juan Basin III: New Mexico Geological Society 28th Annual Fall Field Conference Guidebook p. 147–152.
- Hefner, T.A., and Barrow, K.T., 1992, Rangley field—U.S.A. Uinta/Piceance Basins, Colorado, *in* Foster, N.H., and Beaumont, E.A., eds., TR—Structural traps VII: Tulsa, Okla., American Association of Petroleum Geologists Treatise of Petroleum Geology, Atlas of Oil and Gas Fields, p. 29–56.
- Hemborg, H.T., 1993, Weber Sandstone, *in* Hjellming, C.A., ed., Atlas of major Rocky Mountain gas reservoirs: Socorro, N. Mex., New Mexico Bureau of Mines and Mineral Resources, p. 104.
- Henry, M.E., and Finn, T.M., 2003, Petroleum assessment of the Ferron/Wasatch Plateau total petroleum system, Upper Cretaceous strata, Wasatch Plateau and Castle Valley, Utah, chap. 8 *of* U.S. Geological Survey Uinta-Piceance Assessment Team, comps., Petroleum systems and geologic assessment of oil and gas in the Uinta-Piceance Province, Utah and Colorado: U.S. Geological Survey Digital Data Series DDS–69–B, 39 p., accessed September 4, 2011, at http://pubs.usgs.gov/dds/dds-069/dds-069-b/REPORTS/Chapter_8.pdf.
- Higley, D.K., 2007, Petroleum systems and assessment of undiscovered oil and gas in the Raton Basin—Sierra Grande Uplift Province, Colorado and New Mexico, chap. 2 *of* Higley, D.K. comp., Petroleum systems and assessment of undiscovered oil and gas in the Raton Basin; Sierra Grande Uplift Province, Colorado and New Mexico—USGS Province 41: U.S. Geological Survey Digital Data Series DDS–69–N, 124 p., accessed September 4, 2011, at http://pubs.usgs.gov/dds/dds-069/dds-069-n/REPORTS/69_N_CH_2.pdf.
- Hintze, L.F., 1974, Geologic map of Utah: Salt Lake City, Utah, Utah Geological Survey, 1 sheet, scale 1:2,500,000, accessed August 1, 2011, at http://geology.utah.gov/maps/geomap/statemap/pdf/geoutah_1.pdf.
- Huffman, A.C., 1987, Petroleum geology and hydrocarbon plays of the San Juan Basin petroleum province: U.S. Geological Survey Open-File Report 87–450–B, 67 p., accessed September 22, 2011, at <http://pubs.usgs.gov/of/1987/0450b/report.pdf>.
- Huffman, A.C., Jr., 1995a, Paradox Basin Province (021), *in* Gautier, D.L., Dolton, G.L., Takahashi, K.I., and Varnes, K.L., eds., 1995 National assessment of United States oil and gas resources—Results, methodology, and supporting data: U.S. Geological Survey Digital Data Series DDS–30, release 2, CD-ROM, 10 p., accessed September 4, 2011, at <http://certmapper.cr.usgs.gov/data/noga95/prov21/text/prov21.pdf>.
- Huffman, A.C., Jr., 1995b, San Juan Basin Province (22), *in* Gautier, D.L., Dolton, G.L., Takahashi, K.I., and Varnes, K.L., eds., 1995 National assessment of United States oil and gas resources—Results, methodology, and supporting data: U.S. Geological Survey Digital Data Series DDS–30, release 2, CD-ROM, 10 p., accessed September 4, 2011, at <http://certmapper.cr.usgs.gov/data/noga95/prov21/text/prov21.pdf>.
- Huffman, A.C., Jr., and Condon, S.M., 1993, Stratigraphy, structure, and paleogeography of Pennsylvanian and Permian rocks, San Juan Basin and adjacent areas, Utah, Colorado, Arizona, and New Mexico, *in* Evolution of sedimentary basins—San Juan Basin: U.S. Geological Survey Bulletin 1808–O, p. 1–44. [Also available at <https://pubs.er.usgs.gov/publication/b1808O>.]
- Huffman, A.C., Jr., Lund, W.R., and Godwin, L.H., eds., 1996, Geology and resources of the Paradox Basin: Utah Geological Association Publication 25, 460 p.
- Huntoon, J.E., Dubiel, R.F., Stanesco, J.D., Mickelson, D.L., and Condon, S.M., 2002, Permian-Triassic deposition systems, paleogeography, paleoclimate, and hydrocarbon resources in Canyonlands and Monument Valley, Utah: Geological Society of America Field Guide, p. 33–58.
- IHS Energy Group, 2010, PIDM [Petroleum Information Data Model] relational U.S. well data: Englewood, Colo., IHS Energy Group, database available from IHS Energy Group, 15 Inverness Way East, D205, Englewood, CO 80112, U.S.A. [Includes data current as of December 23, 2009.]

- IHS Energy Group, 2011, ENERDEQ U.S. well data: Englewood, Colo., IHS Energy Group, database available from IHS Energy Group, 15 Inverness Way East, D205, Englewood, CO 80112, U.S.A., accessed January 20, 2011, at <http://energy.ihs.com/>.
- Jentgen, R.W., 1977, Pennsylvanian rocks in the San Juan Basin, New Mexico and Colorado, *in* Fassett, J.E., James, H.L., and Hodgson, H.E., eds., *San Juan Basin III: New Mexico Geological Society 28th Annual Fall Field Conference Guidebook*, p. 129–132.
- Johnson, E.A., 2003, Geologic assessment of the Phosphoria total petroleum system, Uinta-Piceance Province, Utah and Colorado, chap. 9 *of* U.S. Geological Survey Uinta-Piceance Assessment Team, comps., *Petroleum systems and geologic assessment of oil and gas in the Uinta-Piceance Province, Utah and Colorado: U.S. Geological Survey Digital Data Series DDS–69–B*, version 1.0, 42 p., accessed September 4, 2011, at http://pubs.usgs.gov/dds/dds-069/dds-069-b/REPORTS/Chapter_9.pdf.
- Johnson, R.C., 1985, Early Cenozoic history of the Uinta and Piceance Creek basins, Utah and Colorado, with special reference to the development of Eocene Lake Uinta, *in* Flores, R.M., and Kaplan, S.S., eds., *Cenozoic paleogeography of west-central United States—Rocky Mountain Paleogeography, Symposium 3: Denver, Colo., Society of Economic Paleontologists and Mineralogists (SEPM), Rocky Mountain Section*, p. 247–276.
- Johnson, R.C., 1989, Detailed cross sections correlating Upper Cretaceous and lower Tertiary rocks between the Uinta Basin of eastern Utah and western Colorado and the Piceance Basin of western Colorado: U.S. Geological Survey Miscellaneous Investigations Series Map I–1974, 2 sheets. [Also available at <https://pubs.er.usgs.gov/publication/i1974>.]
- Johnson, R.C., and Roberts, S.B., 2003, The Mesaverde total petroleum system, Uinta-Piceance Province, Utah and Colorado, chap. 7 *of* U.S. Geological Survey Uinta-Piceance Assessment Team, comps., *Petroleum systems and geologic assessment of oil and gas the Uinta-Piceance Province, Utah and Colorado: U.S. Geological Survey Digital Data Series DDS–69–B*, version 1.0, 68 p., accessed September 4, 2011, at http://pubs.usgs.gov/dds/dds-069/dds-069-b/REPORTS/Chapter_7.pdf.
- Johnson, S.Y., 1992, Phanerozoic evolution of sedimentary basins in the Uinta-Piceance Basin region, northwestern Colorado and northeastern Utah, chap. FF *of* *Evolution of sedimentary basins—Uinta and Piceance Basins: U.S. Geological Survey Bulletin 1787*, 48 p. [Also available at <https://pubs.er.usgs.gov/publication/b1787FF>.]
- Johnson, S.Y., Chan, M.A., and Konopka, E.A., 1992, Pennsylvanian and early Permian paleogeography of the Uinta-Piceance Basin region, northwestern Colorado and northeastern Utah, chap. CC *of* *Evolution of sedimentary basins—Uinta and Piceance Basins: U.S. Geological Survey Bulletin 1787*, 44 p. [Also available at <https://pubs.er.usgs.gov/publication/b1787CC>.]
- Kelley, V.C., 1958, Tectonics of the region of the Paradox Basin, *in* Sanborn, A.F., ed., *Geology of the Paradox Basin*, 9th Annual Field Conference Guidebook: Intermountain Association of Petroleum Geologists, p. 31–38.
- Kirschbaum, M.A., 2003, Assessment of undiscovered oil and gas resources of the Mancos/Mowry total petroleum system, Uinta-Piceance basin province, Utah and Colorado, chap. 6 *of* U.S. Geological Survey Uinta-Piceance Assessment Team, comps., *Petroleum systems and geologic assessment of oil and gas the Uinta-Piceance Province, Utah and Colorado: U.S. Geological Survey Digital Data Series DDS–69–B*, 51 p., accessed July 24, 2013, at http://pubs.usgs.gov/dds/dds-069/dds-069-b/REPORTS/Chapter_6.pdf.
- Kirschbaum, M.A., and Schenk, C.J., 2011, Sedimentology and reservoir heterogeneity of a valley-fill deposit—A field guide to the Dakota Sandstone of the San Rafael Swell, Utah: U.S. Geological Survey Scientific Investigations Report 2010–5222, 36 p., 1 pl. [Also available at <http://pubs.usgs.gov/sir/2010/5222/>.]
- Kluth, C.F., 1986, Plate tectonics of the Ancestral Rocky Mountains, *in* Peterson, J.A., ed., *Paleotectonics and sedimentation in the Rocky Mountain region, United States: American Association of Petroleum Geologists Memoir 41*, p. 353–369.
- Kluth, C.F., and DuChene, H.R., 2009, Late Pennsylvanian and early Permian structural geology and tectonic history of the Paradox Basin and Uncompahgre uplift, Colorado and Utah, *in* Houston, W.S., Wray, L.L., and Moreland, P.G., eds., *The Paradox Basin revisited—New developments in petroleum systems and basin analysis: Denver, Colo., Rocky Mountain Association of Geologists Special Publication*, p. 178–197.
- Kurtz, D.D., and Anderson, J.B., 1980, Depositional environments and paleocurrents of Chinle Formation (Triassic), eastern San Juan Basin, New Mexico: *New Mexico Geology*, v. 2, p. 22–27.

- LaPointe, D.D., Price, J.G., and Hess, R.H., 2007, Assessment of the potential for carbon dioxide sequestration with enhanced oil recovery in Nevada: Nevada Bureau of Mines and Geology Open-File Report 07-7, 24 p.
- Lawton, T.F., 2008, Laramide sedimentary basins, chap. 12 of Miall, A.D., ed., *Sedimentary basins of the world*: Amsterdam, Elsevier, v. 5, p. 429–450.
- Lessentine, R.H., 1965, Kaiparowits and Black Mesa Basins—Stratigraphic synthesis: *Bulletin of the American Association of Petroleum Geologists*, v. 49, no. 11, p. 1997–2019.
- Levings, G.W., Craig, S.D., Dam, W.L., Kernodle, J.M., and Thorn, C.R., 1990, Hydrogeology of the Menefee Formation in the San Juan structural basin, New Mexico, Colorado, Arizona, and Utah: U.S. Geological Survey Hydrologic Investigations Atlas HA-720-F, 2 sheets. [Also available at <https://pubs.er.usgs.gov/publication/ha720F>.]
- Loughlin, G.F., 1919, General geography and geology, part 1, in Lindgren, W., Loughlin, G.F., and Heikes, V.C., eds., *Geology and ore deposits of the Tintic mining district, Utah, with a historical review*: U.S. Geological Survey Professional Paper 107, p. 15–104. [Also available at <https://pubs.er.usgs.gov/publication/pp107>.]
- Lucia, F.J., 1995, Rock-fabric/petrophysical classification of carbonate pore space for reservoir characterization: *American Association of Petroleum Geologists Bulletin*, v. 70, no. 9, p. 1275–1300.
- Magoon, L.B., and Dow, W.G., 1994, The petroleum system, in Magoon, L.B., and Dow, W.G. eds., *The petroleum system—From source to trap*: American Association of Petroleum Geologists Memoir 60, p. 3–24.
- Mallory, W.W., ed., 1972, *Geologic atlas of the Rocky Mountain region*: Denver, Colo., Rocky Mountain Association of Geologists, 331 p.
- Massé, D.J., and Ray, R.R., 1995, 3-D seismic prospecting for Entrada Sandstone reservoirs on the southeastern flank of the San Juan Basin, New Mexico, in Ray, R.R., ed., *High-definition seismic—2-D, 2-D swath, and 3-D case histories*: Denver, Colo., Rocky Mountain Association of Geologists, p. 143–160.
- Maughan, E.K., 1994, Phosphoria Formation (Permian) and its resource significance in the western interior, U.S.A.: *Canadian Society of Petroleum Geologists Memoir* 17, p. 479–495.
- McClure, K., Morgan, C.D., and Chidsey, T.C., Jr., 2003a, Regional Paradox Formation structure and isochore maps, Blanding sub-basin, Utah, deliverable 1.1.1 of Heterogeneous shallow-shelf carbonate buildups in the Paradox Basin, Utah and Colorado—Targets for increased oil production and reserves using horizontal drilling techniques: Utah Geological Survey, Contract No. DE-2600BC15128, 39 p., accessed December 21, 2015, at <http://geology.utah.gov/emp/paradox2/pdf/deliverable1-1-1.pdf>.
- McClure, K., Morgan, C.D., and Chidsey, T.C., Jr., 2003b, Regional Paradox Formation cross sections, Blanding sub-basin, Utah and Colorado, deliverable 1.1.2 of Heterogeneous shallow-shelf carbonate buildups in the Paradox Basin, Utah and Colorado—Targets for increased oil production and reserves using horizontal drilling techniques: Utah Geological Survey, Contract No. DE-2600BC15128, 10 p., 14 pls., accessed December 21, 2015, at <http://geology.utah.gov/emp/paradox2/pdf/deliverable1-1-2.pdf>.
- McGookey, D.P., 1972, Cretaceous System, in Mallory, W.W., ed., *Geologic atlas of the Rocky Mountain region*: Denver, Colo., Rocky Mountain Association of Geologists, p. 190–228.
- Miller, E.L., and Gans, P.B., 1983, The Snake Range decollement—An exhumed mid-Tertiary ductile-brittle transition: *Tectonics*, v. 2, no. 3, p. 239–263.
- Miller, L.D., Watts, K.R., Ortiz, R.F., and Ivahnenko, T., 2010, Occurrence and distribution of dissolved solids, selenium, and uranium in groundwater and surface water in the Arkansas River Basin from the headwaters to Coolidge, Kansas, 1970–2009: U.S. Geological Survey Scientific Investigations Report 2010–5069, 59 p., accessed October 1, 2011, at <http://pubs.usgs.gov/sir/2010/5069/pdf/SIR10-5069.pdf>.
- Molenaar, C.M., 1974, Correlation of the Gallup Sandstone and associated formations, Upper Cretaceous, eastern San Juan and Acoma Basins, New Mexico, in Siemers, C.T., Woodward, L.A., and Callender, J.F., eds., *Ghost Ranch: New Mexico Geological Society 25th Annual Fall Field Conference Guidebook*, p. 251–258.

- Molenaar, C.M., 1977, Stratigraphy and depositional history of Upper Cretaceous rocks of the San Juan Basin area, New Mexico and Colorado, with a note on economic resources, *in* Fassett, J.E., James, H.L., and Hodgson, H.E., eds., *San Juan Basin III: New Mexico Geological Society 28th Annual Fall Field Conference Guidebook*, p. 159–166.
- Molenaar, C.M., and Baird, J.K., 1992, Regional stratigraphic cross sections of Upper Cretaceous rocks across the San Juan Basin, northwestern New Mexico and southwestern Colorado: U.S. Geological Survey Open-File Report 92–257, 3 sheets, accessed October 18, 2011, at <http://pubs.er.usgs.gov/publication/ofr92257>.
- Molenaar, C.M., Cobban, W.A., Merewether, E.A., Pillmore, C.L., Wolfe, D.G., and Holbrook, J.M., 2002, Regional stratigraphic cross sections of Cretaceous rocks from east-central Arizona to the Oklahoma panhandle: U.S. Geological Survey Miscellaneous Field Studies Map MF–2382, version 1.0, 3 sheets, accessed December 22, 2015, at <http://pubs.usgs.gov/mf/2002/mf-2382/>.
- Morgan, C.D., 1993, Paradox Basin plays, *in* Hjellming, C.A., ed., *Atlas of major Rocky Mountain gas reservoirs: Socorro, N. Mex.*, New Mexico Bureau of Mines and Mineral Resources, p. 90–94.
- Murray, H.F., 1958, Pennsylvanian stratigraphy of the Maroon trough, *in* Symposium on Pennsylvanian rocks of Colorado and adjacent areas, 1958: Denver, Colo., Rocky Mountain Association of Geologists Field Conference Guidebook 10, p. 47–58.
- Nehring Associates Inc., 2010, Significant oil and gas fields of the United States database: Colorado Springs, Colo., Nehring Associates Inc., database available from Nehring Associates Inc., P.O. Box 1655, Colorado Springs, CO 80901, U.S.A. [Includes data current as of December 2008.]
- Nevada Bureau of Mines and Geology, 1999, Generalized geologic map of Nevada: Nevada Bureau of Mines and Geology Education Series E–30, 1 sheet, scale 1:1,000,000, accessed March 21, 2016, at <http://pubs.nbmng.unr.edu/Generalized-geologic-map-of-Nev-p/e030.htm>.
- Noe, D.C., 1993, Greater Piceance—PC-4 Dakota Sandstone, Cedar Mountain Formation, and Morrison Formation, *in* Hjellming, C.A., ed., *Atlas of major Rocky Mountain gas reservoirs: Socorro, N. Mex.*, New Mexico Bureau of Mines and Mineral Resources, p. 101.
- Nuccio, V.F., and Condon, S.M., 1996, Burial and thermal history of the Paradox Basin, Utah and Colorado, and petroleum potential of the Middle Pennsylvanian Paradox Formation, *in* Huffman, A.C., Jr., ed., *Evolution of sedimentary basins—Paradox Basin: U.S. Geological Survey Bulletin 2000–O*, 41 p., 2 pls.
- Nummedal, D., and Molenaar, C.M., 1995, Sequence stratigraphy of ramp-setting strand plain successions—The Gallup Sandstone, New Mexico, *in* Van Wagoner, J.C., and Bertram, G.T., eds., *Sequence stratigraphy of foreland basin deposits: American Association of Petroleum Geologists Memoir 64*, p. 277–310.
- Olsen, T., 1995, Fluvial and fluvio-lacustrine facies and depositional environments of the Maastrichtian to Paleocene North Horn Formation, Price Canyon, Utah: *The Mountain Geologist*, v. 32, no. 2, p. 27–44.
- O’Sullivan, R.B., 1977, Triassic rocks of the San Juan Basin of New Mexico and adjacent areas, *in* Fassett, J.E., James, H.L., and Hodgson, H.E., eds., *San Juan Basin III: New Mexico Geological Society 28th Annual Fall Field Conference Guidebook*, p. 139–146.
- Owen, D.E., 1973, Depositional history of the Dakota Sandstone, San Juan Basin area, New Mexico, *in* Fassett, J.E., ed., *Cretaceous and Tertiary rocks of the southern Colorado Plateau: Durango, Colo.*, Four Corners Geological Society Memoir, p. 37–51.
- Parsons, T., 1995, The Basin and Range Province, *in* Olsen, K., ed., *Continental rifts—Evolution, structure and tectonics: Amsterdam, Elsevier*, p. 277–324.
- Peterson, J.A., 1972, Jurassic System, *in* Mallory, W.W., ed., *Geologic atlas of the Rocky Mountain region: Denver, Colo.*, Rocky Mountain Association of Geologists, p. 177–189.
- Peterson, J.A., 1989, Geology and petroleum resources, Paradox Basin Province: U.S. Geological Survey Open-File Report 88–450–U, 69 p. [Also available at <https://pubs.er.usgs.gov/publication/ofr88450U>.]

- Peterson, J.A., and Grow, J.A., 1995, Eastern Great Basin Province (019), *in* Gautier, D.L., Dolton, G.L., Takahashi, K.I., and Varnes, K.L., eds., 1995 National assessment of United States oil and gas resources—Results, methodology, and supporting data: U.S. Geological Survey Digital Data Series DDS–30, 13 p. accessed May 1, 2014, at <http://pubs.usgs.gov/of/1995/of95-075n/>.
- Poole, F.G., and Claypool, G.E., 1984, Petroleum source-rock potential and crude-oil correlation in the Great Basin, *in* Woodward, J., Meissner, F.F., and Clayton, J.L., eds., Hydrocarbon source rocks of the Greater Rocky Mountain region: Denver, Colo., Rocky Mountain Association of Geologists, p. 179–229.
- Potter, C.J., Tang, R.L., and Hainsworth, T.J., 1991, Late Paleozoic structure of the southern part of the Uinta Basin, Utah, from seismic reflection data, chap. V *of* Evolution of sedimentary basins—Uinta and Piceance Basins: U.S. Geological Survey Bulletin 1787, p. 1–10, 1 pl., accessed June 5, 2013, at <http://pubs.er.usgs.gov/publication/b1787V>.
- Price, J.G., Hess, R.H., Fitch, S., Faulds, J.E., Garside, L.J., Shevenell, L., and Warren, S., 2005, Preliminary assessment of the potential for carbon dioxide disposal by sequestration in geological settings in Nevada: Nevada Bureau of Mines and Geology Report 51, 35 p.
- Rascoe, B., Jr., and Baars, D.L., 1972, Permian System, *in* Mallory, W.W., ed., Geologic atlas of the Rocky Mountain region: Denver, Colo., Rocky Mountain Association of Geologists, p. 143–165.
- Rauzi, S.L., and Spencer, J.E., 2012, An evaluation of CO₂ sequestration potential of Paleozoic sandstone units, northeastern Arizona: Arizona Geological Survey Open-File Report, OFR–12–10, version 1.0, 24 p., accessed February 21, 2014, at http://repository.azgs.gov/uri_gin/azgs/dlio/1460.
- Rauzi, S.L., and Spencer, J.E., 2014, An evaluation of carbon dioxide sequestration potential of the Permian Cedar Mesa Sandstone, northeastern Arizona: Arizona Geological Survey Open-File Report, OFR–14–03, 20 p., accessed April 27, 2014, at http://repository.azgs.gov/sites/default/files/dlio/files/nid1565/ofr-14-03_rmccs.pdf.
- Reneau, W.E., Jr., and Harris, J.D., Jr., 1957, Reservoir characteristics of Cretaceous sands of the San Juan Basin: Durango, Colo., Four Corners Geological Society Guidebook, p. 40.
- Ridgley, J.L., 1977, Stratigraphy and depositional environments of the Jurassic Cretaceous sedimentary rocks in the southwest part of the Chama Basin, New Mexico, *in* Fassett, J.E., James, H.L., and Hodgson, H.E., eds., San Juan Basin III: New Mexico Geological Society 28th Annual Fall Field Conference Guidebook, p. 153–158.
- Ridgley, J.L., Condon, S.M., and Hatch, J.R., 2013, Geology and oil and gas assessment of the Mancos-Menefee composite total petroleum system, San Juan Basin, New Mexico and Colorado, chap. 4 *of* U.S. Geological Survey San Juan Basin Assessment Team, comps., Total petroleum systems and geologic assessment of undiscovered oil and gas resources in the San Juan Basin Province, exclusive of Paleozoic rocks, New Mexico and Colorado: U.S. Geological Survey Digital Data Series DDS–69–F, p. 1–97, available at http://pubs.usgs.gov/dds/dds-069/dds-069-f/REPORTS/Chapter4_508.pdf.
- Ridgley, J.L., and Hatch, J.R., 2013, Geology and oil and gas assessment of the Todilto total petroleum system, San Juan Basin Province, New Mexico and Colorado, chap. 3 *of* U.S. Geological Survey San Juan Basin Assessment Team, comps., Total petroleum systems and geologic assessment of undiscovered oil and gas resources in the San Juan Basin Province, exclusive of Paleozoic rocks, New Mexico and Colorado: U.S. Geological Survey Digital Data Series DDS–69–F, p. 1–29, accessed September 23, 2013, at <http://pubs.usgs.gov/dds/dds-069/dds-069-f/>.
- Roberts, L.N.R., 2003, Structure contour map of the top of the Dakota Sandstone, Uinta-Piceance Province, Utah and Colorado, chap. 16 *of* U.S. Geological Survey Uinta-Piceance Assessment Team, comps., Petroleum systems and geologic assessment of oil and gas the Uinta-Piceance Province, Utah and Colorado: U.S. Geological Survey Digital Data Series DDS–69–B, 14 p., accessed April 29, 2010, at http://pubs.usgs.gov/dds/dds-069/dds-069-b/REPORTS/Chapter_16.pdf.
- Roth, G., 1983, Sheep Mountain and Dike Mountain fields, Huerfano County, Colorado—A source of CO₂ for enhanced oil recovery, *in* Fassett, J.E., Hamilton, W., Jr., Martin, G.W., and Middleman, A.A., eds., Oil and gas fields of the Four Corners area: Durango, Colo., Four Corners Geological Society, v. 3, p. 740–744.
- Ryder, R.T., Fouch, T.D., and Elison, J.H., 1976, Early Tertiary sedimentation in the western Uinta Basin, Utah: Geological Society of America Bulletin, v. 87, no. 4, p. 496–512.

- Sanford, R.F., 1995, Ground-water flow and migration of hydrocarbons to the lower Permian White Rim Sandstone, Tar Sand Triangle, southeastern Utah: U.S. Geological Survey Bulletin 2000–J, 24 p. [Also available at <https://pubs.er.usgs.gov/publication/b00J>.]
- Scott, P.K., 2003, Paradox Basin, Colorado maps, cross sections, and database for oil, gas, and CO₂ fields: Colorado Geological Survey Resource Series 43, 1 CD-ROM.
- Shaw, G.L., 1958, Pennsylvanian history and stratigraphy of the Raton Basin, *in* Symposium on Pennsylvanian rocks of Colorado and adjacent areas: Denver, Colo., Rocky Mountain Association of Geologists Field Conference Guidebook 10, p. 74–79.
- Smith, D.L., and Miller, E.L., 1990, Late Paleozoic extension in the Great Basin, western United States: *Geology*, v. 18, no. 8, p. 712–715.
- Speed, R.C., and Sleep, N.H., 1982, Antler orogeny and foreland basin—A model: *Geological Society of America Bulletin*, v. 93, no. 9, p. 815–828.
- Spencer, C.W., 1995, Uinta-Piceance Basin Province (020), *in* Gautier, D.L., Dolton, G.L., Takahashi, K.I., and Varnes, K.L., eds., 1995 National assessment of United States oil and gas resources—Results, methodology, and supporting data: U.S. Geological Survey Digital Data Series DDS–30, release 2, accessed February 21, 2014, at <http://certmapper.cr.usgs.gov/data/noga95/prov20/text/prov20.pdf>.
- Sprinkel, D.A., 1982, Twin Creek Limestone-Arapien Shale relations in central Utah, *in* Nelson, D.L., ed., Overthrust belt of Utah: 1982 Symposium and Field Conference, Salt Lake City, Utah, Utah Geological Association Publication 10, p. 169–180.
- Sprinkel, D.A., 1993, Wasatch Plateau; Ferron Sandstone, *in* Hjellming, C.A., ed., Atlas of major Rocky Mountain gas reservoirs: Socorro, N. Mex., New Mexico Bureau of Mines and Mineral Resources, p. 89.
- Stanley, K.O., and Collinson, J.W., 1979, Depositional history of Paleocene–lower Eocene Flagstaff Limestone and coeval rocks, central Utah: *American Association of Petroleum Geologists Bulletin*, v. 63, no. 3, p. 311–323.
- Stevenson, G.M., 1983, Oil and gas exploration in the Paradox Basin, 1978 to 1983, *in* Fassett, J.E., Hamilton, W., Jr., Martin, G.W., and Middleman, A.A., eds., Oil and gas fields of the Four Corners area: Durango, Colo., Four Corners Geological Society, v. 3, p. 773–779.
- Stevenson, G.M., and Baars, D.L., 1977, Pre-Carboniferous paleotectonics of the San Juan Basin, *in* Fassett, J.E., James, H.L., and Hodgson, H.E., eds., San Juan Basin III: New Mexico Geological Society 28th Annual Fall Field Conference Guidebook, p. 99–110.
- Stevenson, G.M., and Baars, D.L., 1988, Overview—Carbonate reservoirs of the Paradox Basin, *in* Goolsby, S.M., and Longman, M.W., eds., Occurrence and petrophysical properties of carbonate reservoirs in the Rocky Mountain region: Denver, Colo., Rocky Mountain Association of Geologists, p. 149–162.
- Stone, W.J., Lyford, F.P., Frenzel, P.F., Mizell, N.H., and Padgett, E.T., 1983, Hydrogeology and water resources of San Juan Basin, New Mexico: New Mexico Bureau of Mines and Mineral Resources Hydrologic Report 6, 70 p.
- Teufel, L.W., Chen, H., Engler, T.W., and Hart, B., 2004, Optimization of infill drilling in naturally-fractured tight-gas reservoirs Phase II: Socorro, N. Mex., New Mexico Institute of Mining and Technology Final Report for U.S. Department of Energy and Industry Cooperative Agreement DE–FC26–98FT40486, 150 p.
- Thorman, C.H., Ketner, K.B., Brooks, W.E., Snee, L.W., and Zimmerman, R.A., 1991, Late Mesozoic-Cenozoic tectonics in northeastern Nevada, *in* Raines, G.L., Lisle, R.E., Schafer, R.W., and Wilkinson, N.H., eds., Geology and ore deposits of the Great Basin Symposium Proceedings: Reno, Nev., Geological Society of Nevada, p. 25–46.
- Thorn, C.R., Levings, G.W., Craig, S.D., Dam, W.L., and Kernodle, J.M., 1990, Hydrogeology of the Cliff House Sandstone in the San Juan structural basin, New Mexico, Colorado, Arizona, and Utah: U.S. Geological Survey Hydrologic Investigations Atlas HA–720–E, 2 sheets. [Also available at <https://pubs.er.usgs.gov/publication/ha720E>.]
- Tremain, C., 1993, Low-BTU gas in Colorado, *in* Hjellming, C.A., ed., Atlas of major Rocky Mountain gas reservoirs: Socorro, N. Mex., New Mexico Bureau of Mines and Mineral Resources, p. 172.

- Trexler, J.H., Cole, J.C., and Cashman, P.H., 1996, Middle Devonian-Mississippian stratigraphy on and near the Nevada Test Site—Implication for hydrocarbon potential: *American Association of Petroleum Geologists Bulletin*, v. 80, no. 11, p. 1736–1762.
- Tripp, C.N., 1989, A hydrocarbon exploration model for the Cretaceous Ferron Sandstone Member of the Mancos Shale, and the Dakota Group in the Wasatch Plateau and Castle Valley of east-central Utah, with emphasis on post-1980 subsurface data: *Utah Geological and Mineral Survey Open-File Report 160*, 82 p.
- Tweto, O., 1987, Rock units of the Precambrian basement in Colorado: U.S. Geological Survey Professional Paper 1321–A, 54 p., 1 pl. [Also available at <https://pubs.er.usgs.gov/publication/pp1321A>.]
- Umbach, P.H., 1950, Cretaceous rocks of the San Juan Basin area, *in* Kelley, V.C., Beaumont, E.C., and Silver, C., eds., *San Juan Basin, New Mexico and Colorado: New Mexico Geological Society 1st Annual Fall Field Conference Guidebook*, p. 82–84.
- U.S. Environmental Protection Agency, 2009, Safe Drinking Water Act (SDWA): Washington, D.C., U.S. Environmental Protection Agency Web site, accessed January 14, 2009, at <http://www.epa.gov/ogwdw/sdwa/index.html>.
- U.S. Geological Survey, 2015, Geologic CO₂ sequestration: U.S. Geological Survey Web site accessed October 15, 2015, at <http://energy.usgs.gov/EnvironmentalAspects/EnvironmentalAspectsofEnergyProductionandUse/GeologicCO2Sequestration.aspx>.
- U.S. Geological Survey Eastern Great Basin Assessment Team, 2005, Assessment of undiscovered oil and gas resources of the Eastern Great Basin Province, 2005: U.S. Geological Survey Fact Sheet 2005–3053, 2 p., accessed July 6, 2011, at <http://pubs.usgs.gov/fs/2005/3053/pdf/FS-2005-3053.pdf>.
- U.S. Geological Survey Geologic Carbon Dioxide Storage Resources Assessment Team, 2013a, National assessment of geologic carbon dioxide storage resources—Data (ver. 1.1, September 2013): U.S. Geological Survey Data Series 774, 13 p., plus 2 appendixes and 2 large tables in separate files, accessed September 22, 2013, at <http://pubs.usgs.gov/ds/774/>. (Supersedes ver. 1.0 released June 26, 2013.)
- U.S. Geological Survey Geologic Carbon Dioxide Storage Resources Assessment Team, 2013b, National assessment of geologic carbon dioxide storage resources—Results (ver. 1.1, September 2013): U.S. Geological Survey Circular 1386, 41 p., accessed September 5, 2013, at <http://pubs.usgs.gov/circ/1386/>. (Supersedes ver. 1.0 released June 26, 2013.)
- U.S. Geological Survey Geologic Carbon Dioxide Storage Resources Assessment Team, 2013c, National assessment of geologic carbon dioxide storage resources—Summary (ver. 1.1, September 2013): U.S. Geological Survey Fact Sheet 2013–3020, 6 p., accessed September 5, 2013, at <http://pubs.usgs.gov/fs/2013/3020/>. (Supersedes ver. 1.0 released June 2, 2013.)
- U.S. Geological Survey Raton Basin-Sierra Grande Uplift Province Assessment Team, 2005, Assessment of undiscovered oil and gas resources of the Raton Basin-Sierra Grande Uplift Province of New Mexico and Colorado, 2004: U.S. Geological Survey Fact Sheet 2005–3027, 2 p., accessed September 10, 2011, at http://pubs.usgs.gov/fs/2005/3027/pdf/higley_FS.pdf.
- U.S. Geological Survey San Juan Basin Assessment Team, 2002, Assessment of undiscovered oil and gas resources of the San Juan Basin Province of New Mexico and Colorado, 2002: U.S. Geological Survey Fact Sheet FS–147–02, 2 p., accessed September 19, 2011, at <http://pubs.usgs.gov/fs/fs-147-02/FS-147-02.pdf>.
- U.S. Geological Survey San Juan Basin Assessment Team, 2013, Total petroleum systems and geologic assessment of undiscovered oil and gas resources in the San Juan Basin Province, exclusive of Paleozoic rocks, New Mexico and Colorado: U.S. Geological Survey Digital Data Series DDS–69–F, accessed January 7, 2014, at <http://pubs.usgs.gov/dds/dds-069/dds-069-f/>.
- U.S. Geological Survey Uinta-Piceance Assessment Team, 2002, Assessment of undiscovered oil and gas resources of the Uinta-Piceance Province of Colorado and Utah, 2002: U.S. Geological Survey Fact Sheet FS–026–02, 2 p., accessed August 26, 2010, at <http://pubs.usgs.gov/fs/fs-0026-02/fs-0026-02.pdf>.
- U.S. Geological Survey Uinta-Piceance Assessment Team, 2003, Petroleum systems and geologic assessment of oil and gas in the Uinta-Piceance Province, Utah and Colorado: U.S. Geological Survey Digital Data Series DDS–69–B, accessed August 26, 2010, at <http://pubs.usgs.gov/dds/dds-069/dds-069-b/>.
- U.S. Geological Survey Wyoming Thrust Belt Province Assessment Team, 2003, Assessment of undiscovered oil and gas resources of the Wyoming Thrust Belt Province, 2003: U.S. Geological Survey Fact Sheet 2004–3007, 2 p., accessed January 31, 2011, at <http://pubs.usgs.gov/fs/2004/3025/fs-2004-3025.pdf>.

- Vincelette, R.R., and Chittum, W.E., 1981, Exploration for oil accumulations in Entrada Sandstone, San Juan Basin, New Mexico: American Association of Petroleum Geologists Bulletin, v. 65, no. 2, p. 2,546–2,570.
- Whidden, K.J., 2012, Assessment of undiscovered oil and gas resources in the Paradox Basin Province, Utah, Colorado, New Mexico, and Arizona, 2011: U.S. Geological Survey Fact Sheet 2012–3031, 4 p., accessed December 23, 2015, at <http://pubs.usgs.gov/fs/2012/3031/>.
- Whitehead, N.H., III, 1993, San Juan Basin plays—Mesaverde Group, *in* Hjellming, C.A., ed., Atlas of major Rocky Mountain gas reservoirs: Socorro, N. Mex., New Mexico Bureau of Mines and Mineral Resources, p. 127–131.
- Woodward, L.A., 1983, Geology and hydrocarbon potential of the Raton Basin, New Mexico, *in* Fassett, J.E., Hamilton, W., Jr., Martin, G.W., and Middleman, A.A., eds., Oil and gas fields of the Four Corners area: Durango, Colo., Four Corners Geological Society, v. 3, p. 789–798.
- Worrall, J., 2004, Preliminary geology of Oakdale Field, northwest Raton Basin, Huerfano County, Colorado: American Association of Petroleum Geologists Search and Discovery Article 20017, 14 p., accessed December 22, 2015, at <http://www.searchanddiscovery.com/documents/2004/Worrall>.
- Zawiskie, J., Chapman, D., and Alley, R., 1982, Depositional history of the Paleocene-Eocene Colton Formation, north-central Utah, *in* Nelson, D.L., ed., Overthrust belt of Utah: 1982 Symposium and Field Conference, Salt Lake City, Utah, Utah Geological Association Publication 10, p. 273–284.

